NETWORK LOCALIZATION AND NAVIGATION: FROM THEORY TO PRACTICE

Moe Z. Win and Andrea Conti

http://wgroup.lids.mit.edu/ http://www.andreaconti.info/

Laboratory for Information and Decision Systems
Massachusetts Institute of Technology

Wireless Communication and Localization Network Laboratory
University of Ferrara

Research Areas

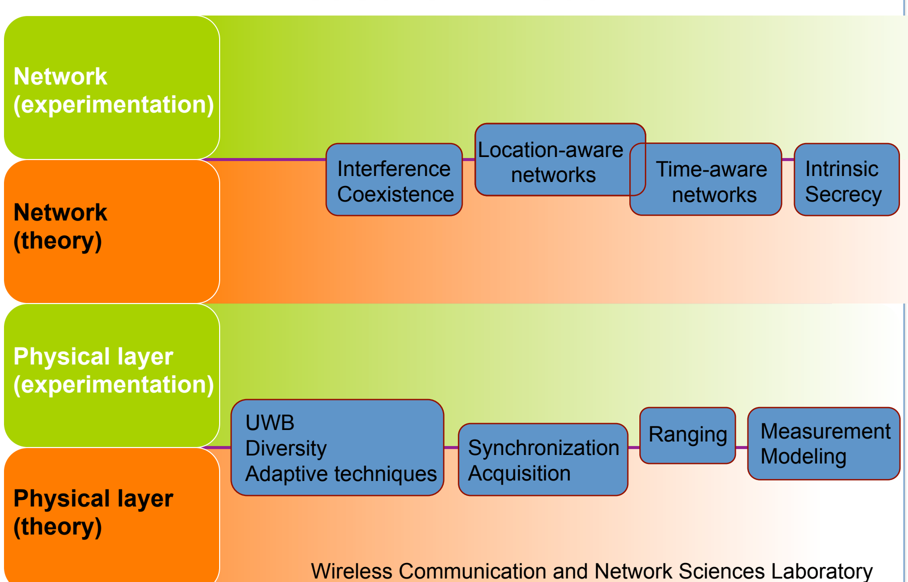

Cycle of cooperative location-aware networks

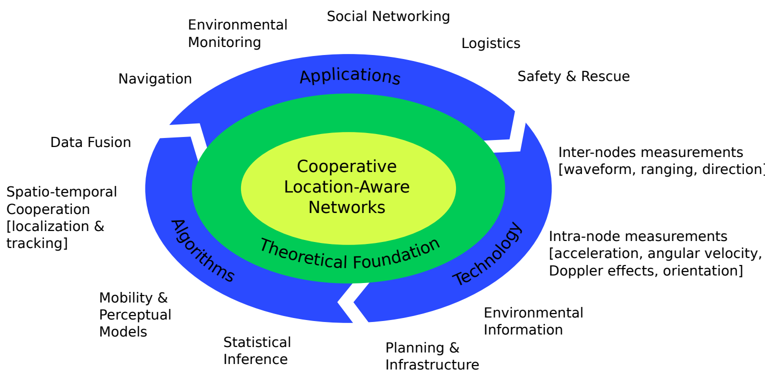

M. Z. Win, A. Conti, S. Mazuelas, Y. Shen, W. M. Gifford, D. Dardari, and M. Chiani, "Network localization and navigation via cooperation," *IEEE Commun. Mag.*, vol. 49, no. 5, pp. 56–62, May 2011.

Cooperative Location-Aware Networks

- Problem:
  - Reliable and efficient localization in harsh GPS-challenged environments with limited infrastructures
  - Current noncooperative techniques are inaccurate either due to limited infrastructures (anchor-based) or velocity drift (inertial-based)
- Main idea:
  - Exploit spatial and temporal cooperation by harnessing inter-nodes (in space) and intra-node (in time) measurements to improve performance
- Challenges
  - Complex information behavior due to joint spatial and temporal cooperation
  - Efficient fusion of information from various cooperation modes
  - Accuracy and reliability in the presence of mobility and uncertainty

Goals: Cooperative Location-Aware Networks

✓ theoretical analysis for determination of fundamental performance limits;
✓ the design of practical algorithms that approach such ultimate limits; and
✓ experimentation, both for validation and for developing realistic statistical models

Outline

- **Part I: Foundations**
  - Wideband Cooperative Localization (S) ✓
  - Cooperative Network Navigation (S) ✓
- **Part II: Network Algorithms**
  - Location Inference and Observation Selection ✓
  - Network Message-Passing Algorithms (S) ✓
  - Belief Condensation Techniques (S)
  - Wideband Ranging ✓
- **Part III: Network Operations**
  - Non-cooperative Network Power Allocation
  - Cooperative Network Power Allocation
  - Sparsity Property of Localization (S) ✓
  - Network Scheduling (S)

Outline

- **Part IV: Network Experimentations**
  - Channel Measurements (S) and Ranging ✓
  - Coopertive Localization ✓
  - Diversity Navigation ✓
- **Part V: Example Applications**
  - Sensor Radar Networks ✓
  - Semipassive Tags ✓
  - RFID Systems
- **Concluding Remarks** ✓
- **References** ✓

WIDEBAND COOPERATIVE LOCALIZATION

Wideband Cooperative Localization

- High-accuracy location-awareness is important for wireless applications
- Wideband transmission
  - Precise range measurements due to fine time resolution
  - Robustness in dense, harsh environments
  - Simultaneous communication & ranging
- Cooperative techniques
  - Measurements are made between agents
  - Agents jointly find spatial topology of the network
  - Dramatic increase in coverage, accuracy, and robustness, especially infrastructure is limited

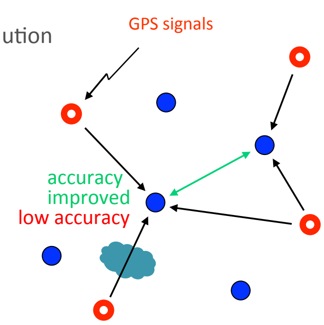

- Our contributions:
  - Determine the fundamental limits of cooperative localization accuracy
  - Introduce a geometric interpretation for the localization information

Outline

- Background
- Problem formulation
- Performance bounds
- Geometric Interpretation
- Conclusion

Problem Formulation

- Cooperative Localization Systems

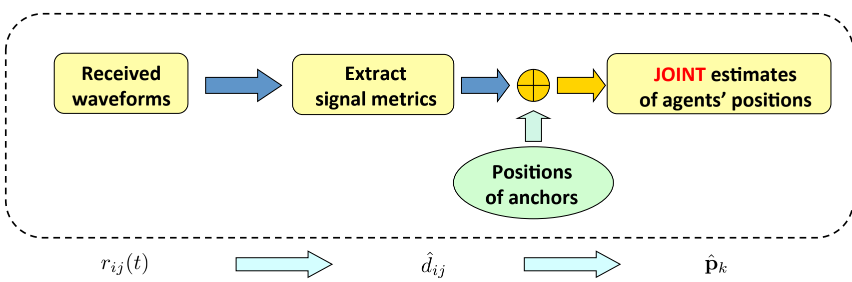

our work

most previous work

Not fundamental – specific signal metric may eliminate relevant localization information inherent in the received waveforms

What are the fundamental limits of wideband cooperative localization?

Problem Formulation

- 2-D Network Setting
  - N_{a} agents (set $\mathcal{N}_{\mathrm{a}}$): position $\mathbf{p}_k = [\, x_k \;\; y_k \,]^{\mathrm{T}}$ $(k \in \mathcal{N}_{\mathrm{a}})$ unknown
  - N_{b} anchors (set $\mathcal{N}_{\mathrm{b}}$): position $\mathbf{p}_j = [\, x_j \;\; y_j \,]^{\mathrm{T}}$ $(j \in \mathcal{N}_{\mathrm{b}})$

- Measurement model
  - Received waveform at agent $k \in \mathcal{N}_{\mathrm{a}}$ from node $j \in \mathcal{N}_{\mathrm{a}} \cup \mathcal{N}_{\mathrm{b}} \backslash \{k\}$

number of multipath — known wideband waveform

$$r_{kj}(t) = \sum_{l=1}^{L_{kj}} \alpha_{kj}^{(l)}\, s\big(t - \tau_{kj}^{(l)}\big) + z_{kj}(t)$$

amplitude — delay — white Gaussian noise

  - Relationship between delays and NLOS biases

$$\tau_{kj}^{(l)} = \frac{1}{c}\big[\, \|\mathbf{p}_k - \mathbf{p}_j\| + b_{kj}^{(l)} \,\big]$$

speed of propagation — positive NLOS biases (LOS signals, $b_{kj}^{(1)} = 0$)

Problem Formulation

- Parameters

$$\boldsymbol{\theta} = [\; \mathbf{P}^{\mathrm{T}} \;\; \boldsymbol{\kappa}_1^{\mathrm{T}} \;\; \boldsymbol{\kappa}_2^{\mathrm{T}} \;\; \cdots \;\; \boldsymbol{\kappa}_{N_{\mathrm{a}}}^{\mathrm{T}} \;]^{\mathrm{T}}$$

  - Agents' positions $\mathbf{P} = [\; \mathbf{p}_1^{\mathrm{T}} \;\; \mathbf{p}_2^{\mathrm{T}} \;\; \cdots \;\; \mathbf{p}_{N_{\mathrm{a}}}^{\mathrm{T}} \;]^{\mathrm{T}}$ — parameters of interest
  - Multipath parameters $\boldsymbol{\kappa}_k$ for agent k include
    - Biases by NLOS propagation $\{b_{kj}^{(l)},\, j \in \mathcal{N}_{\mathrm{a}} \cup \mathcal{N}_{\mathrm{b}}\}$
    - Multipath amplitudes $\{\alpha_{kj}^{(l)},\, j \in \mathcal{N}_{\mathrm{a}} \cup \mathcal{N}_{\mathrm{b}}\}$

  For LOS signals $b_{kj}^{(1)} = 0$ are eliminated

- Received signal vector
  - Received waveforms $r_{kj}(t) \Longrightarrow \mathbf{r}_{kj}$ — Karhunen-Loève expansion
  - Vector $\mathbf{r}$ is composed by all the $\mathbf{r}_{kj}$

- Localization problem: To estimate $\boldsymbol{\theta}$ based on observation $\mathbf{r}$

Fisher Information Matrix

- Bayesian Fisher Information Matrix (FIM)

$$\mathbf{J}_{\boldsymbol{\theta}} = \mathbb{E}_{\mathbf{r},\boldsymbol{\theta}}\left\{-\frac{\partial^2}{\partial\boldsymbol{\theta}\partial\boldsymbol{\theta}^{\mathrm{T}}}\ln f(\mathbf{r},\boldsymbol{\theta})\right\}$$

- Log joint probability function can be factorized as

$$\ln f(\mathbf{r},\boldsymbol{\theta}) = \underbrace{\sum_{k\in\mathcal{N}_{\mathrm{a}}}\sum_{j\in\mathcal{N}_{\mathrm{b}}}\Big[\ln f(\mathbf{r}_{kj}|\boldsymbol{\theta}) + \ln f(\boldsymbol{\kappa}_{kj}|\mathbf{P})\Big]}_{\text{anchor}} + \underbrace{\sum_{k\in\mathcal{N}_{\mathrm{a}}}\sum_{j\in\mathcal{N}_{\mathrm{a}}\backslash\{k\}}\Big[\ln f(\mathbf{r}_{kj}|\boldsymbol{\theta}) + \ln f(\boldsymbol{\kappa}_{kj}|\mathbf{P})\Big]}_{\text{cooperation}}$$

where $f(\mathbf{r}_{kj}|\boldsymbol{\theta})$ is the likelihood of the measurement, and $f(\boldsymbol{\kappa}_{kj}|\mathbf{P})$ is the conditional pdf of channel parameters $\boldsymbol{\kappa}_{kj}$.

- FIM decomposed as $\mathbf{J}_{\boldsymbol{\theta}} = \underbrace{\mathbf{J}_{\boldsymbol{\theta}}^{\mathrm{A}}}_{\text{anchor}} + \underbrace{\mathbf{J}_{\boldsymbol{\theta}}^{\mathrm{C}}}_{\text{cooperation}}$

Performance Metric

- Squared position error bound (SPEB)
  - Metric of localization accuracy
  - Hybrid Cramer-Rao bound

$$\mathbb{E}_{\mathbf{r},\boldsymbol{\theta}}\left\{(\hat{\boldsymbol{\theta}}-\boldsymbol{\theta})(\hat{\boldsymbol{\theta}}-\boldsymbol{\theta})^{\mathrm{T}}\right\} \succeq \mathbf{J}_{\boldsymbol{\theta}}^{-1} \qquad \boldsymbol{\theta} = [\ \mathbf{P}^{\mathrm{T}}\ \overbrace{\boldsymbol{\kappa}_1^{\mathrm{T}}\ \ \boldsymbol{\kappa}_2^{\mathrm{T}}\ \cdots\ \boldsymbol{\kappa}_{N_{\mathrm{a}}}^{\mathrm{T}}}^{\text{multipath parameters}}\ ]^{\mathrm{T}}$$

$$\Longrightarrow \mathbb{E}_{\mathbf{r},\boldsymbol{\theta}}\left\{(\hat{\mathbf{P}}-\mathbf{P})(\hat{\mathbf{P}}-\mathbf{P})^{\mathrm{T}}\right\} \succeq [\mathbf{J}_{\boldsymbol{\theta}}^{-1}]_{\mathbf{P}}$$

  - $[\mathbf{J}_{\boldsymbol{\theta}}^{-1}]_{\mathbf{P}}$ denotes the square submatrix on the diagonal of $\mathbf{J}_{\boldsymbol{\theta}}^{-1}$ corresponding to $\mathbf{P}$
  - Mean squared position error of agent k

$$\mathbb{E}_{\mathbf{r},\boldsymbol{\theta}}\left\{\|\hat{\mathbf{p}}_k - \mathbf{p}_k\|^2\right\} \geq \mathrm{tr}\left\{\left[\mathbf{J}_{\boldsymbol{\theta}}^{-1}\right]_{\mathbf{p}_k}\right\} = \mathcal{P}(\mathbf{p}_k)$$

where $[\mathbf{J}_{\boldsymbol{\theta}}^{-1}]_{\mathbf{p}_k}$ is a 2×2 submatrix on the diagonal of $\mathbf{J}_{\boldsymbol{\theta}}^{-1}$

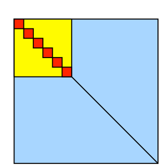

$\mathbf{J}_{\boldsymbol{\theta}}^{-1}$

- SPEB is defined as

$$\boxed{\mathcal{P}(\mathbf{p}_k) := \mathrm{tr}\left\{\left[\mathbf{J}_{\boldsymbol{\theta}}^{-1}\right]_{\mathbf{p}_k}\right\}}$$

Equivalent Fisher Information

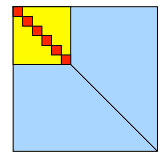

- Remarks:
  - FIM $\mathbf{J}_{\boldsymbol{\theta}}$ is a matrix of high dimensions; however, for SPEB evaluation only $[\mathbf{J}_{\boldsymbol{\theta}}^{-1}]_{\mathbf{P}}$ is of interest
  - Use Schur's complement to reduce the dimension of the FIM

- Equivalent Fisher information matrix (EFIM)
  - Original FIM $\mathbf{J}_{\boldsymbol{\theta}} = \begin{bmatrix} \boxed{\mathbf{A}} & \mathbf{B} \\ \mathbf{B}^{\dagger} & \mathbf{C} \end{bmatrix}$ for $\boldsymbol{\theta} = \begin{bmatrix} \boxed{\boldsymbol{\theta}_1} \\ \boldsymbol{\theta}_2 \end{bmatrix}$
  - EFIM $\boxed{\mathbf{J}_{\mathrm{e}}(\boldsymbol{\theta}_1) := \mathbf{A} - \mathbf{B}\mathbf{C}^{-1}\mathbf{B}^{\mathrm{T}}}$
  - It retains all necessary information to derive the information inequality for $\boldsymbol{\theta}_1$

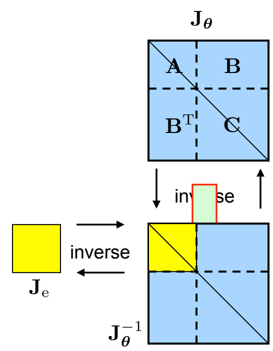

Outline

- Background
- Problem formulation
- **Performance bounds**
- Geometric Interpretation
- Conclusion

EFIM for Cooperative Localization

- **Result:** When prior knowledge of the agents' position is not available, the EFIM for the agents' positions is a $2N_\text{a} \times 2N_\text{a}$ matrix:

FIM: $\mathbf{J}_{\boldsymbol{\theta}} = \mathbf{J}_{\boldsymbol{\theta}}^\text{A} + \mathbf{J}_{\boldsymbol{\theta}}^\text{C}$ $\Longrightarrow$ **EFIM:** $\mathbf{J}_\text{e}(\mathbf{P}) = \mathbf{J}_\text{e}^\text{A} + \mathbf{J}_\text{e}^\text{C}$

where $\mathbf{J}_\text{e}^\text{A}$ and $\mathbf{J}_\text{e}^\text{C}$ are $2N_\text{a} \times 2N_\text{a}$ matrices that characterize the contribution from anchors and cooperation, respectively,

$$\mathbf{J}_\text{e}^\text{A} = \begin{bmatrix} \mathbf{J}_\text{e}^\text{A}(\mathbf{p}_1) & & & \\ & \mathbf{J}_\text{e}^\text{A}(\mathbf{p}_2) & & \\ & & \ddots & \\ & & & \mathbf{J}_\text{e}^\text{A}(\mathbf{p}_{N_\text{a}}) \end{bmatrix}$$

2×2

$$\boxed{\mathbf{J}_\text{e}^\text{A}(\mathbf{p}_k) = \sum_{j \in \mathcal{N}_\text{b}} \boxed{\lambda_{kj}\, \mathbf{J}_\text{r}(\phi_{k,j})}}$$

Ranging information

$$\mathbf{J}_\text{e}^\text{C} = \begin{bmatrix} \sum_{j \in \mathcal{N}_\text{a}\backslash\{1\}} \mathbf{C}_{1,j} & -\mathbf{C}_{1,2} & \cdots & -\mathbf{C}_{1,N_\text{a}} \\ -\mathbf{C}_{1,2} & \sum_{j \in \mathcal{N}_\text{a}\backslash\{2\}} \mathbf{C}_{2,j} & & -\mathbf{C}_{2,N_\text{a}} \\ \vdots & & \ddots & \\ -\mathbf{C}_{1,N_\text{a}} & -\mathbf{C}_{2,N_\text{a}} & & \sum_{j \in \mathcal{N}_\text{a}\backslash\{N_\text{a}\}} \mathbf{C}_{N_\text{a},j} \end{bmatrix}$$

$$\boxed{\mathbf{C}_{k,j} = \mathbf{C}_{j,k} = \boxed{(\lambda_{kj} + \lambda_{jk}) \cdot \mathbf{J}_\text{r}(\phi_{k,j})}}$$

Ranging Information

- EFIM from anchors to agent k

$$\mathbf{J}_\text{e}^\text{A}(\mathbf{p}_k) = \underbrace{\sum_{j \in \mathcal{N}_\text{b}}}_{\text{sum over anchors}} \underbrace{\lambda_{k,j}}_{\text{RII}} \cdot \underbrace{\mathbf{J}_\text{r}(\phi_{k,j})}_{2\times 2 \text{ RDM}}$$

  - Canonical form: weighted sum of RDM from individual anchors
  - Each anchor provides "one-dimensional" information since RDM has rank 1

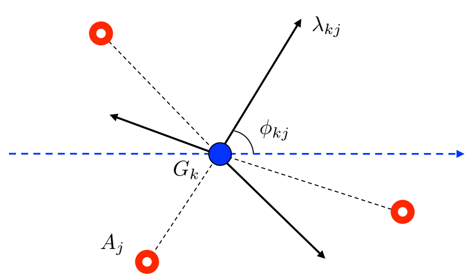

Geometric Interpretation

Ranging Information Intensity

- **Result:** When channel knowledge is not available, the RII of LOS signals is determined by the first contiguous-cluster of the signals:

$$\lambda_{kj} = \frac{8\pi^2\beta^2}{c^2}(1-\chi_{kj})\cdot \text{SNR}_{kj}^{(1)}$$

SNR of the first path

effective bandwidth
$\beta = (\int f^2 \cdot S(f)^2 df)^{1/2}$

$\chi_{kj} \in [0,1]$ path-overlap coefficient: determined ONLY by the NLOS biases

  – Special case: if the first path is resolvable then

$$\lambda_{kj} = \frac{8\pi^2\beta^2}{c^2}\cdot \text{SNR}_{kj}^{(1)} \qquad (\chi_{kj}=0)$$

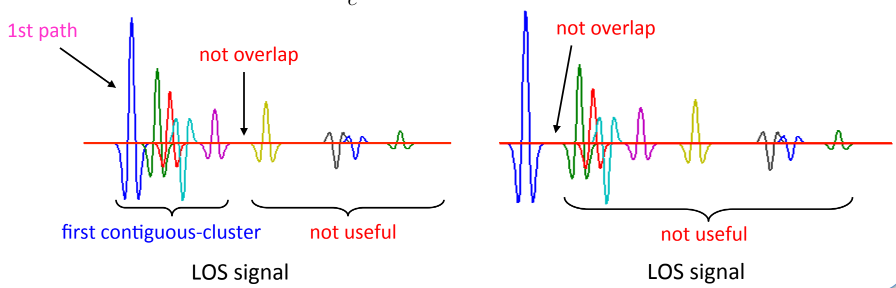

Outline

- Background
- Problem formulation
- Performance bounds
- Geometric Interpretation
- Conclusion

Geometric Interpretation

- Information Ellipse of EFIM
  - Eigen-decomposition

$$\mathbf{J}_{\mathrm{e}}(\mathbf{p}) = \mathbf{U}_{\vartheta} \begin{bmatrix} \mu & 0 \\ 0 & \eta \end{bmatrix} \mathbf{U}_{\vartheta}^{\mathrm{T}} \qquad \mathbf{U}_{\vartheta} = \begin{bmatrix} \cos\vartheta & -\sin\vartheta \\ \sin\vartheta & \cos\vartheta \end{bmatrix}$$

  - Set of points $\{\mathbf{y} \in \mathbb{R}^2 : \mathbf{y}^{\dagger}\, \mathbf{J}_{\mathrm{e}}^{-1}\, \mathbf{y} = 1\}$

- Ellipse evolution:
  - $\sqrt{\mu},\ \sqrt{\eta},\ \vartheta$
  - RI can be viewed as a degenerate information ellipse

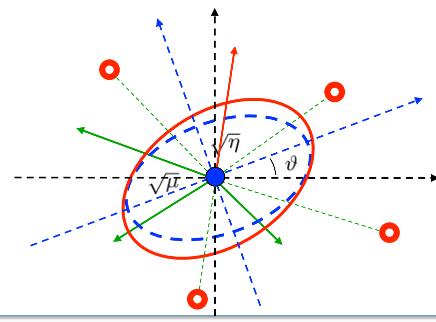

Geometric Interpretation

- Two-agent cooperation with $\mathbf{S}_{12} = \lambda_{12}\, \mathbf{J}_{\mathrm{r}}(\phi_{12})$
  - EFIM for agent 1

$$\mathbf{J}_{\mathrm{e}}(\mathbf{x}_1) = \mathbf{J}_{\mathrm{e}}^{\mathrm{A}}(\mathbf{x}_1) + \xi_{12}\, \mathbf{S}_{12}$$

where

$$\xi_{12} = \frac{1}{1 + \lambda_{12}\, \underbrace{\mathbf{u}_{\phi_{12}}^{\dagger}\, \left[\mathbf{J}_{\mathrm{e}}^{\mathrm{A}}(\mathbf{x}_2)\right]^{-1} \mathbf{u}_{\phi_{12}}^{\dagger}}_{\text{projected position error}}}$$

  - Effective intensity $\xi_{12}\, \lambda_{12}$ $(\xi_{12} \leq 1)$
  - Agent -> anchor when projected error diminishes

- More agents in cooperation

$$\mathbf{J}_{\mathrm{e}}(\mathbf{x}_k) \approx \mathbf{J}_{\mathrm{e}}^{\mathrm{A}}(\mathbf{x}_k) + \sum_{j \in \mathcal{N}_{\mathrm{a}} \setminus \{k\}} \xi_{kj}\, \mathbf{S}_{kj}$$

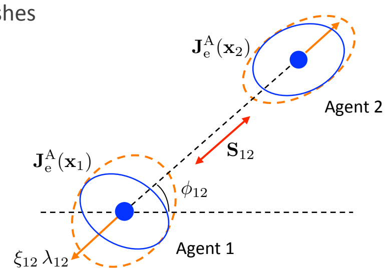

Geometric Interpretation

- **Result:** The SPEB is coordinate system independent.

$$\mathcal{P}(\mathbf{p}) = \mathcal{P}(\mathbf{p}^*) = \mathrm{tr}\left\{ \begin{bmatrix} \mu & 0 \\ 0 & \eta \end{bmatrix}^{-1} \right\} = \frac{1}{\mu} + \frac{1}{\eta}$$

where $\mathbf{p}^*$ is the agent's position in the new coordinate system that is rotated by ϑ .

  - Remark: The localization information is decoupled in the new coordinate system.

- **Result:** An agent has EFIM $\mathbf{J}_{\mathrm{e}}(\mathbf{p}) = \mathbf{F}(\mu, \eta, \vartheta)$ and corresponding SPEB $\mathcal{P}(\mathbf{p})$ If the agent obtains RI $\mathbf{F}(\nu, 0, \phi)$ from a new anchor, then the agent's SPEB becomes

$$\tilde{\mathcal{P}}(\mathbf{p}) = \frac{1}{\tilde{\mu}} + \frac{1}{\tilde{\eta}} = \frac{\mu + \eta + \nu}{\mu\eta + \nu\left[\eta + (\mu - \eta)\sin^2(\phi - \vartheta)\right]}$$

  - Minimum SPEB for a fixed RII is

$$\min_{\phi} \tilde{\mathcal{P}}(\mathbf{p}) = \frac{\mu + \eta + \nu}{\mu(\eta + \nu)} \qquad \phi = \vartheta \pm \pi/2$$

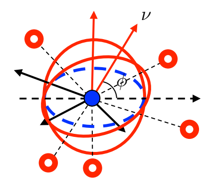

Geometric Interpretation

Overall $2N_{\mathrm{a}} \times 2N_{\mathrm{a}}$ **EFIM** $\mathbf{J}_{\mathrm{e}}(\mathbf{P}) = \mathbf{J}_{\mathrm{e}}^{\mathrm{A}} + \mathbf{J}_{\mathrm{e}}^{\mathrm{C}}$

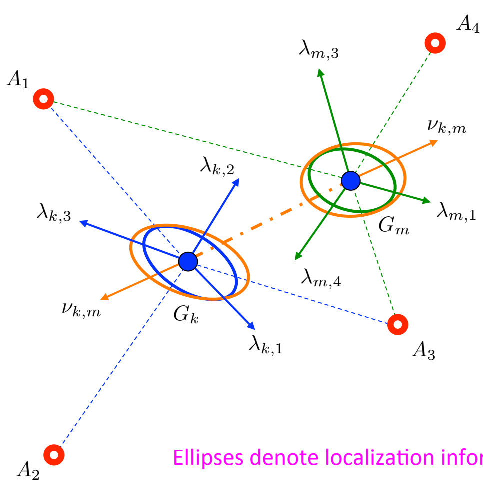

Comment:

- Cooperative information for localization is coupled
- $\nu_{k,m}$ cannot to be fully utilized
- The strength is weighed by $\chi_{km} \in [0, 1]$

Ellipses denote localization information.

Numerical Example

- Agents randomly locate in an area of 20 m by 20 m
- Two set of anchor deployments (red/magenta)
- SPEB decreases at the rate of the number of agents

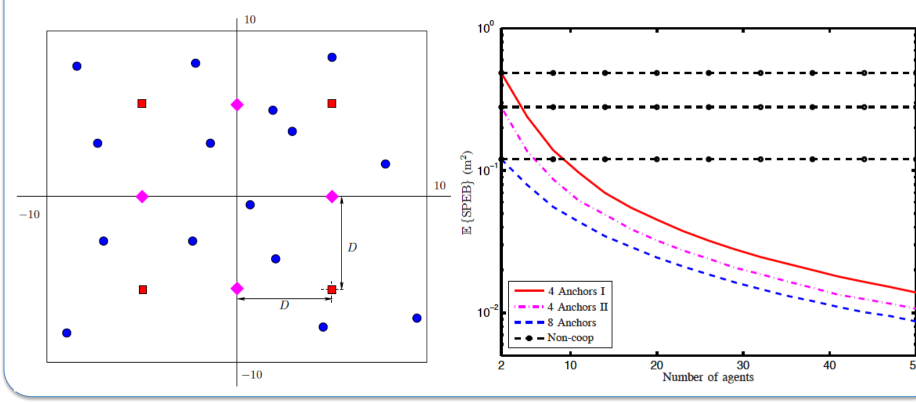

Outline

- Background
- Problem formulation
- Performance bounds
- Geometric Interpretation
- Conclusion

Conclusion

- Developed a framework to study *wideband cooperative opportunistic location-aware networks*, and determined their localization accuracy
- Introduced the notions of *equivalent Fisher information* and *ranging information*, and unified the localization information from anchors and that from agents in a canonical form
- Provided a *geometric interpretation* of the localization information in cooperative networks, and used *information ellipse* for localization information to characterize the cooperation benefits

References

- M. Z. Win, A. Conti, S. Mazuelas, Y. Shen, W. M. Gifford, D. Dardari, and M. Chiani, "Network localization and navigation via cooperation," *IEEE Commun. Mag.,* vol. 49, no. 5, pp. 56–62, May 2011.
- Y. Shen and M. Z. Win, "Fundamental Limits of Wideband Localization - Part I: A General Framework," *IEEE Trans. Inform. Theory*, vol. 56, no. 10, pp. 4956-4980, Oct. 2010.
- Y. Shen, H. Wymeersch, and M. Z. Win, "Fundamental limits of wideband cooperative localization – Part II: Cooperative Networks," *IEEE Trans. Inform. Theory*, vol. 56, no. 10, pp. 4981-5000, Oct. 2010.
- Y. Shen and M. Z. Win, "On the accuracy of localization systems using wideband antenna arrays," *IEEE Trans. Commun.*, vol. 58, no. 1, pp. 270–280, Jan. 2010.
- D. B. Jourdan, D. Dardari, and M. Z. Win, "Position error bound for UWB localization in dense cluttered environments," *IEEE Trans. Aerosp. Electron. Syst.,* vol. 44, no. 2, pp. 613–628, Apr. 2008.

BACKUP SLIDES

Ranging Information

- Ranging Information
  - Basic building block of the EFIM
  - Definition: a 2×2 matrix of the form $\lambda \cdot \mathbf{J}_{\mathrm{r}}(\phi)$
  - $\lambda \in \mathbb{R}^+$ is called the ranging information intensity (RII)
  - $\mathbf{J}_{\mathrm{r}}(\phi)$ is called the ranging direction matrix (RDM), given by

$$\mathbf{J}_{\mathrm{r}}(\phi) := \mathbf{u}(\phi)\,\mathbf{u}(\phi)^{\mathrm{T}} = \begin{bmatrix} \cos^2\phi & \cos\phi\sin\phi \\ \cos\phi\sin\phi & \sin^2\phi \end{bmatrix}$$

    where $\mathbf{u}(\phi) = [\cos\phi \quad \sin\phi]^{\mathrm{T}}$
  - The RDM is one-dimensional along the direction of ϕ , exactly one non-zero eigenvalue equal to 1 with corresponding eigenvector $\mathbf{u}(\phi) = [\cos\phi \quad \sin\phi]^{\mathrm{T}}$

Geometric Interpretation

- Information Ellipse – EFIM
  - Eigen-decomposition

$$\mathbf{J}_{\mathrm{e}}(\mathbf{p}) = \mathbf{U}_{\vartheta} \begin{bmatrix} \mu & 0 \\ 0 & \eta \end{bmatrix} \mathbf{U}_{\vartheta}^{\mathrm{T}}$$

  - Set of points $\mathbf{x} \in \mathbb{R}^2$ satisfying $\mathbf{x}^{\mathrm{T}}\mathbf{J}_{\mathrm{e}}\mathbf{x} = 1$

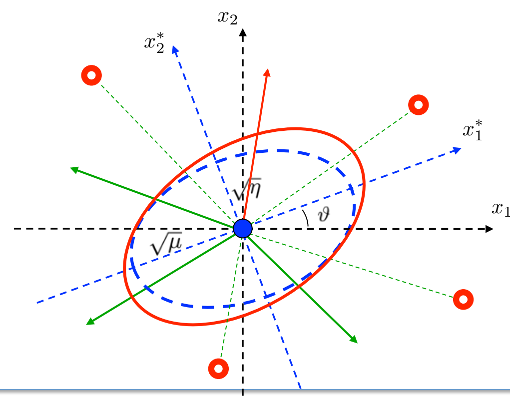

COOPERATIVE NETWORK NAVIGATION

Network Navigation

- Challenges in wireless localization
  - GPS-challenged and dynamic environments
  - High accuracy and reliability
  - Time-critical operation and resource constraints
  - Heterogeneous information fusion

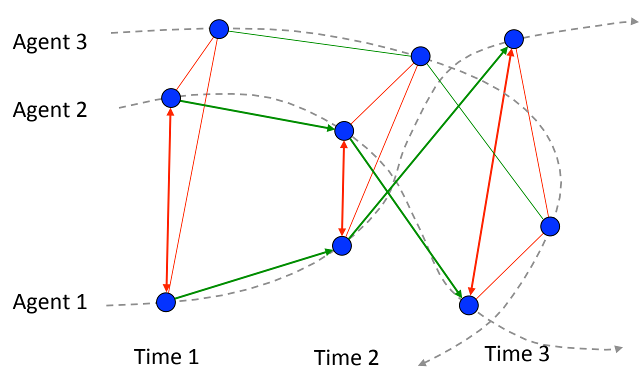

Network Navigation

- Network navigation: exploit both spatial and temporal cooperation
  - Spatial cooperation: inter-node measurements (e.g., ranges)
  - Temporal cooperation: intra-node measurements (e.g., accelerations)
  - Dramatic increase in coverage, accuracy, and robustness
- Contributions
  - develop a theoretical framework for network navigation
  - characterize the information behavior and benefit of joint cooperation

Outline

- Background
- System Model
- EFIM for Network Navigation
- Navigation Information Evolution
- Numerical Example
- Conclusion

System Model

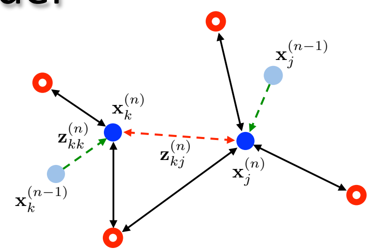

- Network model
  - N_{a} agents and N_{b} anchors
  - Discrete time instants $n \in \{1, 2, \ldots, N\}$
  - Node positional state $\mathbf{x}_k^{(n)}$ 2-D position
- Measurements
  - Inter-node: $\mathbf{z}_{kj}^{(n)}$ with parameter $\boldsymbol{\kappa}_{kj}^{(n)}$ (e.g., wireless channel) distance
  - Intra-node: $\mathbf{z}_{kk}^{(n)}$ with parameter $\boldsymbol{\kappa}_{kk}^{(n)}$ (e.g., clock drift) velocity
- Parameters $\boldsymbol{\theta} = \left[\, \mathbf{x}_{1:N_{\mathrm{a}}}^{(1)\dagger} \;\; \boldsymbol{\kappa}_{1:N_{\mathrm{a}}}^{(1)\dagger} \;\; \cdots \;\; \mathbf{x}_{1:N_{\mathrm{a}}}^{(N)\dagger} \;\; \boldsymbol{\kappa}_{1:N_{\mathrm{a}}}^{(N)\dagger} \,\right]^{\dagger}$ deterministic

$$\mathbf{x}_{k_1:k_2} = \left[\, \mathbf{x}_{k_1} \;\; \ldots \;\; \mathbf{x}_{k_2} \,\right]$$
$$\mathbf{x}_{k_1:k_2}^{(t_1:t_2)} = \left[\, \mathbf{x}_{k_1:k_2}^{(t_1)} \;\; \ldots \;\; \mathbf{x}_{k_1:k_2}^{(t_2)} \,\right]$$

- Likelihood function

$$f(\mathbf{z}|\boldsymbol{\theta}) = \prod_{n=1}^{N} \prod_{k \in \mathcal{N}_{\mathrm{a}}} \Bigg[\underbrace{\prod_{j \in \mathcal{N}_{\mathrm{a}} \cup \mathcal{N}_{\mathrm{b}} \backslash \{k\}} f\left(\mathbf{z}_{kj}^{(n)} | \mathbf{x}_k^{(n)} - \mathbf{x}_j^{(n)}, \boldsymbol{\kappa}_{kj}^{(n)}\right)}_{\text{inter-node}} \cdot \underbrace{f\left(\mathbf{z}_{kk}^{(n)} | \mathbf{x}_k^{(n)} - \mathbf{x}_k^{(n-1)}, \boldsymbol{\kappa}_{kk}^{(n)}\right)}_{\text{intra-node}} \Bigg]$$

Localization Performance Metric

- Location inference from inter-node and intra-node measurements
  - Performance bound for positional errors

$$\mathbb{E}_{\mathbf{z}}\left\{ \left(\hat{\mathbf{x}}_k^{(n)} - \mathbf{x}_k^{(n)}\right)\left(\hat{\mathbf{x}}_k^{(n)} - \mathbf{x}_k^{(n)}\right)^{\dagger} \right\} \succeq \left[\mathbf{J}_{\boldsymbol{\theta}}^{-1}\right]_{\mathbf{x}_k^{(n)}}$$

  - Fisher information matrix (FIM) for $\boldsymbol{\theta} = \left[\, \mathbf{x}_{1:N_{\mathrm{a}}}^{(1)\dagger} \;\; \boldsymbol{\kappa}_{1:N_{\mathrm{a}}}^{(1)\dagger} \;\; \cdots \;\; \mathbf{x}_{1:N_{\mathrm{a}}}^{(N)\dagger} \;\; \boldsymbol{\kappa}_{1:N_{\mathrm{a}}}^{(N)\dagger} \,\right]^{\dagger}$

nuisance parameters

$$\mathbf{J}_{\boldsymbol{\theta}} = \mathbb{E}_{\mathbf{z}}\left\{ -\frac{\partial^2}{\partial \boldsymbol{\theta} \partial \boldsymbol{\theta}^{\mathrm{T}}} \ln f(\mathbf{z}|\boldsymbol{\theta}) \right\}$$

  - $\left[\mathbf{J}_{\boldsymbol{\theta}}^{-1}\right]_{\mathbf{x}_k^{(n)}}$: square submatrix on the diagonal corresp. to $\mathbf{x}_k^{(n)}$

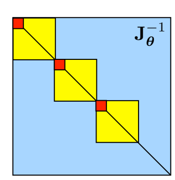

- Equivalent Fisher information
  - Original FIM $\mathbf{J}_{\boldsymbol{\theta}} = \begin{bmatrix} \boxed{\mathbf{A}} & \mathbf{B} \\ \mathbf{B}^{\dagger} & \mathbf{C} \end{bmatrix}$ for parameter $\boldsymbol{\theta} = \begin{bmatrix} \boxed{\boldsymbol{\theta}_1} \\ \boldsymbol{\theta}_2 \end{bmatrix}$
  - EFIM $\mathbf{J}_{\mathrm{e}}(\boldsymbol{\theta}_1) := \mathbf{A} - \mathbf{B}\mathbf{C}^{-1}\mathbf{B}^{\dagger}$
  - Reduce the matrix dimension without loss of relevant information

Outline

- Background
- System Model
- EFIM for Network Navigation
- Navigation Information Evolution
- Numerical Example
- Conclusion

EFIM for Network Navigation

- **Theorem:** The EFIM for the agents' positions $\mathbf{x} = \mathbf{x}_{1:N_\mathrm{a}}^{(1:N)}$ from time 1 to N is given by

$$\mathbf{J}_\mathrm{e}(\mathbf{x}) = \mathbf{J}_\mathrm{e}^\mathrm{s}(\mathbf{x}) + \mathbf{J}_\mathrm{e}^\mathrm{t}(\mathbf{x})$$

  - $\mathbf{J}_\mathrm{e}^\mathrm{s}(\mathbf{x})$ is the EFIM corresponding to spatial cooperation

$$\mathbf{J}_\mathrm{e}^\mathrm{s}(\mathbf{x}) = \mathrm{diag}\{\mathbf{S}^{(1)}, \mathbf{S}^{(2)}, \ldots, \mathbf{S}^{(N)}\}$$

  in which

$$\mathbf{S}^{(n)} = \begin{bmatrix} \sum_{j\in\mathcal{N}_\mathrm{a}\cup\mathcal{N}_\mathrm{b}\backslash\{1\}} \mathbf{S}_{1,j}^{(n)} & -\mathbf{S}_{1,2}^{(n)} & \cdots & -\mathbf{S}_{1,N_\mathrm{a}}^{(n)} \\ -\mathbf{S}_{1,2}^{(n)\dagger} & \sum_{j\in\mathcal{N}_\mathrm{a}\cup\mathcal{N}_\mathrm{b}\backslash\{2\}} \mathbf{S}_{2,j}^{(n)} & & -\mathbf{S}_{2,N_\mathrm{a}}^{(n)} \\ \vdots & & \ddots & \\ -\mathbf{S}_{1,N_\mathrm{a}}^{(n)\dagger} & -\mathbf{S}_{2,N_\mathrm{a}}^{(n)\dagger} & & \sum_{j\in\mathcal{N}_\mathrm{a}\cup\mathcal{N}_\mathrm{b}\backslash\{N_\mathrm{a}\}} \mathbf{S}_{N_\mathrm{a},j}^{(n)} \end{bmatrix}$$

2×2

  - Remarks:
    - $\mathbf{J}_\mathrm{e}^\mathrm{s}(\mathbf{x})$ has block-diagonal structure due to independence in time
    - Each component $\mathbf{S}_{kj}^{(n)}$ associated with inter-node measurement

EFIM for Network Navigation

- **Theorem:** (cont')
  - $\mathbf{J}_\mathrm{e}^\mathrm{t}(\mathbf{x})$ is the EFIM corresponding to temporal cooperation

$$\mathbf{J}_\mathrm{e}^\mathrm{t}(\mathbf{x}) = \begin{bmatrix} \mathbf{T}^{(2)} & -\mathbf{T}^{(2)} & & & \\ -\mathbf{T}^{(2)} & \mathbf{T}^{(2)}+\mathbf{T}^{(3)} & -\mathbf{T}^{(3)} & & \\ & -\mathbf{T}^{(3)} & \mathbf{T}^{(3)}+\mathbf{T}^{(4)} & \ddots & \\ & & \ddots & \mathbf{T}^{(N-1)}+\mathbf{T}^{(N)} & -\mathbf{T}^{(N)} \\ & & & -\mathbf{T}^{(N)} & \mathbf{T}^{(N)} \end{bmatrix}$$

in which $\mathbf{T}^{(n)} = \mathrm{diag}\{\mathbf{T}_1^{(n)}, \mathbf{T}_2^{(n)}, \ldots, \mathbf{T}_{N_\mathrm{a}}^{(n)}\}$

2×2

  - Remarks
    - $\mathbf{J}_\mathrm{e}^\mathrm{t}(\mathbf{x})$ has block tri-diagonal structure
    - $\mathbf{T}^{(n)}$ has block-diagonal structure
    - Each component $\mathbf{T}_k^{(n)}$ associated with intra-node measurement

EFIM for NLN

- **Theorem:** The EFIM for the agents' positions $\mathbf{x} = \mathbf{x}_{1:N_\mathrm{a}}^{(1:N)}$ from time 1 to N is

$$\mathbf{J}_\mathrm{e}(\mathbf{x}) = \mathbf{J}_\mathrm{e}^\mathrm{s}(\mathbf{x}) + \mathbf{J}_\mathrm{e}^\mathrm{t}(\mathbf{x})$$

spatial + temporal

$$\mathbf{J}_\mathrm{e}^\mathrm{s}(\mathbf{x}) = \mathrm{diag}\{\mathbf{S}^{(1)}, \mathbf{S}^{(2)}, \ldots, \mathbf{S}^{(N)}\}$$

$$\mathbf{J}_\mathrm{e}^\mathrm{t}(\mathbf{x}) = \begin{bmatrix} \mathbf{T}^{(2)} & -\mathbf{T}^{(2)} & & & \\ -\mathbf{T}^{(2)} & \mathbf{T}^{(2)}+\mathbf{T}^{(3)} & -\mathbf{T}^{(3)} & & \\ & -\mathbf{T}^{(3)} & \mathbf{T}^{(3)}+\mathbf{T}^{(4)} & \ddots & \\ & & \ddots & \mathbf{T}^{(N-1)}+\mathbf{T}^{(N)} & -\mathbf{T}^{(N)} \\ & & & -\mathbf{T}^{(N)} & \mathbf{T}^{(N)} \end{bmatrix}$$

Time — indep. | corr.

Space — corr. | indep.

each block

$$\mathbf{S}^{(n)} = \begin{bmatrix} \sum_{j \in \mathcal{N}_\mathrm{a} \cup \mathcal{N}_\mathrm{b} \backslash \{1\}} \mathbf{S}_{1,j}^{(n)} & -\mathbf{S}_{1,2}^{(n)} & \cdots & -\mathbf{S}_{1,N_\mathrm{a}}^{(n)} \\ -\mathbf{S}_{1,2}^{(n)\dagger} & \sum_{j \in \mathcal{N}_\mathrm{a} \cup \mathcal{N}_\mathrm{b} \backslash \{2\}} \mathbf{S}_{2,j}^{(n)} & & -\mathbf{S}_{2,N_\mathrm{a}}^{(n)} \\ \vdots & & \ddots & \\ -\mathbf{S}_{1,N_\mathrm{a}}^{(n)\dagger} & -\mathbf{S}_{2,N_\mathrm{a}}^{(n)\dagger} & & \sum_{j \in \mathcal{N}_\mathrm{a} \cup \mathcal{N}_\mathrm{b} \backslash \{N_\mathrm{a}\}} \mathbf{S}_{N_\mathrm{a},j}^{(n)} \end{bmatrix}$$

each block

$$\mathbf{T}^{(n)} = \mathrm{diag}\{\mathbf{T}_1^{(n)}, \mathbf{T}_2^{(n)}, \ldots, \mathbf{T}_{N_\mathrm{a}}^{(n)}\}$$

2×2 building block

inter-node meas. intra-node meas.

Building Blocks

- Spatial measurement (inter-node distance)

$$\mathbf{S}_{kj}^{(n)} = \lambda_{kj}^{(n)} \cdot \mathbf{J}_{\mathrm{r}}(\phi_{kj}^{(n)})$$

$$\boxed{\begin{aligned}\mathbf{J}_{\mathrm{r}}(\phi) &:= \mathbf{u}_\phi \, \mathbf{u}_\phi^\dagger \\ \mathbf{u}_\phi &= [\cos\phi \ \ \sin\phi]^\dagger\end{aligned}}$$

  - $\lambda_{kj}^{(n)}$ is the ranging information intensity
  - Example: wideband transmission

$$\lambda_{kj} = \frac{8\pi^2\beta^2}{c^2}(1-\chi_{kj}) \cdot \mathsf{SNR}_{kj}^{(1)}$$

β : effective bandwidth
$\mathsf{SNR}_{kj}^{(1)}$: SNR of first path
χ_{kj} : path-overlap coefficient on $[0,\,1]$

- Temporal measurement (intra-node velocity)

$$\mathbf{T}_{k}^{(n)} = \lambda_{kk}^{(n)} \cdot \mathbf{J}_{\mathrm{r}}(\phi_{kk}^{(n)}) + \nu_{kk}^{(n)} \cdot \mathbf{J}_{\mathrm{r}}(\phi_{kk}^{(n)} + \pi/2)$$

  - $\lambda_{kk}^{(n)}$ and $\nu_{kk}^{(n)}$ are the amplitude and direction information intensities

Spatial and Temporal Cooperation

Fundamental Limits | **Inference Algorithms**

Cooperation in Space

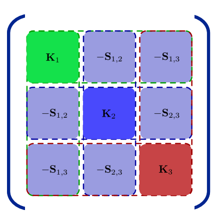

Fisher Information Matrix

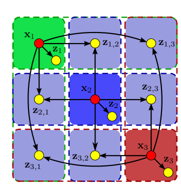

Bayesian Network

Spatial and Temporal Cooperation

Fundamental Limits **Inference Algorithms**

Cooperation in Space and Time

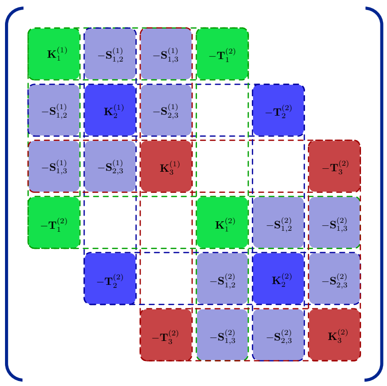

Fisher Information Matrix

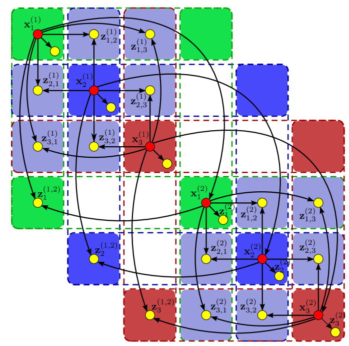

Bayesian Network

Outline

- Background
- System Model
- EFIM for Network Navigation
- Navigation Information Evolution
- Numerical Example
- Conclusion

Navigation Information Evolution

- Filtering application: to infer the state at time N based on the observations up to time N ; the performance is characterized by $\mathbf{J}_{\mathrm{e}}(\mathbf{x}^{(N)})$

- The block-tri-diagonal structure of the EFIM $\mathbf{J}_{\mathrm{e}}(\mathbf{x}^{(1:N)})$ allows to derive the EFIM $\mathbf{J}_{\mathrm{e}}(\mathbf{x}^{(N)})$ through a recursion $\mathbf{J}_{\mathrm{e}}(\mathbf{x}^{(1:N)}) \to \mathbf{J}_{\mathrm{e}}(\mathbf{x}^{(2:N)}) \to \cdots \to \mathbf{J}_{\mathrm{e}}(\mathbf{x}^{(N)})$

$$\mathbf{J}_{\mathrm{e}}(\mathbf{x}^{(1:N)}) = \begin{bmatrix} \mathbf{S}^{(1)} + \mathbf{T}^{(2)} & -\mathbf{T}^{(2)} & & & \\ -\mathbf{T}^{(2)} & \mathbf{S}^{(2)} + \mathbf{T}^{(2)} + \mathbf{T}^{(3)} & -\mathbf{T}^{(3)} & & \\ & -\mathbf{T}^{(3)} & \mathbf{S}^{(3)} + \mathbf{T}^{(3)} + \mathbf{T}^{(4)} & \ddots & \\ & & \ddots & \mathbf{S}^{(N-1)} + \mathbf{T}^{(N-1)} + \mathbf{T}^{(N)} & -\mathbf{T}^{(N)} \\ & & & -\mathbf{T}^{(N)} & \mathbf{S}^{(N)} + \mathbf{T}^{(N)} \end{bmatrix}$$

$$\mathbf{J}_{\mathrm{e}}(\mathbf{x}^{(2:N)}) = \begin{bmatrix} \mathbf{S}^{(2)} + \boxed{\widetilde{\mathbf{T}}^{(2)}} + \mathbf{T}^{(3)} & -\mathbf{T}^{(3)} & & \\ -\mathbf{T}^{(3)} & \mathbf{S}^{(3)} + \mathbf{T}^{(3)} + \mathbf{T}^{(4)} & \ddots & \\ & \ddots & \mathbf{S}^{(N-1)} + \mathbf{T}^{(N-1)} + \mathbf{T}^{(N)} & -\mathbf{T}^{(N)} \\ & & -\mathbf{T}^{(N)} & \mathbf{S}^{(N)} + \mathbf{T}^{(N)} \end{bmatrix}$$

carry-over information

Navigation Information Evolution

- **Proposition:** The carry-over information can be recursively obtained as

$$\widetilde{\mathbf{T}}^{(n)} = \mathbf{T}^{(n)} - \mathbf{T}^{(n)} \left(\mathbf{S}^{(n-1)} + \widetilde{\mathbf{T}}^{(n-1)} + \mathbf{T}^{(n)} \right)^{-1} \mathbf{T}^{(n)}$$

with $\widetilde{\mathbf{T}}^{(1)} := \mathbf{0}$

- The spatial cooperation $\mathbf{S}^{(n-1)}$ is highly-coupled inference, i.e., the agents' positions after spatial cooperation are correlated

- In *distributed* networks, each agent only obtains its own position estimate after spatial cooperation; the accuracy of each agent is characterized by its *individual* EFIM

Navigation Information Evolution

- Under the distributed condition, ignoring spatial coupling

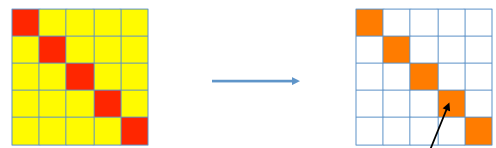

$$\mathbf{S}^{(n-1)} + \widetilde{\mathbf{T}}^{(n-1)}$$

$$\widetilde{\mathbf{S}}_k^{(n-1)} = \left\{ \left[\left(\mathbf{S}^{(n-1)} + \widetilde{\mathbf{T}}^{(n-1)} \right)^{-1} \right]_{\mathbf{x}_k^{(n-1)}} \right\}^{-1}$$

Individual EFIM after spatial coop.

- **Proposition:** The carry-over information in distributed networks can be approximated as

$$\widetilde{\mathbf{T}}^{(n)} = \mathrm{diag}\left\{ \widetilde{\mathbf{T}}_1^{(n)}, \widetilde{\mathbf{T}}_2^{(n)}, \ldots, \widetilde{\mathbf{T}}_{N_{\mathrm{a}}}^{(n)} \right\}$$

where

$$\widetilde{\mathbf{T}}_k^{(n)} = \mathbf{T}_k^{(n)} - \mathbf{T}_k^{(n)} \left(\widetilde{\mathbf{S}}_k^{(n-1)} + \mathbf{T}_k^{(n)} \right)^{-1} \mathbf{T}_k^{(n)}$$

Geometric Interpretation: Spatial

- EFIM from anchors to agent k

$$\mathbf{J}_{\mathrm{e}}^{\mathrm{A}}(\mathbf{x}_k) = \sum_{j \in \mathcal{N}_{\mathrm{b}}} \lambda_{kj} \cdot \mathbf{J}_{\mathrm{r}}(\phi_{kj})$$

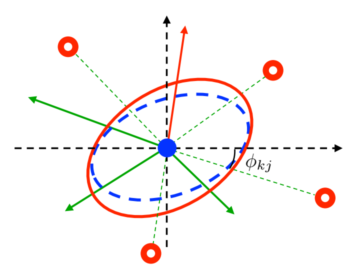

- Information ellipse $\{\mathbf{y} \in \mathbb{R}^2 : \mathbf{y}^\dagger \, \mathbf{J}_{\mathrm{e}} \, \mathbf{y} = 1\}$
- Two-agent cooperation with $\mathbf{S}_{12} = \lambda_{12} \, \mathbf{J}_{\mathrm{r}}(\phi_{12})$
  - EFIM for agent 1

$$\mathbf{J}_{\mathrm{e}}(\mathbf{x}_1) = \mathbf{J}_{\mathrm{e}}^{\mathrm{A}}(\mathbf{x}_1) + \xi_{12} \, \mathbf{S}_{12}$$

where

$$\xi_{12} = \frac{1}{1 + \lambda_{12} \, \underbrace{\mathbf{u}_{\phi_{12}}^\dagger \left[\mathbf{J}_{\mathrm{e}}^{\mathrm{A}}(\mathbf{x}_2) \right]^{-1} \mathbf{u}_{\phi_{12}}^\dagger}_{\text{projected position error}}}$$

  - Effective intensity $\xi_{12} \, \lambda_{12} \; (\xi_{12} \leq 1)$

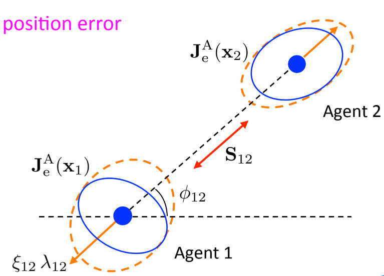

- More agents in cooperation

$$\mathbf{J}_{\mathrm{e}}(\mathbf{x}_k) \approx \mathbf{J}_{\mathrm{e}}^{\mathrm{A}}(\mathbf{x}_k) + \sum_{j \in \mathcal{N}_{\mathrm{a}} \backslash \{k\}} \xi_{kj} \, \mathbf{S}_{kj}$$

Geometric Interpretation: Temporal

- Carry-over information for individual agent

$$\begin{aligned}\widetilde{\mathbf{T}}_k^{(n)} &= \mathbf{T}_k^{(n)} - \mathbf{T}_k^{(n)}\big(\widetilde{\mathbf{S}}_k^{(n-1)} + \mathbf{T}_k^{(n)}\big)^{-1}\mathbf{T}_k^{(n)} \\ &= \Big[\big(\widetilde{\mathbf{S}}_k^{(n-1)}\big)^{-1} + \big(\mathbf{T}_k^{(n)}\big)^{-1}\Big]^{-1}\end{aligned}$$

  - "Harmonic mean" of the information from previous time and from intra-node measurement

- Effective information
  - $\widetilde{\mathbf{T}} \preceq \mathbf{T}$ with equality $\mathbf{S} \to \mathrm{diag}\{\infty, \infty\}$
  - $\widetilde{\mathbf{T}} \preceq \mathbf{S}$ with equality $\mathbf{T} \to \mathrm{diag}\{\infty, \infty\}$

- Intra-node measurement is speed $\mathbf{T} = \lambda\,\mathbf{J}_{\mathrm{r}}(\psi)$ then

$$\widetilde{\mathbf{T}} = \xi_2\,\mathbf{T}$$

$$\xi_2 = (1 + \lambda\,\mathbf{u}_\psi^\dagger\,\mathbf{S}^{-1}\,\mathbf{u}_\psi)^{-1}$$

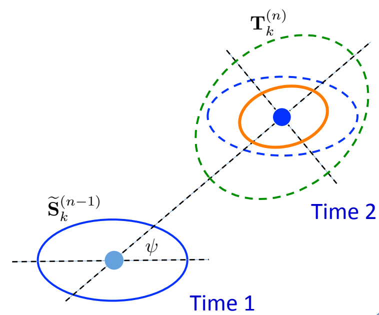

Information Evolution

- Spatial cooperation
  - Information increases in the direction connecting the agents
  - Cooperative information degrades due to position uncertainty
- Temporal cooperation
  - Combination of measurement information and previous localization information

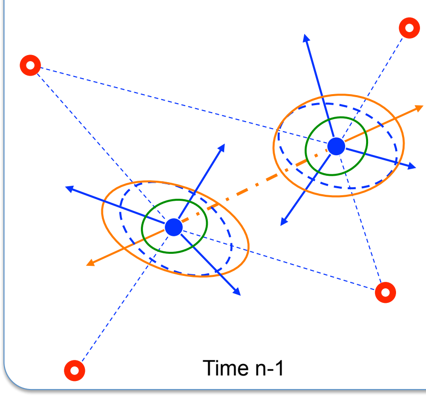

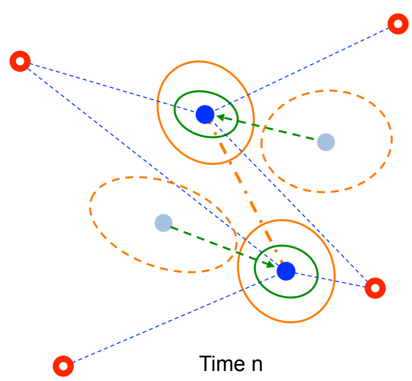

Outline

- Background
- System Model
- EFIM for Network Navigation
- Navigation Information Evolution
- Numerical Example
- Conclusion

Numerical Example

- Agents placed randomly in a 20 m by 20 m area and follow random walks
- Anchors provide a localization accuracy of 2 m^2
- Inter- and intra-node distance error variances are 0.2 m^2

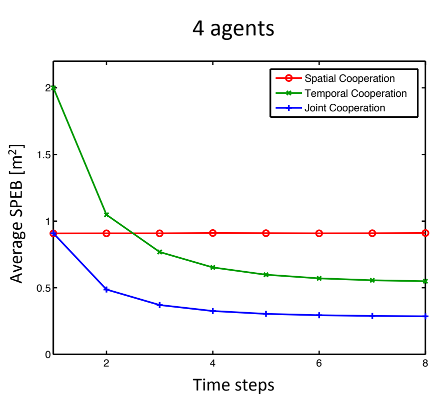

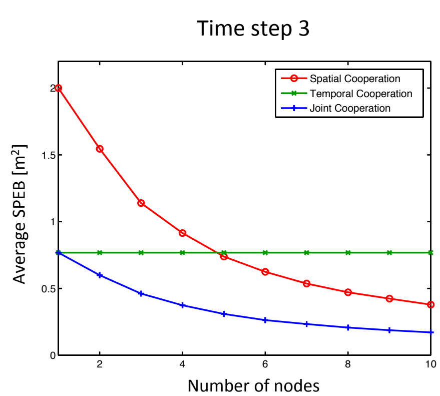

Outline

- Background
- System Model
- EFIM for Network Navigation
- Navigation Information Evolution
- Numerical Example
- Conclusion

Conclusion

- Established a framework for network navigation to determine the fundamental limits of navigation accuracy
- Derived the *navigation information* by the EFI analysis, and showed that
  - it can be decomposed as the sum of the information corresponding to spatial and temporal cooperation
  - each part can be further decomposed into basic building blocks associated with each measurement
- Introduced the notion of carry-over information, and characterized the information evolution and cooperation benefit in distributed navigation networks

References

- M. Z. Win, A. Conti, S. Mazuelas, Y. Shen, W. M. Gifford, D. Dardari, and M. Chiani, "Network localization and navigation via cooperation," *IEEE Commun. Mag.*, vol. 49, no. 5, pp. 56–62, May 2011.
- Y. Shen, S. Mazuelas, and M. Z. Win, "Network Navigation: A Theoretical Foundation," *IEEE J. Sel. Commun.*, vol. 30, no. 10, Oct. 2012.
- S. Mazuelas, Y. Shen, and M. Z. Win, "Information coupling in cooperative localization," *IEEE Commun. Lett.*, vol. 15, no. 7, pp. 737–739, Jul. 2011.

LOCATION INFERENCE AND OBSERVATION SELECTION

Location inference

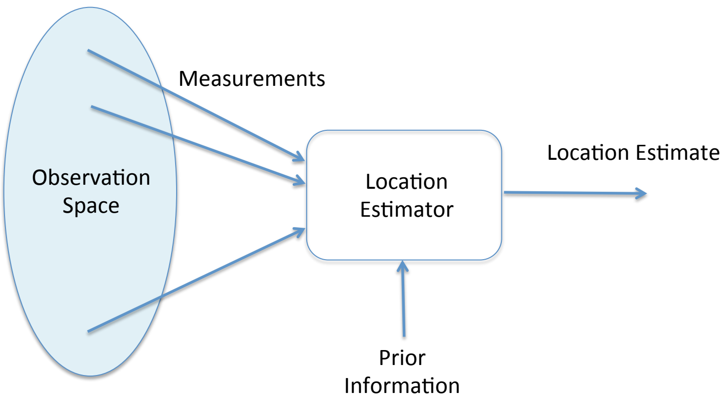

The purpose of location-aware networks is to determine the unknown positions of agents based on intra-node and inter-node measurements (e.g., IMU and RMU) and prior information (e.g., environment and mobility)

Cycle of cooperative location-aware networks

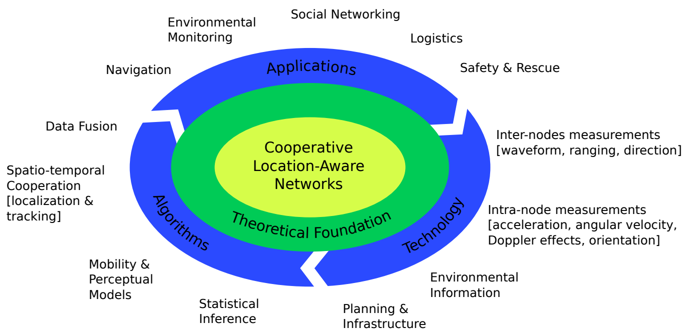

M.Z.Win et al., "Network Localization and Navigation via Cooperation," IEEE Communications Magazine, May 2011

Classification

- Anchor-based: some nodes in known position (anchors/beacons); targets/agents estimate their position through measures with anchors (direct/single-hop, indirect/multi-hop) and other agents (cooperation)

- Anchor-free: all nodes in unknown position, only relative coordinates can be obtained

Depending on the type of measurements used…

Range-based

Angle-based

Proximity-based

… and others like scene-based, optical, inertial, etc.

Classification based on technology

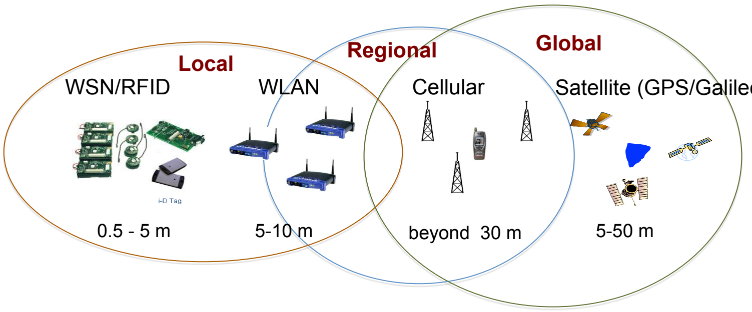

- None of the technologies can guarantee global coverage and high-accuracy
- Integration for seamless localization
- UWB-based localization (submetric localization)

Technology	Measurement technique	Accuracy	Pros	Cons
GPS	TDOA	10-20m	Earth scale coverage	Expensive infrastructure, Only outdoor
Galileo	TDOA	1-5m	Earth scale coverage	Expensive infrastructure, Only outdoor
A-GNSS	TDOA	< 5m	Country coverage	Scarce indoor accuracy
Cellular	E-OTD / OTDOA	50-500m	Country coverage	Requires synchronized base stations
Cellular	CellID	Cell size	Country coverage	Scarce accuracy
WLAN	RSS - Fingerprinting	1-5m	Indoor coverage, low cost	Data base required for fingerprinting, low accuracy
WSN (ZigBee)	RSS	1-10m	Indoor coverage, Low power consumption, low cost	low accuracy
WSN (UWB)	TOA/TDOA/AOA	0.1-1m	Indoor coverage, High accuracy	Short range (<20m), problems in NLOS conditions
RFID	Proximity	Connectivity range	Indoor coverage, low power consumption, low cost	low accuracy, one tag per location
NFR	e.m. near-field characteristics	1-5m	Indoor coverage, low cost	low frequency, large antennas
INS	Acceleration/Angular rate/Earth magnetic field	1-5% of the traveled distance/angle	Works everywhere	position/orientation drift, magnetic disturbance in indoor

UWB-based localization

- UWB technology offers the potential of achieving this high ranging accuracy through TOA measurements also in harsh environments due to its ability to resolve multipath and penetrate obstacles.

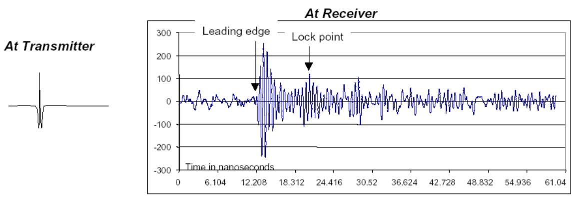

Worldwide UWB Emission Masks

Band	EIRP	Mitigation technique
China		
4.2–4.8 GHz	–41.3 dBm/MHz	DAA
6.3–8.9 GHz	–41.3 dBm/MHz	No mitigation
Europe		
3.1–4.8 GHz	–41.3 dBm/MHz	LDC or DAA
2.7–3.4 GHz	–70 dBm/MHz	No mitigation
3.4–3.8 GHz	–80 dBm/MHz	No mitigation
3.4–6 GHz	–70 dBm/MHz	No mitigation
6–8.5 GHz	–41.3 dBm/MHz	No mitigation
8.5–9 GHz	–41.3 dBm/MHz	DAA
Japan		
3.4–4.8 GHz	–41.3 dBm/MHz	DAA
4.8–7.25 GHz	–70 dBm/MHz	No mitigation
7.25–10.25 GHz	–41.3 dBm/MHz	No mitigation
Korea		
3.1–4.8 GHz	–41.3 dBm/MHz	LDC or DAA
7.25–10.25 GHz	–41.3 dBm/MHz	No mitigation
United States		
3.1–10.6 GHz	–41.3 dBm/MHz	No mitigation

- UWB with low complexity, cost and size
- Existence of standards IEEE802.15.4a and 4f: with ranging accuracy

M. Z. Win and R. A. Scholtz, "On the energy capture of ultra-wide bandwidth signals in dense multipath environments," IEEE Commun. Lett., Sep. 1998 - S. Gezici et al., "Localization via ultra-wideband radios: A look at positioning aspects for future sensor networks," IEEE Signal Process. Mag., Jul. 2005.

Ingredients for localization-awareness

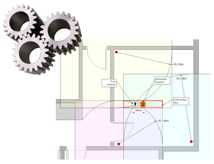

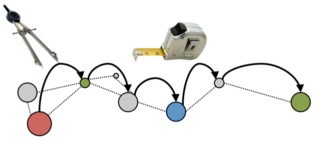

Position-Based Applications

Robust
w/o memory
Range-, angle-, proximity-based
w/o cooperation

Algorithms

Error sources
Uncertainty

RSSI, ToA, TDoA, AoA, …

Technologies

Localization requirements

Accuracy: (e.g., Root Mean Squared Error of location estimation averaged in space and time). Localization error $e(\mathbf{p}) = ||\hat{\mathbf{p}} - \mathbf{p}||$

Outage: fraction of times for which the target precision is not reached. Localization error outage (LEO) probability* $Po = \mathbb{P}\{e(\mathbf{p}) > e_{\text{th}}\}$

Refresh rate, Robustness, Coverage

The chosen technology/algorithm should satisfy all and it is environment dependent (e.g., indoor/ outdoor, office, home, open-space,…)

Design: which nodes' density is required to reach a target performance (accuracy, outage, refresh-rate) in different kinds of environments?

*The concept of LEO is driven by that of bit error outage (BEO) in communications, *A.Conti et al., "Bit error outage for diversity reception in shadowing environment," IEEE Comm. Lett., Jan. 2003*

Location estimation

- To determine the location of objects based on observations (i.e., measurements) is a “classical” estimation problem

- Several approaches for the estimation of state/parameter $\mathbf{x}$ from observation $\mathbf{z}$ affected by noise are applicable to localization

  – $\mathbf{x}$ unknown deterministic: Non-Bayesian Estimation (e.g., least square, maximum likelihood)

  – $\mathbf{x}$ unknown RV: Bayesian Estimation (e.g., minimum mean square error, maximum a posteriori)

  – Approximate Inference (e.g., based on Kullback-Leibler divergence)

Navigation and Localization algorithms

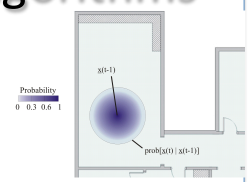

- Beliefs evolution in Bayesian inference

State vector at time *t*

Intra- & inter-node meas. From time *1* to *t-1*

Mobility model

(i) prediction: $$f(\boldsymbol{x}^{(t)}|\boldsymbol{z}^{(1:t-1)}) = \int f(\boldsymbol{x}^{(t-1)}|\boldsymbol{z}^{(1:t-1)})\, f(\boldsymbol{x}^{(t)}|\boldsymbol{x}^{(t-1)})\, d\boldsymbol{x}^{(t-1)}$$

(ii) correction: $$f(\boldsymbol{x}^{(t)}|\boldsymbol{z}^{(1:t)}) \propto f(\boldsymbol{x}^{(t)}|\boldsymbol{z}^{(1:t-1)})\, f(\boldsymbol{z}^{(t)}|\boldsymbol{x}^{(t)})$$

$$f(\boldsymbol{z}^{(t)}|\boldsymbol{x}^{(t)}) = f(\boldsymbol{z}^{(t)}_{\text{intra}}|\boldsymbol{x}^{(t)})\, f(\boldsymbol{z}^{(t)}_{\text{inter}}|\boldsymbol{x}^{(t)})$$

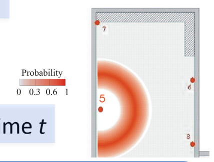

Intra- & inter-node measurement model at time *t*

The quality of range information affects the localization accuracy depending on network intrinsic properties, signal features, and signal processing techniques

Inference through Factor Graph

If $f_{\mathsf{X}|\mathsf{Z}}(\boldsymbol{x}|\boldsymbol{z})$ can be factorized and then described through factor graphs and message passing algorithms (e.g., sum-product)

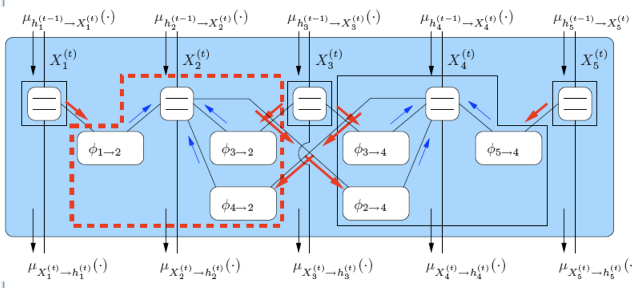

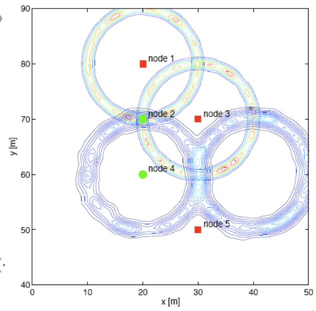

H. Wymeersch, J.Lien, M.Win, "Cooperative Localization in Wireless Networks," Proceedings of the IEEE, Feb. 2009

From theoretical limits

The performance of network localization and navigation depends mainly on two factors:

- the geometric configuration of the system, and
- the quality of the waveform and range measurements

The characterization of each possible link, by means of ranging and waveform measurements, enables the system designer to understand how to

- harness environmental knowledge,
- identify LOS and NLOS conditions,
- take advantage of cooperation, and
- choose cooperating nodes.

M.Z.Win et al., "Network Localization and Navigation via Cooperation," IEEE Communications Magazine, May 2011

Cooperation

- Cooperation is an emerging paradigm for wireless communications and location-aware networks; e.g., at the PHY layer is an efficient method to improve the performance and extend the coverage

- The connectivity and cooperation diversity achieved depend on channel conditions in each link

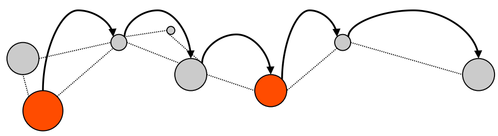

For the design of cooperative wireless networks carefully characterize the wireless channels associated with all links.

Cooperation in localization

- To extend coverage of the localization system (through multi-hop)

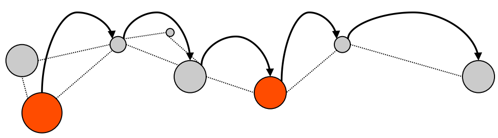

- To increase the number of visible anchors (e.g., an agent can be virtual anchor for another → iterative approach)

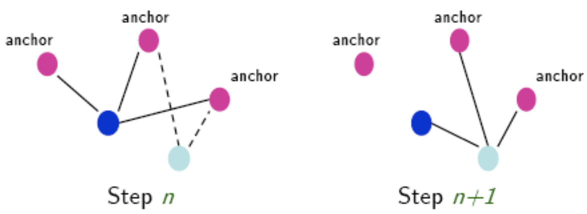

Harnessing environmental information

• The ranging error degrades the performance of localization.

• When a priori information of the environment topology is available, we can harness such information to refine ranging and position estimates.

• Three-step procedure, regardless of the particular range-based localization algorithm used:

(i) Initial position estimate

(ii) Range error mitigation

(iii) Position refinement

When no a priori information on the environment topology is available, such condition can be determined by analyzing the received waveform

Choice of features for NLOS detection

• Features are extracted from the received waveform *v(t)* observed within the interval *T* under a particular channel condition. Examples are

• Temporal dispersion (RMS delay spread) (*higher for NLOS*)

$$\tau_{\text{rms}} = \left[\frac{\int_T (t-\tau_{\text{m}})^2 \, |v(t)|^2 \, dt}{\int_T |v(t)|^2 \, dt} \right]^{1/2}$$

mean excess delay

$$\tau_{\text{m}} = \frac{\int_T t \, |v(t)|^2 \, dt}{\int_T |v(t)|^2 \, dt}$$

$$\text{Decide}: \begin{cases} \text{LOS} & \text{if } \tau_{\text{rms}} < \lambda_\tau \\ \text{NLOS} & \text{if } \tau_{\text{rms}} > \lambda_\tau \end{cases}$$

• Kurtosis (*higher for LOS*)

$$\mathcal{K} = \frac{1}{\sigma_{|v|}^4 T} \int_T (|v(t)| - \mu_{|v|})^4 \, dt$$

$$\text{Decide}: \begin{cases} \text{NLOS} & \text{if } \mathcal{K} < \lambda_{\mathcal{K}} \\ \text{LOS} & \text{if } \mathcal{K} > \lambda_{\mathcal{K}} \end{cases}$$

Selection of Representative Observations

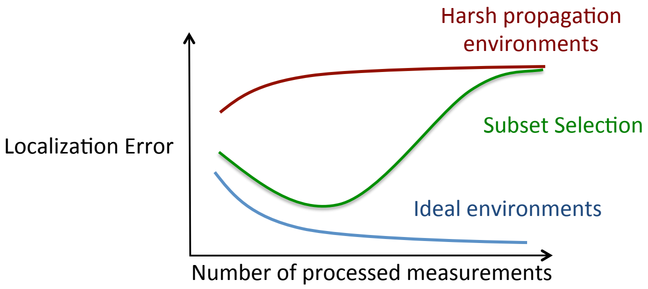

S. Bartoletti et al., "Blind Selection of Representative Observations for Sensor Radar Networks," IEEE Trans. On Vevhicular Technol., Apr. 2015

Observations Selection in a Sensor Radar Network Scenario

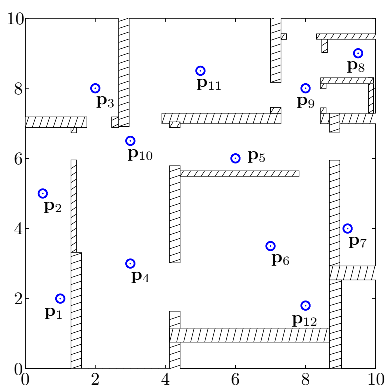

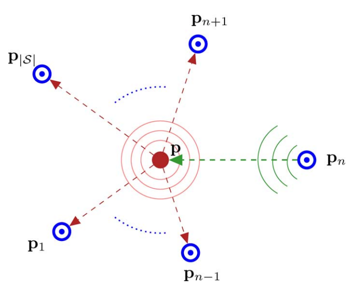

Scenario including: clutter, multipath, excess delay, obstruction loss and excess delay

Localization with Observation Selection: the idea

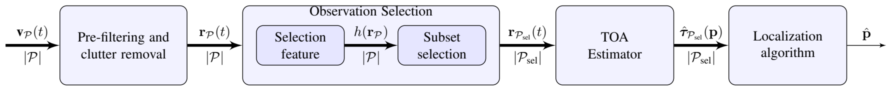

Samples characterization for energy detection based ranging

$$r_{ij}(t) = \sum_{p=0}^{N_{\text{p}}-1} \sum_{l=0}^{L_{\text{p}}-1} \alpha_{ij}^{(l)} s\left(t - pT_{\text{g}} - \tau_{ij}^{(l)}\right) + n_{ij}(t)$$

$$\epsilon_{ij}^{(p,q)} = \int_{qT_{\text{dwell}}+pT_{\text{g}}}^{(q+1)T_{\text{dwell}}+pT_{\text{g}}} r_{ij}^2(t)\, dt$$

$$\boxed{\bar{\epsilon}_{ij}^{(q)} = \frac{1}{N_{\text{p}}} \sum_{p=0}^{N_{\text{p}}-1} \epsilon_{ij}^{(p,q)}}$$

$$f_{ij}(q) = \frac{\bar{\epsilon}_{ij}^{(q)}}{\sum_{k=0}^{N_{\text{b}}-1} \bar{\epsilon}_{ij}^{(k)}}$$ PMF

$$F_{ij}(x) = \sum_{q \le x} f_{ij}(q)$$ CDF

$$\bar{\mu}_{ij} = \sum_{q=0}^{N_{\text{b}}-1} q f_{ij}(q)$$ *1*-st moment

$$\mu_{ij}^{(n)} = \sum_{q=0}^{N_{\text{b}}-1} (q - \bar{\mu}_{ij})^n f_{ij}(q)$$ *n*-th central moment

Localization with Observation Selection: signal features

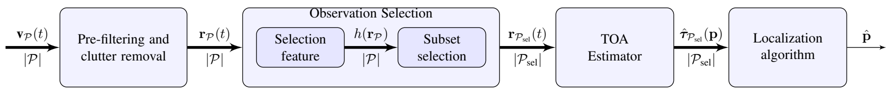

Temporal dispersion features

$$\sigma_{ij}^2 = \mu_{ij}^{(2)}$$ variance

$$\mathsf{IQR}_{ij} = F_{ij}^{-1}(0.75) - F_{ij}^{-1}(0.25)$$ interquartile range

$$\kappa_{ij} = \frac{\mu_{ij}^{(4)}}{\left(\mu_{ij}^{(2)}\right)^2}$$ kurtosis

$$\chi_{ij} = \frac{\mu_{ij}^{(3)}}{\left(\sqrt{\mu_{ij}^{(2)}}\right)^3}.$$ skewness

Amplitude dispersion features

$$\mathsf{M}_{ij} = \max_q \bar{\epsilon}_{ij}^{(q)}$$ maximum value

sample variance

$$\mathsf{s}_{ij}^2 = \frac{1}{N_{\text{b}}} \sum_{q=0}^{N_{\text{b}}-1} \left[\bar{\epsilon}_{ij}^{(q)} - \left(\frac{1}{N_{\text{b}}} \sum_{k=0}^{N_{\text{b}}-1} \bar{\epsilon}_{ij}^{(k)}\right)\right]^2$$

$$\mathsf{r}_{ij} = \left|\max_q \bar{\epsilon}_{ij}^{(q)} - \min_q \bar{\epsilon}_{ij}^{(q)}\right|$$ sample range

sample skewness

$$\mathsf{c}_{ij} = \frac{\sum_{q=0}^{N_{\text{b}}-1} \left[\bar{\epsilon}_{ij}^{(q)} - \frac{1}{N_{\text{b}}} \left(\sum_{k=0}^{N_{\text{b}}-1} \bar{\epsilon}_{ij}^{(q)}\right)\right]^3}{N_{\text{b}} \left(\mathsf{s}_{ij}^2\right)^{\frac{3}{2}}}.$$

Localization Error Outage

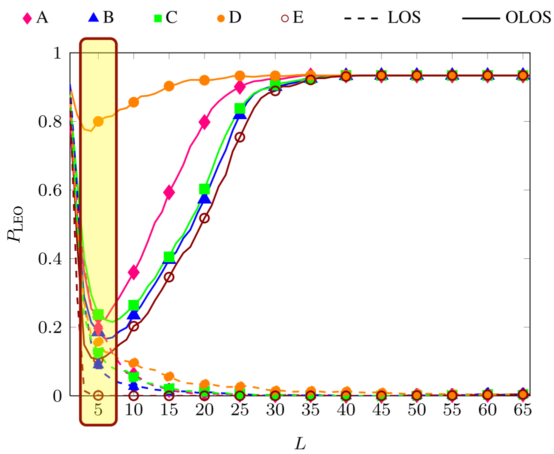

Fig. 9. LEO as a function of $L = 1, 2, ..., N_{\text{obs}}$ for $e_{\text{th}} = 1$ m, with (solid) and without (dashed) walls, for the cases (A) $h(\overline{\epsilon}_{ij}) = \sigma^2_{ij}$, (B) $h(\overline{\epsilon}_{ij}) = \kappa_{ij}$, and (C) $h(\overline{\epsilon}_{ij}) = \mathsf{M}_{ij}$. The case (D) represents the random choice of L observations. The case (E) refers to the non-blind case $h(\overline{\epsilon}_{ij}) = \mathsf{e}_{ij}$.

Localization Error Outage

$L = 5$

Without walls

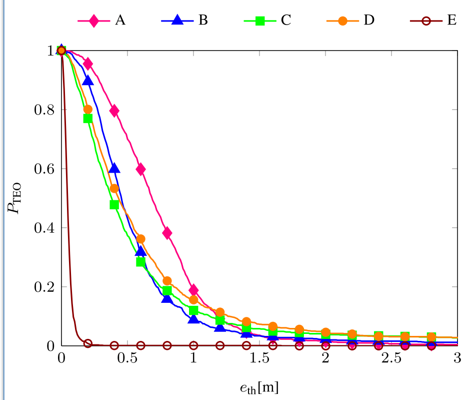

With walls

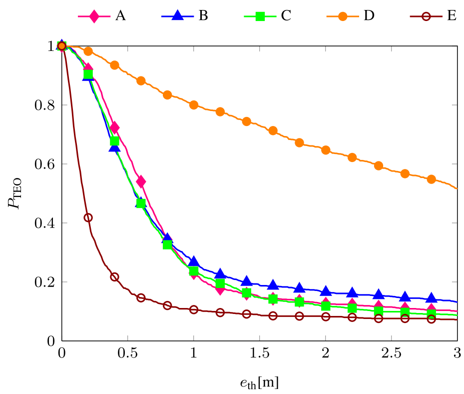

D: random choice of L observations

E: non-blind case

NETWORK MESSAGE-PASSING ALGORITHMS

Two Non-Trivial Cases

- One mobile agent

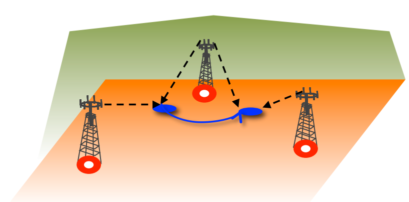

- Multiple static agents

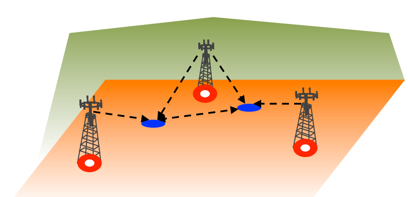

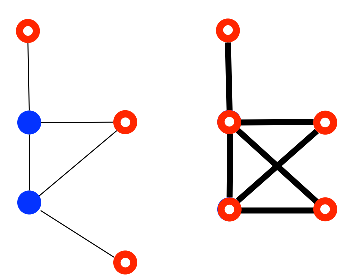

Multiple Static Agents

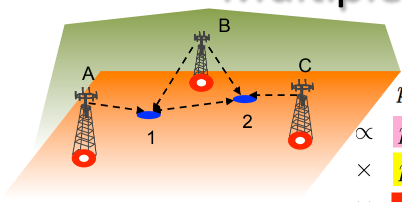

$$
\begin{aligned}
&p(x_1,x_2,x_A,x_B,x_C|z_{A,1},z_{B,1},z_{B,2},z_{C,2},z_{1,2},z_{2,1})\\
\propto\ &p(x_1)p(x_2)\delta(x_A-x_A^*)\delta(x_B-x_B^*)\delta(x_C-x_C^*)\\
\times\ &p(z_{A,1}|x_1,x_A)p(z_{B,1}|x_1,x_B)p(z_{B,2}|x_2,x_B)\\
\times\ &p(z_{1,2}|x_1,x_2)p(z_{2,1}|x_1,x_2)p(z_{C,2}|x_2,x_C)
\end{aligned}
$$

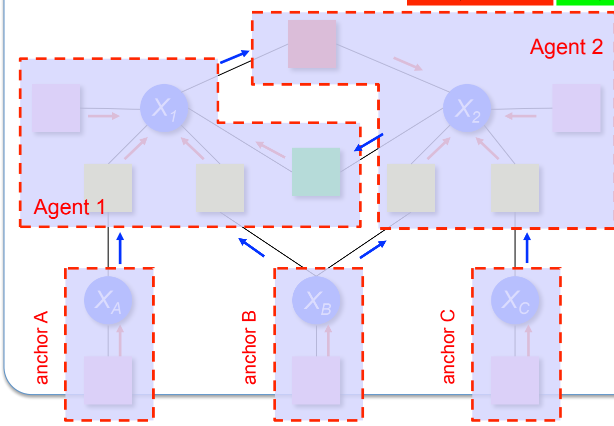

Net-Factor Graph

Net-Message Passing

Cooperative Localization Process

- Cooperative localization
  - 3 anchors
  - 2 agents
- Cooperation between
  - Pairs of anchors and single agents
  - Two agents

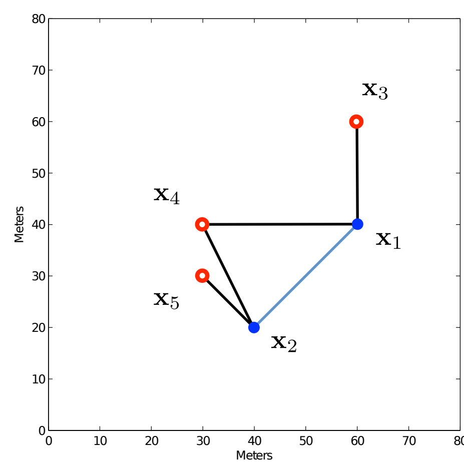

Cooperative Localization Process

- Cooperative localization
  - Agent 1 and Anchors 3, 4
- Ranging between Agt 1 and Anc 3
  - Likelihood $f(\widehat{d}_{13}|\mathbf{x}_1)$
- Ranging between Agt 1 and Anc 4
  - Likelihood $f(\widehat{d}_{14}|\mathbf{x}_1)$
- Location belief of Agt 1

$$b^{(1)}(\mathbf{x}_1) = f(\mathbf{x}_1|\widehat{d}_{13}, \widehat{d}_{14})$$
$$\propto f(\mathbf{x}_1|\widehat{d}_{13}) \times f(\mathbf{x}_2|\widehat{d}_{14})$$

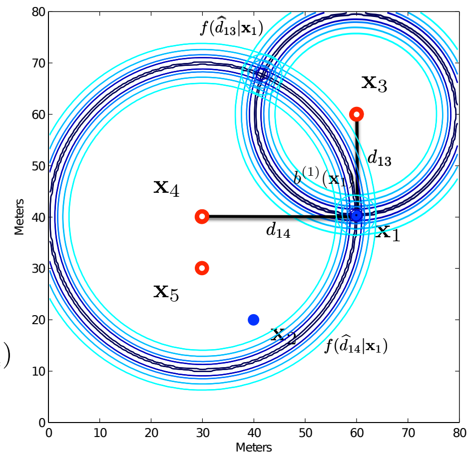

Cooperative Localization Process

- Cooperative localization
  - Agent 2 and Anchors 4, 5
- Ranging between Agt 2 and Anc 4
  - Likelihood $f(\widehat{d}_{24}|\mathbf{x}_2)$
- Ranging between Agt 2 and Anc 5
  - Likelihood $f(\widehat{d}_{25}|\mathbf{x}_2)$
- Location belief of Agt 2

$$b^{(1)}(\mathbf{x}_2) = f(\mathbf{x}_2|\widehat{d}_{24}, \widehat{d}_{25})$$
$$\propto f(\mathbf{x}_2|\widehat{d}_{24}) \times f(\mathbf{x}_2|\widehat{d}_{25})$$

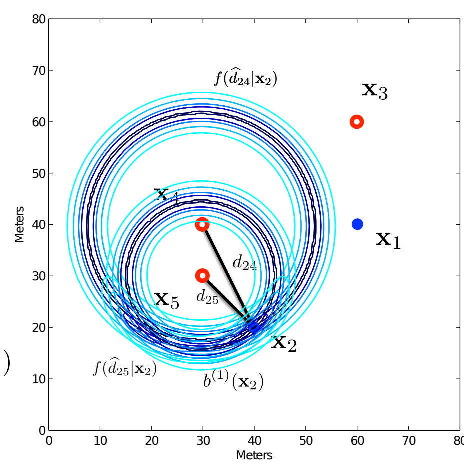

Cooperative Localization Process

- Cooperative localization
  - Agent 1 and Agent 2
- Ranging between Agt 1 and Agt 2
  - Likelihood: $f(\widehat{d}_{21}|\mathbf{x}_1,\mathbf{x}_2)$
- Information from Agt 1 to Agt 2

$$\int f(\widehat{d}_{21}|\mathbf{x}_1,\mathbf{x}_2)b^{(1)}(\mathbf{x}_1)\mathrm{d}\mathbf{x}_1$$

- Location belief of Agt 2
  - Previous: $b^{(1)}(\mathbf{x}_2)$
  - Updated: $b^{(2)}(\mathbf{x}_2)$

$$b^{(1)}(\mathbf{x}_2)\int f(\widehat{d}_{21}|\mathbf{x}_1,\mathbf{x}_2)b^{(1)}(\mathbf{x}_1)d\mathbf{x}_1$$

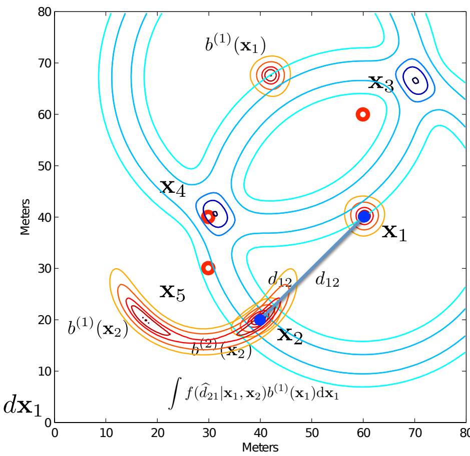

Cooperative Localization Process

- Cooperative localization
  - Agent 1 and Agent 2
- Ranging between Agt 1 and Agt 2
  - Likelihood: $f(\widehat{d}_{12}|\mathbf{x}_1,\mathbf{x}_2)$
- Information from Agt 2 to Agt 1

$$\int f(\widehat{d}_{12}|\mathbf{x}_1,\mathbf{x}_2)b^{(1)}(\mathbf{x}_2)\mathrm{d}\mathbf{x}_2$$

- Location belief of Agt 2
  - Previous: $b^{(1)}(\mathbf{x}_1)$
  - Updated: $b^{(2)}(\mathbf{x}_1)$

$$b^{(1)}(\mathbf{x}_1)\int f(\widehat{d}_{12}|\mathbf{x}_1,\mathbf{x}_2)b^{(1)}(\mathbf{x}_2)\mathrm{d}\mathbf{x}_2$$

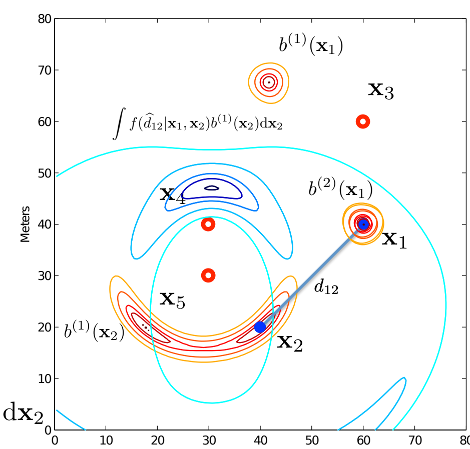

Algorithm Design

- Developed concept of Space-Time Network Factor Graph

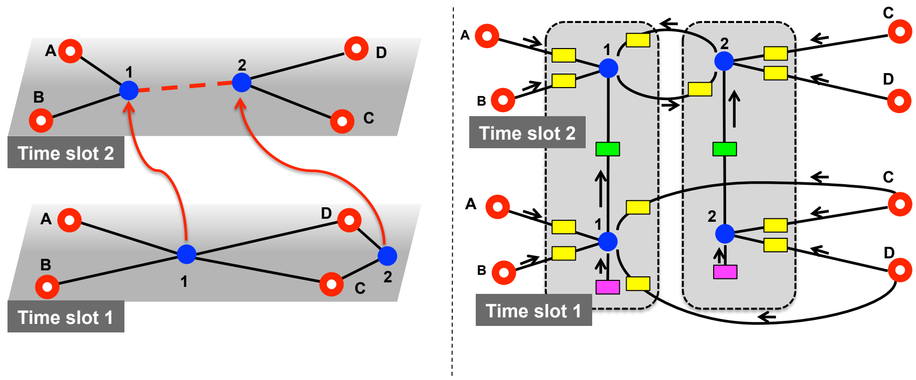

- Underlying frameworks: Bayesian Inference, graphical models, statistics, machine learning

Case Study: Advantages of Our Approach

- Indoor environment, covers 100m x 100m area, 13 anchors, 100 agents
- Nodes can communicate within 20m range, using UWB peer-to-peer transmission (experiment at MIT)
- Underlying frameworks: Bayesian Inference, graphical models, statistics, machine learning

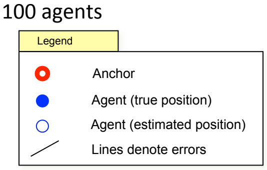

Non-cooperative

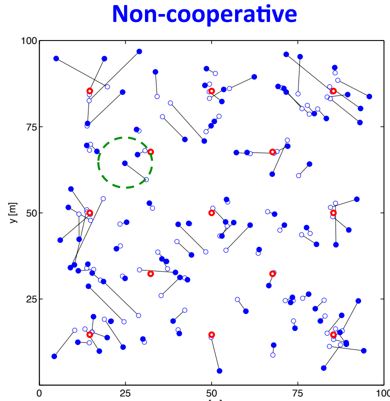

Cooperative

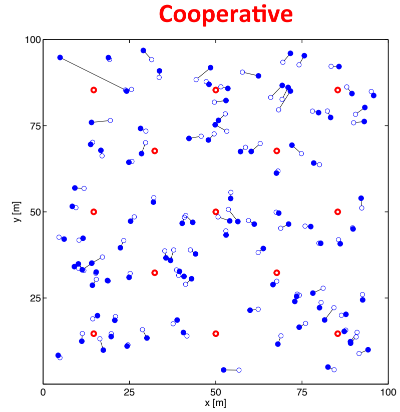

Iteration Advantage

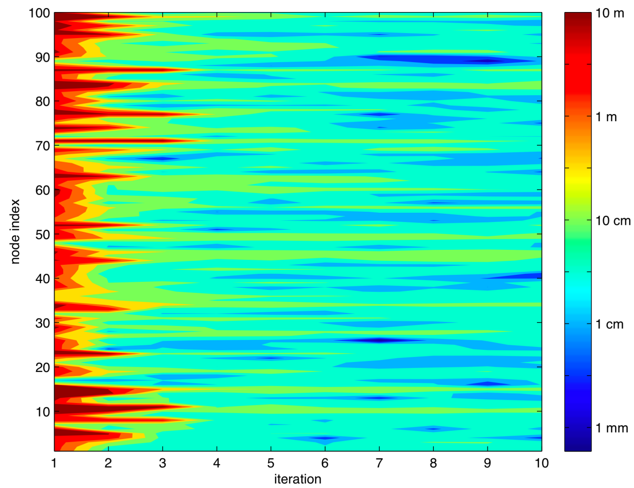

References

- H. Wymeersch, J. Lien, and M. Z. Win, "Cooperative localization in wireless networks," *Proc. IEEE*, vol. 97, no. 2, pp. 427–450, Feb. 2009.
- M. Z. Win, A. Conti, S. Mazuelas, Y. Shen, W. M. Gifford, and D. Dardari, "Network localization and navigation via cooperation," *IEEE Commun. Mag.*, vol. 49, no. 5, pp. 56–62, May 2011.

WIDEBAND RANGING

Distance estimation (ranging)

- Ranging is the technique employed by two nodes in the network to determine the physical distance between them.
- Ranging techniques significantly affect localization accuracy and system complexity.

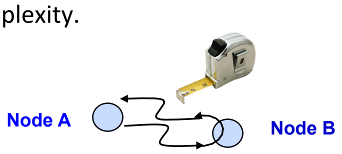

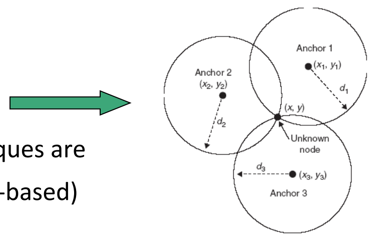

- Two most widely used ranging techniques are
  - Received Signal Strength-based (RSS-based)
  - Time-based (with variants)

- Possibility of heterogeneous techniques depending on complexity

D.Dardari, A.Conti, U.Ferner, A.Giorgetti, M.Z.Win, "Ranging with Ultrawide Bandwidth Signals in Multipath Environments," Proceedings of the IEEE, Feb. 2009

RSS-based Ranging

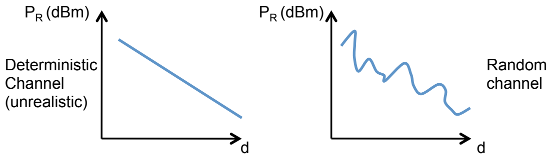

- Theoretical and empirical models are used to translate the difference between the transmitted signal strength and the RSS into a range estimate.
- Propagation effects (refraction, reflection, shadowing, and multipath) cause the attenuation to poorly correlate with distance

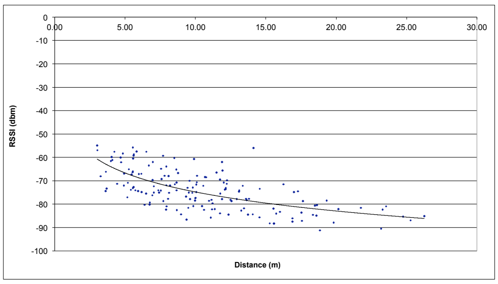

Inaccurate distance estimates

Time synch between nodes is not required

Time-based ranging measurements

- Time-of-flight $\tau_f = d/c$ (e.g., *1 ns* corresponds to *30 cm*)

Accomplished by using (TOA/TDOA stand for time/time difference-of-arrival):

One-way TOA	Two-way TOA	TDOA many-1	TDOA 1-many
(perfect synch req.)		(e.g., GPS)	

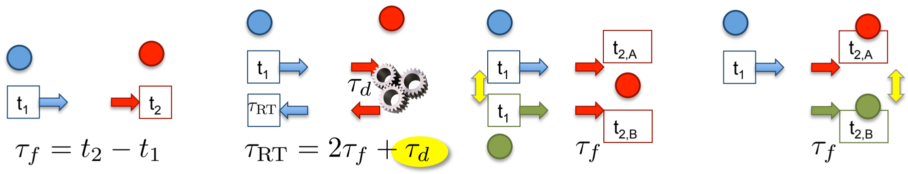

Time-based ranging

- Distance between two nodes is estimated from measurements on propagation delay of e.m. waves (light speed $c \simeq 3 \cdot 10^8$ m/s)
- Applicable if nodes can measure the time between events → TOA/TDOA

Time-of-flight $\tau_f = d/c$

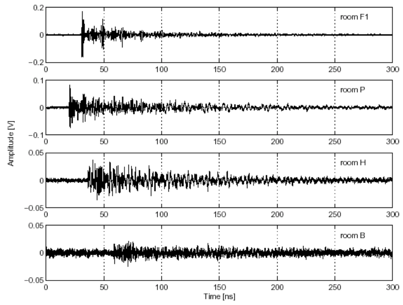

Error sources

- Clock drift (within node)
- Propagation: multipath, clutter, excess delay, blockage, LOS/NLOS
- Interference: narrowband interference (NBI), wideband interference (WBI), multi-user interference (MUI)

Multipath propagation and excess delay

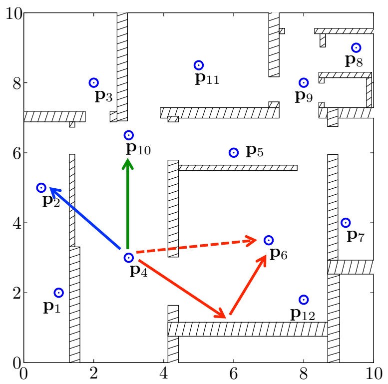

direct path (DP), LOS
DP excess delay, non-DP, NLOS
DP blockage, non-DP, NLOS

Narrowband systems are often unable to resolve paths in cluttered environments.

Wideband systems can resolve paths, but if they are dense it is hard to detect DP.

TOA Estimation in Multipath

$$\sqrt{E_p}p(t) \rightarrow r(t) = \sqrt{E_p}\sum_{l=1}^{L}\alpha_l p(t-\tau_l) + n(t)$$

It may be difficult to recognize the first path, especially at low and medium SNRs

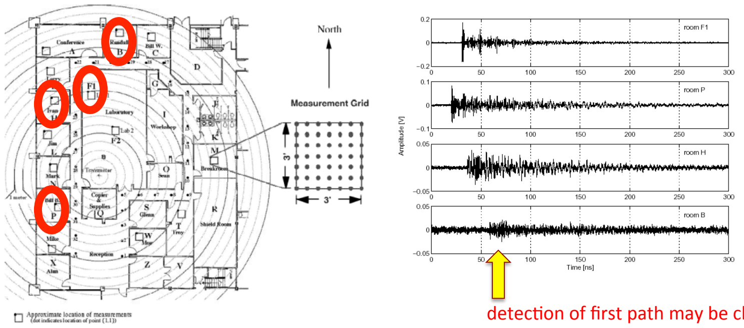

detection of first path may be challenging

M.Win, R.Scholtz, "Characterization of Ultra-Wide Bandwidth Wireless Indoor Channels: A Communication-Theoretic View", IEEE JSAC, Dec.2002

CRB and ZZB for ML TOA Estimator in multipath

Log-likelihood function $\mathcal{L}(\mathcal{V}) = -\frac{1}{N_0}\int_0^{T_{ob}}\left|r(t) - \sqrt{E_p}\sum_{l=1}^{L}\alpha_l p(t-\tau_l)\right|^2 dt$

$$E_1 \triangleq \int_0^{T_{ob}} p(t)\,p^{(1)}(t)\,dt$$

$$\boxed{\mathrm{CRB} = \frac{N_0}{8\pi^2 E_p \alpha_1^2(\beta^2 - E_1^2/E_p)}}$$

$$d_{k,i}^2(z) = \frac{1}{E_p}\int_{T_{ob}}\left[s^{(k)}(t|\tau) - s^{(i)}(t|\tau+z)\right]^2 dt$$

$$P_{\min}(z) \simeq \frac{1}{N_{ch}}\sum_{k=1}^{N_{ch}} Q\left(\sqrt{\frac{\mathrm{SNR}}{2}d_{k,i^*}^2(z)}\right)$$

$$\boxed{\mathrm{ZZB} = \frac{1}{T_a}\int_0^{T_a} z\,(T_a - z)\,P_{\min}(z)\,dz}$$

Ziv-Zakai bound

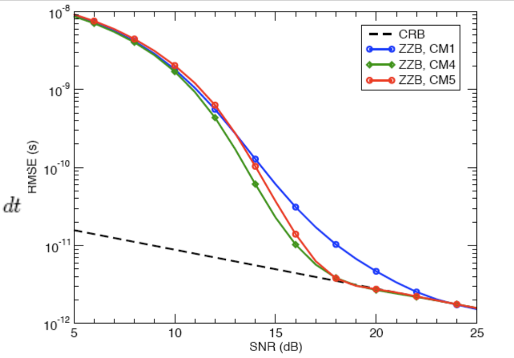

Fig. 5. ZZB as a function of SNR for the IEEE 802.15.4a channel models. Also shown is the CRB in AWGN channel for band-pass pulse with RRC envelope, $f_0 = 4$ GHz, $\nu = 0.6$, $\tau_p = 0.8$ ns and $T_a = 100$ ns.

D.Dardari et al., "Ranging with Ultrawide Bandwidth Signals in Multipath Environments," Proceedings of the IEEE, Feb. 2009

ML TOA estimation

- Classical non-linear parameter estimation problem
- Maximum likelohood (ML) TOA estimator (matched filter and maximum search)
- It requires sampling at Nyquist rate

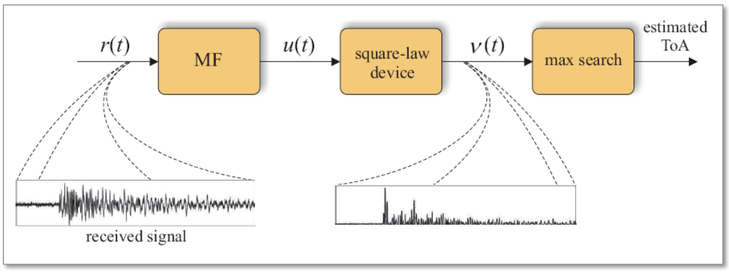

Energy detection-based TOA Estimators

- Low complexity (sub-Nyquist sampling rate, non-coherent)
- TOA resolution is bounded by the ED integration time

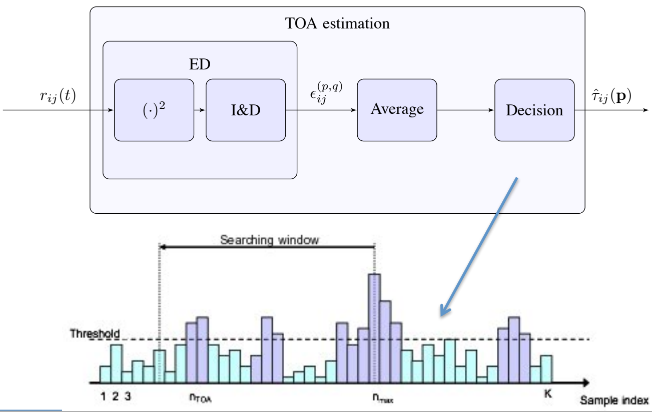

ED TOA Estimators: 1st path detection

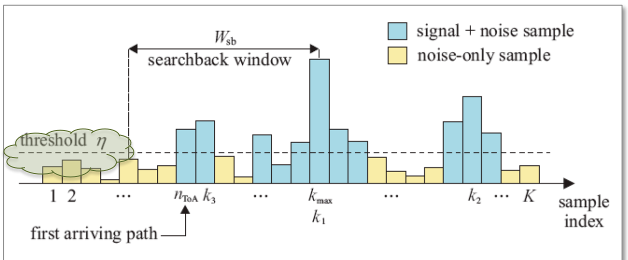

Fig. 9. Illustration of the Max, P-Max, simple thresholding, JBSF, SBS and SBSMC algorithms.

Maximum Bin Search

Threshold Crossing Search

Jump Back and Search Forward

Serial Backward Search

D.Dardari, C.-C.Chong, M.Win, "Analysis of threshold based ToA estimators in UWB channels", EUSIPCO2006

I.Guvenc, Z.Sahinoglu, "Threshold-based TOA estimation for impulse radio UWB systems", ICUWB2005

S.Gezici, Z.Tian, G.B.Giannakis, H.Kobayashi, A.F.Molisch, H.V.Poor, Z.Sahinoglu, "Localization via ultra-wideband radios: a look at positioning aspects for future sensor networks", IEEE Signal Proc. Mag., Jul. 2005

D.Dardari, A.Conti, U.Ferner, A.Giorgetti, M.Z.Win, "Ranging with Ultrawide Bandwidth Signals in Multipath Environments," Proceedings of the IEEE, Feb. 2009

Soft-decision and hard-decision ranging based on energy detection

$\boldsymbol{\theta} = [\tau \ \boldsymbol{\theta}_{\mathrm{h}} \ \boxed{\boldsymbol{\theta}_{\mathrm{d}}}]$ true TOA, wireless channel, energy detector parameters

$h(t;\varsigma) = \sum_{l=1}^{L(t)} \alpha_l(t)\,\delta(\varsigma - \tau_l(t))$ wideband CIR

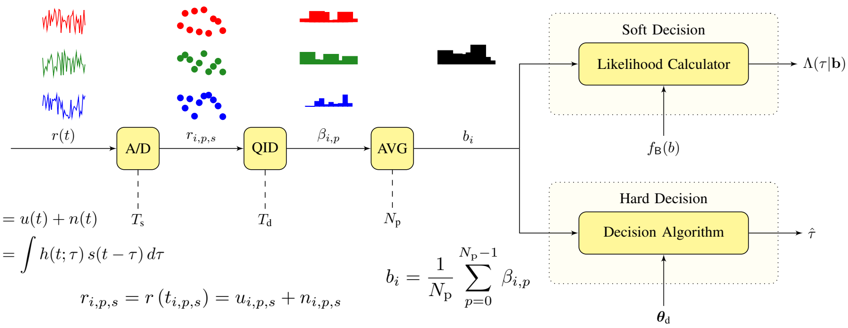

$r(t) = u(t) + n(t)$

$u(t) = \int h(t;\tau)\, s(t-\tau)\, d\tau$

$b_i = \frac{1}{N_{\mathrm{p}}} \sum_{p=0}^{N_{\mathrm{p}}-1} \beta_{i,p}$

$r_{i,p,s} = r\left(t_{i,p,s}\right) = u_{i,p,s} + n_{i,p,s}$

$$\beta_{i,p} = \sum_{s=0}^{N_{\mathrm{sb}}-1} r^2\left(t_{i,p,s}\right) = \sum_{s=0}^{N_{\mathrm{sb}}-1} \left(u_{i,p,s} + n_{i,p,s}\right)^2$$

S. Bartoletti et al., "A Mathematical Model for Wideban Ranging," IEEE J. of Select. Topics in Signal Proc., Mar. 2015

Energy samples

- Typically, ranging is based on hard-decision which provides the TOA estimate from the energy bins
- If the distribution function of energy bins is known, then a soft-decision ranging can be conceived providing a posterior probability function of the TOA estimates
- Models for both hard-decision and soft-decision ranging depend on the analysis of the energy samples distribution

$$\mathsf{B}_i \frac{N_\mathrm{p}}{\sigma^2} \overset{|\boldsymbol{\theta}}{\sim} \chi^2_{N_\mathrm{p} N_\mathrm{sb}}(\lambda_i)$$

$$f_{\mathsf{B}_i}(b|\boldsymbol{\theta}) = \frac{N_\mathrm{p}}{2\sigma^2} e^{-\frac{bN_\mathrm{p}+\lambda_i\sigma^2}{2\sigma^2}} \left(\frac{bN_\mathrm{p}}{\lambda_i \sigma^2}\right)^{\frac{N_\mathrm{p}N_\mathrm{sb}-2}{4}} I_{\frac{N_\mathrm{p}N_\mathrm{sb}-2}{2}}\left(\sqrt{\frac{\lambda_i b N_\mathrm{p}}{\sigma^2}}\right)$$

$$\lambda_i = \sum_{p=0}^{N_\mathrm{p}-1} \sum_{s=0}^{N_\mathrm{sb}-1} \frac{u^2_{i,p,s}}{\sigma^2}$$

$$F_{\mathsf{B}_i}(b|\boldsymbol{\theta}) = e^{-\frac{\lambda_i}{2}} \sum_{r=0}^{+\infty} \frac{(\lambda_i/2)^r}{r!} \frac{\gamma\left(\frac{N_\mathrm{p}N_\mathrm{sb}}{2}+r, \frac{bN_\mathrm{p}}{2\sigma^2}\right)}{\Gamma\left(\frac{N_\mathrm{p}N_\mathrm{sb}}{2}+r\right)}$$

Range Likelihood

- The RL is obtained from the observations of the bins and their distribution as

$$\Lambda(\varsigma|\mathbf{b}) = \prod_{i=0}^{N_\mathrm{b}-1} f_{\mathsf{B}_i}(b_i|\varsigma, \boldsymbol{\theta}_\mathrm{h}, \boldsymbol{\theta}_\mathrm{d})$$

- It can be directly used for localization (localization based on soft-decision ranging)

Range Estimate

- E.g., detection of the first arrival path → selection of the first bin index containing a portion of the signal

$$\hat{\imath} \in \mathcal{B} = \{0, 1, \dots, N_{\mathrm{b}} - 1\}$$

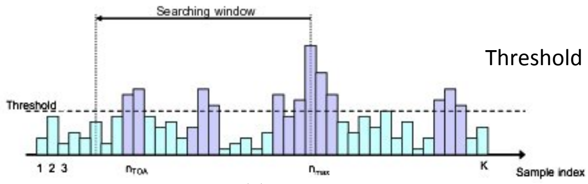

Threshold $\{\xi_i\}$

$$\hat{\tau} = g(\hat{\imath})$$

$$g(\hat{\imath}) = \hat{\imath}\, T_{\mathrm{d}} + T_{\mathrm{d}}/2$$

- Popular hard-decision algorithms: TCS, MBS, JBSF, SBS
- Localization based on hard-decision ranging

Threshold crossing event & PMF of selected bin

- HD algorithms involve comparison of bins with thresholds
- Threshold crossing event

$$\mathcal{C}_{\mathrm{th}} = \{\exists i \in \mathcal{B} : \mathsf{B}_i > \xi_i\}$$

$$\mathbb{P}\{\mathcal{C}_{\mathrm{th}} | \boldsymbol{\theta}\} = 1 - \prod_{n \in \mathcal{B}} F_{\mathsf{B}_n}(\xi_n | \boldsymbol{\theta})$$

- PMF of the selected bin

$$f_{\mathsf{I}}(i|\boldsymbol{\theta}) = \mathbb{P}\{\mathcal{S}_i \cap \mathcal{C}_{\mathrm{th}} | \boldsymbol{\theta}\} / \mathbb{P}\{\mathcal{C}_{\mathrm{th}} | \boldsymbol{\theta}\}$$

$$\mathcal{S}_i \cap \mathcal{C}_{\mathrm{th}} | \boldsymbol{\theta} = \{i \text{ is selected}, \, \mathcal{C}_{\mathrm{th}} | \boldsymbol{\theta}\}$$

Threshold crossing search

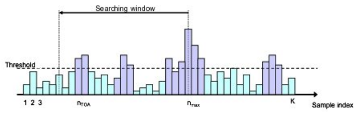

$$\mathcal{I}_W(m) = \mathcal{B} \cap \{m-W, m-W+1, \ldots, m-1\}$$
$$\mathcal{I}_W^{\mathrm{c}}(m) = \mathcal{B} \backslash \mathcal{I}_W(m)$$

$$\hat{\imath} \overset{|\mathcal{C}_{\mathrm{th}}}{=} \min\{i \in \mathcal{B} | b_i > \xi_i\}$$

$$\mathcal{S}_i \cap \mathcal{C}_{\mathrm{th}} | \boldsymbol{\theta} = \{\mathsf{B}_j \leq \xi_j \, \forall j \in \mathcal{I}_i(i), \mathsf{B}_i > \xi_i | \boldsymbol{\theta}\}$$

$$f_{\mathsf{I}}(i|\boldsymbol{\theta}) = \left[1 - F_{\mathsf{B}_i}(\xi_i|\boldsymbol{\theta})\right] \prod_{j \in \mathcal{I}_i(i)} F_{\mathsf{B}_j}(\xi_j|\boldsymbol{\theta}) \left[1 - \prod_{n \in \mathcal{B}} F_{\mathsf{B}_n}(\xi_n|\boldsymbol{\theta})\right]^{-1}$$

$\mathcal{B} = \{0, 1, \ldots, 7\}$ $\quad$ $\boldsymbol{\xi} = [1.3, 1.1, 0.9, 2.5, 1.4, 2.9, 1.9, 1.4]$

$\mathbf{b} = [0.8, 1.2, 1.3, 2.3, 2.5, 2.8, 2.4, 1.2]$

Maximum bin search

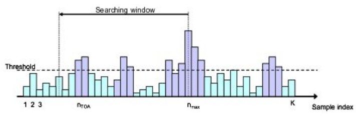

$$\mathcal{I}_W(m) = \mathcal{B} \cap \{m-W, m-W+1, \ldots, m-1\}$$
$$\mathcal{I}_W^{\mathrm{c}}(m) = \mathcal{B} \backslash \mathcal{I}_W(m)$$

$$\hat{\imath} \overset{|\mathcal{C}_{\mathrm{th}}}{=} \operatorname*{argmax}_{i \in \mathcal{B}} b_i$$

$$\begin{aligned}\mathcal{S}_i \cap \mathcal{C}_{\mathrm{th}} | \boldsymbol{\theta} = {} & \{\mathsf{B}_j \leq \mathsf{B}_i \forall j \in \mathcal{B} \backslash \{i\} | \boldsymbol{\theta}\} \\ & \backslash \{\mathsf{B}_j \leq \xi_j \forall j \in \mathcal{B}, \mathsf{B}_j \leq \mathsf{B}_i \forall j \in \mathcal{B} \backslash \{i\} | \boldsymbol{\theta}\}\end{aligned}$$

$$f_{\mathsf{I}}(i|\boldsymbol{\theta}) = \Big[\int_0^{+\infty} \prod_{j \in \mathcal{B} \backslash \{i\}} F_{\mathsf{B}_j}(b|\boldsymbol{\theta}) \, f_{\mathsf{B}_i}(b|\boldsymbol{\theta}) \, db - \int_0^{\xi_i} \prod_{j \in \mathcal{B} \backslash \{i\}} F_{\mathsf{B}_j}(\check{\xi}_j(b)|\boldsymbol{\theta}) \, f_{\mathsf{B}_i}(b|\boldsymbol{\theta}) \, db\Big] \Big[1 - \prod_{n \in \mathcal{B}} F_{\mathsf{B}_n}(\xi_n|\boldsymbol{\theta})\Big]^{-1}$$

$\mathcal{B} = \{0, 1, \ldots, 7\}$ $\quad$ $\boldsymbol{\xi} = [1.3, 1.1, 0.9, 2.5, 1.4, 2.9, 1.9, 1.4]$

$\mathbf{b} = [0.8, 1.2, 1.3, 2.3, 2.5, 2.8, 2.4, 1.2]$

Jump back search forward (W)

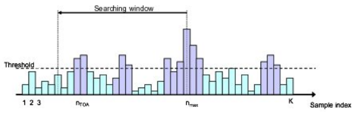

$$\mathcal{I}_W(m) = \mathcal{B} \cap \{m-W, m-W+1, \ldots, m-1\}$$
$$\mathcal{I}_W^{\mathrm{c}}(m) = \mathcal{B} \backslash \mathcal{I}_W(m)$$

$$\hat{\imath} \stackrel{|\mathcal{C}_{\mathrm{th}}}{=} \min\{\{i \in \mathcal{I}_W(m) | b_i > \xi_i\} \cup \{m\}\}$$

$$\mathcal{S}_i \cap \mathcal{C}_{\mathrm{th}} | \boldsymbol{\theta} = \mathcal{M}_i | \boldsymbol{\theta} \cup \mathcal{M}_i^{\mathrm{c}} | \boldsymbol{\theta}$$
$$\mathcal{M}_i | \boldsymbol{\theta} = \{\mathsf{B}_j \leq \xi_j \forall j \in \mathcal{I}_W(i), \mathsf{B}_j \leq \mathsf{B}_i \forall j \in \mathcal{B} \backslash \{i\} | \boldsymbol{\theta}\} \backslash \{\mathsf{B}_j \leq \xi_j \forall j \in \mathcal{B}, \mathsf{B}_j \leq \mathsf{B}_i \forall j \in \mathcal{B} \backslash \{i\} | \boldsymbol{\theta}\}$$
$$\mathcal{M}_i^{\mathrm{c}} | \boldsymbol{\theta} = \bigcup_{m \in \mathcal{I}_W(i+W+1)} \{\mathsf{B}_j \leq \xi_j \forall j \in \mathcal{I}_{i-m+W}(i), \mathsf{B}_i > \xi_i, \mathsf{B}_j \leq \mathsf{B}_m \forall j \in \mathcal{B} \backslash \{m\} | \boldsymbol{\theta}\}$$

$$f_{\mathsf{I}}(i|\boldsymbol{\theta}) = \Big[\int_0^{+\infty} \prod_{j \in \mathcal{I}_W(i)} F_{\mathsf{B}_j}(\breve{\xi}_j(b)|\boldsymbol{\theta}) \prod_{j \in \mathcal{I}_W^{\mathrm{c}}(i) \backslash \{i\}} F_{\mathsf{B}_j}(b|\boldsymbol{\theta})\, f_{\mathsf{B}_i}(b|\boldsymbol{\theta})\, db - \int_0^{\xi_i} \prod_{j \in \mathcal{B} \backslash \{i\}} F_{\mathsf{B}_j}(\breve{\xi}_j(b)|\boldsymbol{\theta})\, f_{\mathsf{B}_i}(b|\boldsymbol{\theta})\, db$$
$$+ \sum_{m \in \mathcal{I}_W(i+W+1)} \int_{\xi_i}^{+\infty} \prod_{j \in \mathcal{I}_{i-m+W}(i)} F_{\mathsf{B}_j}(\breve{\xi}_j(b)|\boldsymbol{\theta}) \left[F_{\mathsf{B}_i}(b|\boldsymbol{\theta}) - F_{\mathsf{B}_i}(\xi_i|\boldsymbol{\theta})\right] \prod_{j \in \mathcal{I}_{i-m+W}^{\mathrm{c}}(i) \backslash \{i,m\}} F_{\mathsf{B}_j}(b|\boldsymbol{\theta})\, f_{\mathsf{B}_m}(b|\boldsymbol{\theta})\, db\Big] \Big[1 - \prod_{n \in \mathcal{B}} F_{\mathsf{B}_n}(\xi_n|\boldsymbol{\theta})\Big]^{-1}$$

$\mathcal{B} = \{0, 1, \ldots, 7\}$ $\qquad \boldsymbol{\xi} = [1.3, 1.1, 0.9, 2.5, 1.4, 2.9, 1.9, 1.4]$

$W = 3$ $\qquad \mathbf{b} = [0.8, 1.2, \boxed{1.3,} 2.3, 2.5, 2.8, 2.4, 1.2]$

Serial backward search

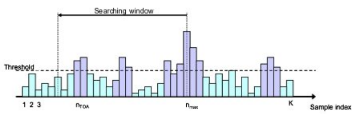

$$\mathcal{I}_W(m) = \mathcal{B} \cap \{m-W, m-W+1, \ldots, m-1\}$$
$$\mathcal{I}_W^{\mathrm{c}}(m) = \mathcal{B} \backslash \mathcal{I}_W(m)$$

$$\hat{\imath} \stackrel{|\mathcal{C}_{\mathrm{th}}}{=} \min\{\{i \in \mathcal{I}_m(m) | b_j > \xi_j, j \in \mathcal{I}_{m-i}(m)\} \cup \{m\}\}$$

$$\mathcal{S}_i \cap \mathcal{C}_{\mathrm{th}} | \boldsymbol{\theta} = \mathcal{M}_i | \boldsymbol{\theta} \cup \mathcal{M}_i^{\mathrm{c}} | \boldsymbol{\theta}$$
$$\mathcal{M}_i | \boldsymbol{\theta} = \{\mathsf{B}_{i-1} \leq \xi_{i-1} \text{ if } i > 0, \mathsf{B}_j \leq \mathsf{B}_i \forall j \in \mathcal{B} \backslash \{i\} | \boldsymbol{\theta}\}\, \{\mathsf{B}_j \leq \xi_j \forall j \in \mathcal{B}, \mathsf{B}_j \leq \mathsf{B}_i \forall j \in \mathcal{B} \backslash \{i\} | \boldsymbol{\theta}\}$$
$$\mathcal{M}_i^{\mathrm{c}} | \boldsymbol{\theta} = \bigcup_{m \in \mathcal{I}_{N_{\mathrm{bin}}-i-1}(N_{\mathrm{bin}})} \{\mathsf{B}_{i-1} \leq \xi_{i-1} \text{ if } i > 0,\ \mathsf{B}_j > \xi_j \forall j \in \mathcal{I}_{m-i}(m), \mathsf{B}_j \leq \mathsf{B}_m \forall j \in \mathcal{B} \backslash \{m\} | \boldsymbol{\theta}\}$$

$$f_{\mathsf{I}}(i|\boldsymbol{\theta}) = \Big[\int_0^{+\infty} \breve{F}_{\mathsf{B}_{i-1}}(\breve{\xi}_{i-1}(b)|\boldsymbol{\theta}) \prod_{j \in \mathcal{B} \backslash \{i-1,i\}} F_{\mathsf{B}_j}(b|\boldsymbol{\theta}) f_{\mathsf{B}_i}(b|\boldsymbol{\theta})\, db - \int_0^{\xi_i} \prod_{j \in \mathcal{B} \backslash \{i\}} F_{\mathsf{B}_j}(\breve{\xi}_j(b)|\boldsymbol{\theta})\, f_{\mathsf{B}_i}(b|\boldsymbol{\theta})\, db$$
$$+ \sum_{m \in \mathcal{I}_{N_{\mathrm{bin}}-i-1}(N_{\mathrm{bin}})} \int_{\breve{\xi}_{m,i}}^{+\infty} \breve{F}_{\mathsf{B}_{i-1}}(\breve{\xi}_{i-1}(b)|\boldsymbol{\theta}) \prod_{j \in \mathcal{I}_{m-i}(m)} \left[F_{\mathsf{B}_j}(b|\boldsymbol{\theta}) - F_{\mathsf{B}_j}(\xi_j|\boldsymbol{\theta})\right] \prod_{j \in \mathcal{I}_{m-i}^{\mathrm{c}}(m) \backslash \{i-1,m\}} F_{\mathsf{B}_j}(b|\boldsymbol{\theta})\, f_{\mathsf{B}_m}(b|\boldsymbol{\theta})\, db\Big] \Big[1 - \prod_{n \in \mathcal{B}} F_{\mathsf{B}_n}(\xi_n|\boldsymbol{\theta})\Big]^{-1}$$

$\mathcal{B} = \{0, 1, \ldots, 7\}$ $\qquad \boldsymbol{\xi} = [1.3, 1.1, 0.9, 2.5, 1.4, 2.9, 1.9, 1.4]$

$\mathbf{b} = [0.8, 1.2, 1.3, 2.3, \boxed{2.5,} 2.8, 2.4, 1.2]$

TOA estimation error

$$f_{\mathsf{E}}(e|\boldsymbol{\theta}_{\mathrm{d}}) = \frac{1}{T_{\mathrm{obs}}} \int_0^{T_{\mathrm{obs}}} f_{\mathsf{E}}(e|\boldsymbol{\theta}_{\mathrm{d}}, \tau)\, d\tau$$

$$f_{\mathsf{E}}(e|\boldsymbol{\theta}_{\mathrm{d}}, \tau) = \mathbb{E}_{\boldsymbol{\theta}_{\mathrm{h}}}\{f_{\mathsf{E}}(e|\boldsymbol{\theta})\}$$

$$f_{\mathsf{I}}(i|\boldsymbol{\theta}_{\mathrm{d}}, \tau) = \mathbb{E}_{\boldsymbol{\theta}_{\mathrm{h}}}\{f_{\mathsf{I}}(i|\boldsymbol{\theta})\}$$

$$f_{\mathsf{E}}(e|\boldsymbol{\theta}_{\mathrm{d}}, \tau) = \begin{cases} |\frac{d\, g^{-1}(e+\tau)}{d\, e}| f_{\mathsf{I}}(g^{-1}(e+\tau)|\boldsymbol{\theta}_{\mathrm{d}}, \tau) & \text{for } e \in \mathcal{E}_\tau \\ 0 & \text{otherwise} \end{cases}$$

$$\varrho_{\mathrm{t}}(\boldsymbol{\theta}_{\mathrm{d}}) = \int_{-\infty}^{+\infty} e^2 f_{\mathsf{E}}(e|\boldsymbol{\theta}_{\mathrm{d}})\, de$$

Tractable range information model

- Approximation of the range information model to enable the design of soft-decision and hard-decision ranging systems

$$\mathsf{B}_i \frac{N_{\mathrm{p}}}{\sigma^2} \xrightarrow{\mathrm{d}} \tilde{\mathsf{B}}_i \frac{N_{\mathrm{p}}}{\sigma^2} \overset{|\boldsymbol{\theta}}{\sim} \mathcal{N}(N_{\mathrm{p}}N_{\mathrm{sb}} + \lambda_i, 2(N_{\mathrm{p}}N_{\mathrm{sb}} + 2\lambda_i))$$

- Lemma $\quad \mathsf{B}_i \simeq \frac{1}{N_{\mathrm{p}}} \sum_{s=0}^{N_{\mathrm{sb}}-1} \sum_{p=0}^{N_{\mathrm{p}}-1} \left(\sqrt{\mathbb{E}\left\{\mathsf{U}_{i,p,s}^2\right\}} + \mathsf{N}_{i,p,s} \right)^2$

$$\overline{\lambda}_i = \sum_{s=0}^{N_{\mathrm{sb}}-1} \sum_{p=0}^{N_{\mathrm{p}}-1} \frac{\mathbb{E}\left\{\mathsf{U}_{i,p,s}^2\right\}}{\sigma^2}\,.$$

- Tapped delay line $\quad \overline{\lambda}_i = \sum_{s=0}^{N_{\mathrm{sb}}-1} \sum_{p=0}^{N_{\mathrm{p}}-1} \sum_{l=1}^{\breve{L}} \frac{\mathbb{E}\left\{\breve{\alpha}_l^2\right\}}{\sigma^2} s^2(t_{i,p,s} - \breve{\tau}_l)$

PMF od selected bin index

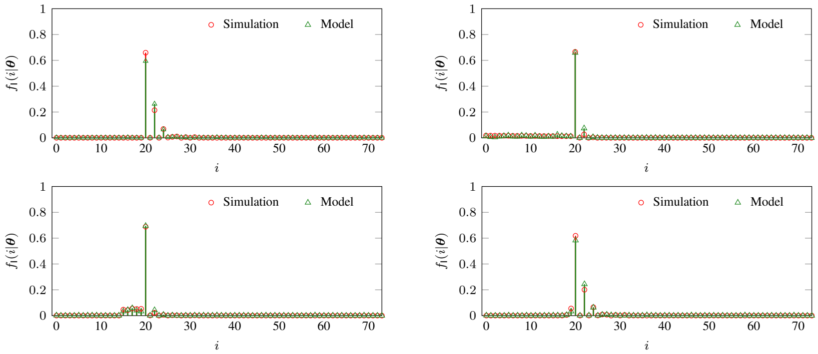

Fig. 2. Example PMF of the selected bin index for the TCS (top left), MBS (top right), JBSF with $W = 5$ (bottom left), and SBS (bottom right) algorithms with $T_{\rm d} = 2\,$ns, $N_{\rm p} = 128$, and $\gamma = -10\,$dB. The first bin containing the transmitted signal has index $i = 20$.

Range information model accuracy

- Distance between the PMF of selected index obtained from the proposed range information model and those obtained through sample-level simulation

$$\mathbb{D}_{\rm JS}\{p_1, p_2\} = \frac{1}{2}\sum_{i\in\mathcal{X}} p_1(i)\,\log\left(\frac{2\,p_1(i)}{p_1(i)+p_2(i)}\right) + \frac{1}{2}\sum_{i\in\mathcal{X}} p_2(i)\,\log\left(\frac{2\,p_2(i)}{p_1(i)+p_2(i)}\right)$$

$$\mathbb{D}_{\rm RMSE}\{p_1, p_2\} = \left[\frac{1}{|\mathcal{X}|}\sum_{i\in\mathcal{X}} |p_1(i) - p_2(i)|^2\right]^{1/2}$$

$$\mathbb{D}_{\rm ME}\{p_1, p_2\} = \max_{i\in\mathcal{X}}\{|p_1(i) - p_2(i)|\}$$

$\mathbb{D}_{\rm JS}\{p_1, p_2\}$ (TOP), $\mathbb{D}_{\rm RMSE}\{p_1, p_2\}$ (MIDDLE), AND $\mathbb{D}_{\rm ME}\{p_1, p_2\}$ (BOTTOM) FOR THEORETICAL AND SIMULATED PMF OF THE SELECTED BIN FOR HARD-DECISION ALGORITHMS.

	$N_{\rm p} = 16$		$N_{\rm p} = 128$	
	$\gamma = -20\,$dB	$\gamma = -10\,$dB	$\gamma = -20\,$dB	$\gamma = -10\,$dB
TCS	0.015	0.013	0.017	0.009
MBS	0.009	0.013	0.010	0.016
JBSF	0.009	0.012	0.010	0.015
SBS	0.009	0.012	0.010	0.015
	$N_{\rm p} = 16$		$N_{\rm p} = 128$	
	$\gamma = -20\,$dB	$\gamma = -10\,$dB	$\gamma = -20\,$dB	$\gamma = -10\,$dB
TCS	0.006	0.007	0.006	0.011
MBS	0.004	0.006	0.004	0.012
JBSF	0.004	0.006	0.004	0.009
SBS	0.004	0.006	0.004	0.010
	$N_{\rm p} = 16$		$N_{\rm p} = 128$	
	$\gamma = -20\,$dB	$\gamma = -10\,$dB	$\gamma = -20\,$dB	$\gamma = -10\,$dB
TCS	0.023	0.037	0.028	0.061
MBS	0.010	0.040	0.011	0.089
JBSF	0.010	0.040	0.010	0.054
SBS	0.010	0.038	0.010	0.070

Energy detector design

- The proposed range information model enables the design of the ranging system.

- Detection and false-alarm probabilities

$$P_{\mathrm{d}}(\boldsymbol{\theta}_{\mathrm{d}}) = \sum_{i \in \mathcal{B}} \check{f}_{\mathsf{I}}(i|\boldsymbol{\theta}_{\mathrm{d}}, \boldsymbol{\lambda} \neq \mathbf{0}) \qquad P_{\mathrm{fa}}(\boldsymbol{\theta}_{\mathrm{d}}) = \sum_{i \in \mathcal{B}} \check{f}_{\mathsf{I}}(i|\boldsymbol{\theta}_{\mathrm{d}}, \boldsymbol{\lambda} = \mathbf{0})$$

- MSE of the TOA estimate

$$\varrho_{\mathrm{t}}(\boldsymbol{\theta}_{\mathrm{d}}) = \int_{-\infty}^{+\infty} e^2 f_{\mathsf{E}}\left(e|\boldsymbol{\theta}_{\mathrm{d}}\right) de$$

ED design criteria

- Different criteria for the design of ED parameters based on the proposed range information model (classical approaches based on detection and false-alarm probabiltiy only)

$$\hat{\boldsymbol{\theta}}_{\mathrm{d}} = \underset{\left\{\boldsymbol{\theta}_{\mathrm{d}} : P_{\mathrm{d}}(\boldsymbol{\theta}_{\mathrm{d}}) \geq P_{\mathrm{d}}^{\star}\right\}}{\operatorname{argmin}} \varrho_{\mathrm{t}}(\boldsymbol{\theta}_{\mathrm{d}})$$

$$\hat{\boldsymbol{\theta}}_{\mathrm{d}} = \underset{\left\{\boldsymbol{\theta}_{\mathrm{d}} : P_{\mathrm{fa}}(\boldsymbol{\theta}_{\mathrm{d}}) \leq P_{\mathrm{fa}}^{\star}\right\}}{\operatorname{argmin}} \varrho_{\mathrm{t}}(\boldsymbol{\theta}_{\mathrm{d}})$$

$$\hat{\boldsymbol{\theta}}_{\mathrm{d}} = \underset{\left\{\boldsymbol{\theta}_{\mathrm{d}} : \varrho_{\mathrm{t}}(\boldsymbol{\theta}_{\mathrm{d}}) \leq \varrho_{\mathrm{t}}^{\star}\right\}}{\operatorname{argmax}} P_{\mathrm{d}}(\boldsymbol{\theta}_{\mathrm{d}})$$

$$\hat{\boldsymbol{\theta}}_{\mathrm{d}} = \underset{\boldsymbol{\theta}_{\mathrm{d}}}{\operatorname{argmin}}\, \upsilon_{\mathrm{t}}(\boldsymbol{\theta}_{\mathrm{d}})$$

$$\upsilon_{\mathrm{t}}(\boldsymbol{\theta}_{\mathrm{d}}) = \varrho_{\mathrm{t}}(\boldsymbol{\theta}_{\mathrm{d}})\, P_{\mathrm{d}}(\boldsymbol{\theta}_{\mathrm{d}}) + \nu(\boldsymbol{\theta}_{\mathrm{d}}) \left[1 - P_{\mathrm{d}}(\boldsymbol{\theta}_{\mathrm{d}})\right]$$

Ranging accuracy

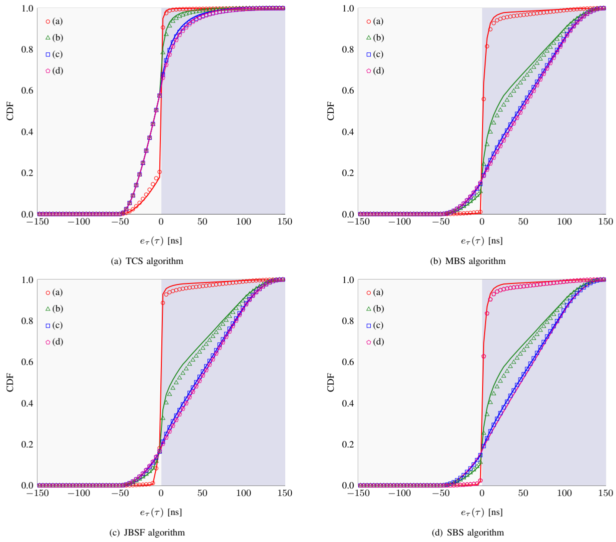

Fig. 4. Example CDF of the TOA estimation error for the TCS, MBS, JBSF with $W = 5$, and SBS algorithms with different values of N_p and γ: (a) $N_\mathrm{p} = 128$, $\gamma = -10\,\mathrm{dB}$; (b) $N_\mathrm{p} = 16$, $\gamma = -10\,\mathrm{dB}$; (c) $N_\mathrm{p} = 128$, $\gamma = -20\,\mathrm{dB}$; and (d) $N_\mathrm{p} = 16$, $\gamma = -20\,\mathrm{dB}$. Simulation results are shown in symbols and theoretical results are shown in solid lines.

RMSE of TOA estimate

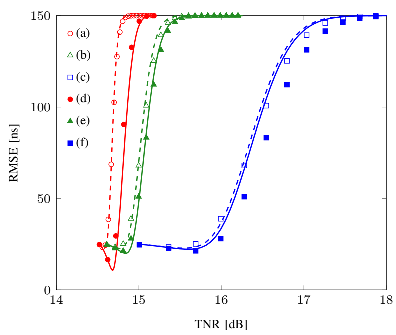

Fig. 5. RMSE of the TOA estimate as a function of TNR per pulse $\xi/(N_\mathrm{p}\,\sigma^2)$ for $\gamma = -20\,\mathrm{dB}$ and $-10\,\mathrm{dB}$, and different values of N_p: (a) $N_\mathrm{p} = 128$, $\gamma = -20\,\mathrm{dB}$; (b) $N_\mathrm{p} = 16$, $\gamma = -20\,\mathrm{dB}$; and (c) $N_\mathrm{p} = 1$, $\gamma = -20\,\mathrm{dB}$; (d) $N_\mathrm{p} = 128$, $\gamma = -10\,\mathrm{dB}$; (e) $N_\mathrm{p} = 16$, $\gamma = -10\,\mathrm{dB}$; and (f) $N_\mathrm{p} = 1$, $\gamma = -10\,\mathrm{dB}$. Simulation results are shown with symbols and theoretical results are shown in solid lines.

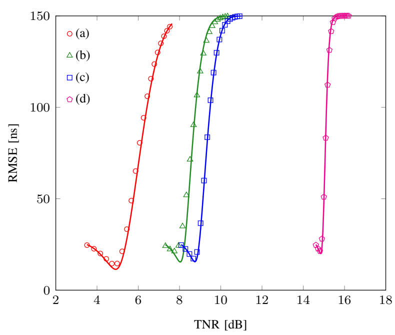

Fig. 6. RMSE of the TOA estimate as a function of TNR per pulse $\xi/(N_\mathrm{p}\,\sigma^2)$ for $N_\mathrm{p} = 16$, $\gamma = -10\,\mathrm{dB}$, and different emission masks: (a) China; (b) Japan; (c) Europe/Korea; and (d) USA. Simulation results are shown with symbols and theoretical results are shown in solid lines.

Localization accuracy

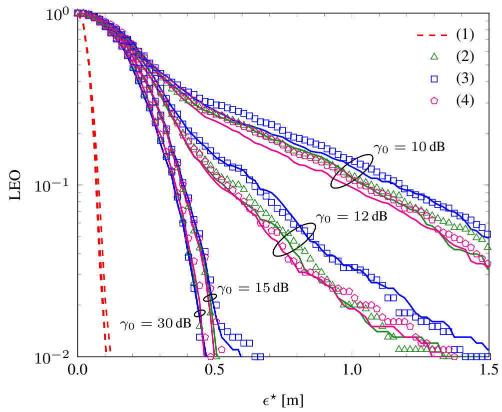

Fig. 7. LEO as a function of the maximum tolerable localization error for soft-decision and hard-decision localization with $T_{\rm d} = 2\,$ns, $N_{\rm p} = 128$, and different values of γ_0: (1) soft decision (dashed curves from left to right are for γ_0 from 30 to 10 dB); (2) JBSF with $N_{\rm w} = 5$; (3) JBSF with $N_{\rm w} = 2$; and (4) TCS. Theoretical results are shown in solid lines and simulation results are shown in symbols.

SPARSITY PROPERTY OF LOCALIZATION

Power Allocation in Network Localization

- High accuracy localization is crucial for numerous location-based applications
- Power allocation not only affects the localization accuracy, but also determines the network lifetime
- The aim of power allocation is to maximize localization accuracy under transmit power constraints
- Existing works on power allocation for network localization
  - Used heuristic ideas and relaxation methods to provide suboptimal strategies
  - Obtained numerical results by using standard optimization packages
  - Numerical results suggest that certain transmitters are more effective in improving localization accuracy
- More insight is desirable for the design and operation of networks
- Contributions
  - Develop a unifying framework for power allocation in network localization
  - Develop an algebraic method to obtain optimal strategies for power allocation problem analytically

Outline

- Background
- Problem Formulation
- Sparsity of Optimal Power Allocation Vector
- Optimal Power Allocation Strategies
- Numerical Results
- Conclusion

System Model

- Wireless Network Localization (WNL): determine the agent's position based on ranging measurements with respect to anchors

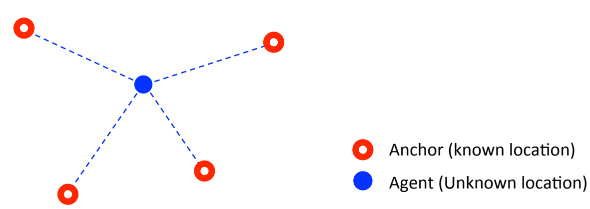

- System Model
  - $N_{\rm b}$ anchors with location $\mathbf{p}_j \in \mathbb{R}^d$, agent position $\mathbf{p}$
  - distance between anchor j and the agent d_j
  - ranging coefficient (RC) ζ_j
  - power allocation vector $\mathbf{x} := [\, x_1, \, x_2, \, \cdots, \, x_{N_{\rm b}} \,]^{\rm T}$

System Model

- Square position error bound (SPEB)
  - A lower bound of the mean square error, i.e.,

$$\mathcal{P}(\mathbf{p};\mathbf{x}) := \mathrm{tr}\left\{\mathbf{J}_{\mathrm{e}}^{-1}(\mathbf{p};\mathbf{x})\right\} \leq \mathbb{E}\left\{\|\hat{\mathbf{p}}-\mathbf{p}\|^2\right\}$$

  where $\mathbf{J}_{\mathrm{e}}(\mathbf{p};\mathbf{x})$ is the *equivalent Fisher information matrix* (EFIM)

- The EFIM is a $d \times d$ matrix for the agent's position

$$\mathbf{J}_{\mathrm{e}}(\mathbf{p};\mathbf{x}) = \sum_{k=1}^{N_{\mathrm{b}}} x_k \cdot \frac{\zeta_k}{d_k^{2\beta}} \cdot \mathbf{u}_k \mathbf{u}_k^{\mathrm{T}}$$

$\mathbf{u}_k = (\mathbf{p}-\mathbf{p}_k)/d_k$ angle vector

sum over anchors

amplitude loss exponent

- Problem Formulation: minimize SPEB under a total power constraint

$$\begin{aligned} \min_{\{\mathbf{x}\}} \quad & \mathrm{tr}\left\{\mathbf{J}_{\mathrm{e}}^{-1}(\mathbf{x})\right\} \\ \mathrm{s.t.} \quad & \boxed{\mathbf{1}^{\mathrm{T}} \cdot \mathbf{x} \leq 1} \\ & \mathbf{x} \succeq \mathbf{0} \end{aligned}$$

total power constraint

System Model

- Radar Network Localization (RNL): obtain the position of the target based on ranging measurements of total distance from transmitters to receivers reflected by the target

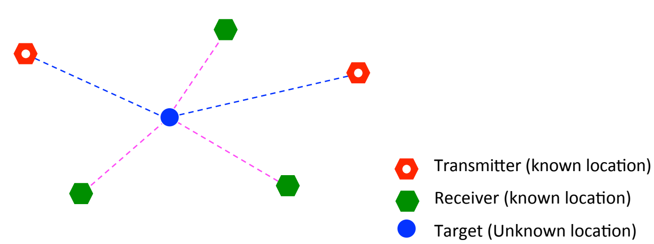

- System Model
  - N_{t} transmit antennas and N_{r} receive antennas with position $\mathbf{p}_j$, target position $\mathbf{p}_0$
  - distance between antenna j and the target: d_j
  - ranging coefficient (RC) ζ_{kj}
  - power allocated to transmit antenna k : x_k

System Model

- Square position error bound (SPEB)
  - A lower bound of the mean square error, i.e.,

$$\mathcal{P}(\mathbf{p}_0;\mathbf{x}) := \mathrm{tr}\left\{\mathbf{J}_\mathrm{e}^{-1}(\mathbf{p}_0;\mathbf{x})\right\} \le \mathbb{E}\left\{\|\widehat{\mathbf{p}_0} - \mathbf{p}_0\|^2\right\}$$

  where $\mathbf{J}_\mathrm{e}(\mathbf{p}_0;\mathbf{x})$ is the *equivalent Fisher information matrix* (EFIM)

- The EFIM is a $d \times d$ matrix for the agent's position

$\mathbf{u}_k = (\mathbf{p}_0 - \mathbf{p}_k)/d_k$

angle vector

$$\mathbf{J}_\mathrm{e}(\mathbf{p}_0;\mathbf{x}) = \sum_{j=1}^{N_\mathrm{t}} \frac{x_j}{d_j^{2\beta}} \sum_{k=1}^{N_\mathrm{r}} \frac{\zeta_{kj}}{d_k^{2\beta}} [\mathbf{u}_k + \mathbf{u}_j][\mathbf{u}_k + \mathbf{u}_j]^\mathrm{T}$$

sum over Tx and Rx

- Problem Formulation: minimize SPEB under a total power constraint

$$\begin{aligned} \min_{\{\mathbf{x}\}} \quad & \mathrm{tr}\left\{\mathbf{J}_\mathrm{e}^{-1}(\mathbf{x})\right\} \\ \text{s.t.} \quad & \boxed{\mathbf{1}^\mathrm{T}\cdot\mathbf{x} \le 1} \longleftarrow \text{total power constraint} \\ & \mathbf{x} \succeq \mathbf{0} \end{aligned}$$

Unification of Power Allocation Problem

- Comparison of SPEB and FIM for WNL and RNL

WNL

$$\mathcal{P}(\mathbf{p};\mathbf{x}) = \boxed{\mathrm{tr}\left\{\mathbf{J}_\mathrm{e}^{-1}\right.}\left.(\mathbf{p};\mathbf{x})\right\}$$

$$\mathbf{J}_\mathrm{e}(\mathbf{p};\mathbf{x}) = \sum_{j=1}^{N_\mathrm{b}} \boxed{x_j} \cdot \boxed{\frac{\zeta_j}{d_j^{2\beta}} \cdot \mathbf{u}_j\mathbf{u}_j^\mathrm{T}}$$

RNL

$$\mathcal{P}(\mathbf{p}_0;\mathbf{x}) = \boxed{\mathrm{tr}\left\{\mathbf{J}_\mathrm{e}^{-1}\right.}\left.(\mathbf{p}_0;\mathbf{x})\right\}$$

$$\mathbf{J}_\mathrm{e}(\mathbf{p}_0;\mathbf{x}) = \sum_{j=1}^{N_\mathrm{t}} \boxed{x_j} \boxed{\sum_{k=1}^{N_\mathrm{r}} \frac{\zeta_{kj}}{d_k^{2\beta} d_j^{2\beta}} [\mathbf{u}_k + \mathbf{u}_j][\mathbf{u}_k + \mathbf{u}_j]^\mathrm{T}}$$

$$\mathcal{P}(\mathbf{x}) = \mathrm{tr}\left\{\mathbf{J}_\mathrm{e}^{-1}(\mathbf{x})\right\}$$

Power Allocation Vector

$\mathbf{x} := [x_1, x_2, \cdots, x_m]^\mathrm{T}$

$$\mathbf{J}_\mathrm{e}(\mathbf{x}) = \sum_{j\in\mathcal{N}_1} \sum_{k\in\mathcal{N}_2} \xi_{kj} x_j \cdot \mathbf{u}_{kj}\mathbf{u}_{kj}^\mathrm{T}$$

Transmitting nodes $\mathcal{N}_1 = \{1, 2, \cdots, m\}$

unit vector

Receiving nodes $\mathcal{N}_2 = \{1, 2, \cdots, n\}$

equivalent RC

- Power Allocation Problem: minimize SPEB under a total power constraint

$$\begin{aligned} \mathscr{P}: \quad \min_{\{\mathbf{x}\}} \quad & \mathrm{tr}\left\{\mathbf{J}_\mathrm{e}^{-1}(\mathbf{x})\right\} \\ \text{s.t.} \quad & \boxed{\mathbf{1}^\mathrm{T}\cdot\mathbf{x} \le 1} \longleftarrow \text{total power constraint} \\ & \mathbf{x} \succeq \mathbf{0} \end{aligned}$$

Prior Positional Knowledge

- A prior positional knowledge can improve the localization accuracy and is useful for a wide range applications such as tracking and navigation

- When prior positional knowledge of the agent/target is available, the SPEB can be approximated as $\mathcal{P}_{\mathrm{p}}(\mathbf{x}) = \mathrm{tr}\left\{\mathbf{J}_{\mathrm{p}}^{-1}(\mathbf{x})\right\}$, where

$$\mathbf{J}_{\mathrm{p}}(\mathbf{x}) = \underbrace{\mathbf{J}_0}_{\text{Prior positional knowledge}} + \sum_{j\in\mathcal{N}_1}\sum_{k\in\mathcal{N}_2} \xi_{kj} x_j \cdot \mathbf{u}_{kj}\mathbf{u}_{kj}^{\mathrm{T}}$$

ξ_{kj} and $\mathbf{u}_{kj}$ are evaluated at position $\bar{\mathbf{p}} = \mathbb{E}\{\mathbf{p}\}$

- Power Allocation Problem with Prior Positional Knowledge

$$\mathscr{P}_{\mathrm{p}}: \quad \min_{\{\mathbf{x}\}} \quad \mathrm{tr}\left\{\mathbf{J}_{\mathrm{p}}^{-1}(\mathbf{x})\right\}$$
$$\text{s.t.} \quad \mathbf{1}^{\mathrm{T}}\cdot\mathbf{x} \le 1$$
$$\mathbf{x} \succeq \mathbf{0}$$

Outline

- Background
- Problem Formulation
- Sparsity of Optimal Power Allocation Vector
- Optimal Power Allocation Strategies
- Numerical Results
- Conclusion

The Sparsity of Optimal Power Allocation

- Main theorem: For d-dimensional network, there exist an optimal solution $\mathbf{x}^*$ of $\mathscr{P}$ (or $\mathscr{P}_\mathrm{p}$) such that

Zero-norm: The number of non-zero elements

$$\|\mathbf{x}^*\|_0 \le \binom{d+1}{2}$$

- At most $\binom{d+1}{2}$ transmitting nodes need to be activated for achieving the optimal localization accuracy (i.e., the minimum SPEB) in d-dimensional networks (e.g., 3 transmitting nodes for 2-D networks and 6 for 3-D) under a total power constraint

- Remark:
  - Only a small subset of transmitting nodes need to be activated for the optimal localization accuracy
  - Sparsity-inspired power allocation strategies

The Sparsity of Optimal Power Allocation

- Illustration: Sparsity of optimal power allocation in WNL
  - Some anchors contribute more to improve localization accuracy
  - closer to the agent, good channel condition, and forming a “good” topology

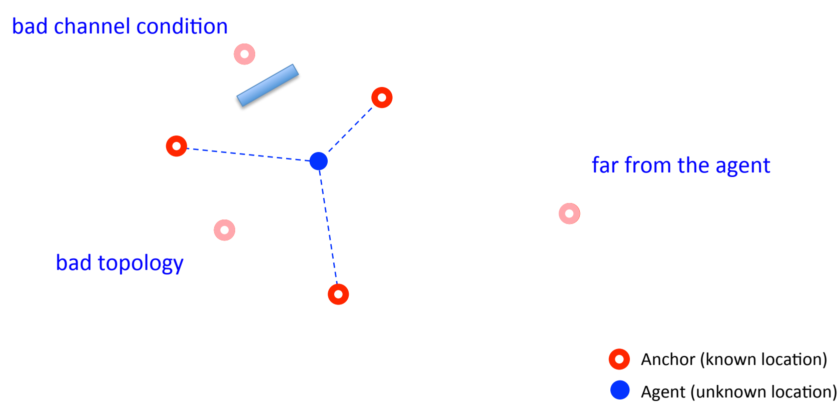

Outline

- Background
- Problem Formulation
- Sparsity of Optimal Power Allocation Vector
- Optimal Power Allocation Strategies
- Numerical Results
- Conclusion

Power Allocation Strategies: 2-D networks

- Since at most three active transmitting nodes are needed to achieve the optimal localization accuracy, we start with a network with three transmitting nodes.
- We will first develop strategies for $\mathscr{P}$ and then transform the problem $\mathscr{P}_{\mathrm{p}}$ to $\mathscr{P}$

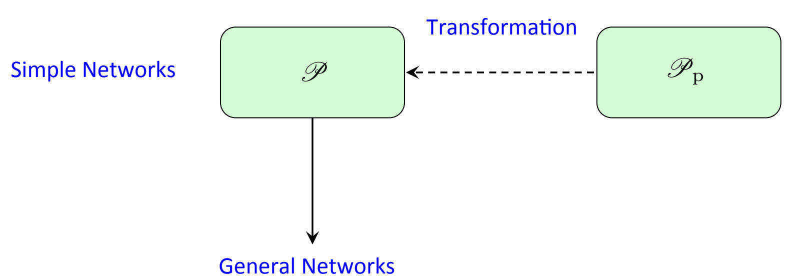

SPEB in 2-D Networks

- Notations
  - $\mathbf{u}_{kj} = [\cos\phi_{kj} \;\; \sin\phi_{kj}\,]^{\mathrm{T}}$
  - $\mathbf{R} = [\mathbf{R}_1 \;\; \mathbf{R}_2 \;\; \cdots \;\; \mathbf{R}_n\,]^{\mathrm{T}}$, where $\mathbf{R}_k = \mathrm{diag}\{\xi_{k1}, \xi_{k2}, \cdots, \xi_{km}\}$
  - Topology matrix matrix $\boldsymbol{\Lambda}$ is a mn by mn symmetric matrix, given by

$$[\boldsymbol{\Lambda}]_{(i-1)m+j,(k-1)m+l} = 2\sin^2(\phi_{ij} - \phi_{kl}) \qquad \begin{matrix} 1 \le i, k \le n \\ 1 \le j, l \le m \end{matrix}$$

- SPEB in 2-D networks is given by

$$\boxed{\mathcal{P}(\mathbf{x}) = \mathrm{tr}\Big\{\Big(\sum_{j\in\mathcal{N}_1}\sum_{k\in\mathcal{N}_2} \xi_{kj}x_j \cdot \mathbf{u}_{kj}\mathbf{u}_{kj}^{\mathrm{T}}\Big)^{-1}\Big\} = \frac{4\cdot\mathbf{1}^{\mathrm{T}}\,\mathbf{R}\,\mathbf{x}}{\mathbf{x}^{\mathrm{T}}\,\mathbf{R}^{\mathrm{T}}\boldsymbol{\Lambda}\,\mathbf{R}\,\mathbf{x}}}$$

- SPEB Properties
  - $\mathcal{P}(\mathbf{x})$ is a convex function of $\mathbf{x}$
  - $\mathcal{P}(\mathbf{x})$ is a non increasing function in $\mathbf{x}$
  - Low rank property of topology matrix $\boldsymbol{\Lambda}$: $\mathrm{rank}(\boldsymbol{\Lambda}) \le 3$

Power Allocation Strategy: Simple Networks

- The methodology is to check Karush-Kuhn-Tucker conditions

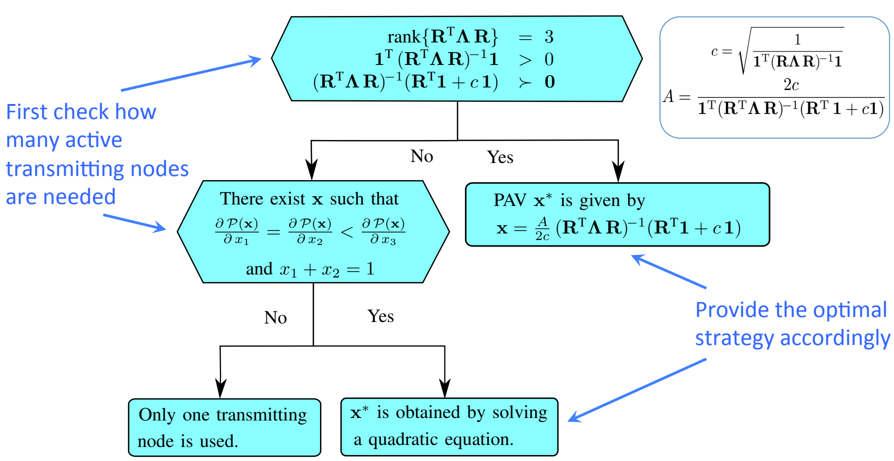

- The algorithm can be extended to the general case, with complexity $O(m^3)$

Power Allocation Strategy: Prior Positional Knowledge

- For problem $\mathscr{P}_{\mathrm{p}}$, though we can apply KKT conditions directly to give the optimal strategy, the process is difficult since $\mathcal{P}_{\mathrm{p}}(\mathbf{x})$ has a complex structure
- Recall performance metric:

SPEB without prior positional knowledge

$$\mathcal{P}(\mathbf{x}) = \mathrm{tr}\left\{\mathbf{J}_{\mathrm{e}}^{-1}(\mathbf{x})\right\}$$

$$\mathbf{J}_{\mathrm{e}}(\mathbf{x}) = \sum_{j\in\mathcal{N}_1}\sum_{k\in\mathcal{N}_2}\xi_{kj}x_j\cdot\mathbf{u}_{kj}\mathbf{u}_{kj}^{\mathrm{T}}$$

SPEB with prior positional knowledge

$$\mathcal{P}_{\mathrm{p}}(\mathbf{x}) = \mathrm{tr}\left\{\mathbf{J}_{\mathrm{p}}^{-1}(\mathbf{x})\right\}$$

$$\mathbf{J}_{\mathrm{p}}(\mathbf{x}) = \boxed{\mathbf{J}_0} + \sum_{j\in\mathcal{N}_1}\sum_{k\in\mathcal{N}_2}\xi_{kj}x_j\cdot\mathbf{u}_{kj}\mathbf{u}_{kj}^{\mathrm{T}}$$

- Basic idea
  - Transform the problem to the case without prior positional knowledge
  - Decompose $\mathbf{J}_0$ as the combination of FIM obtained by three transmitting nodes

Power Allocation Strategy: Prior Positional Knowledge

- Problem Transformation
  - Decomposition $\mathbf{J}_0 = \sum_{j=1,2,3} x_0^{(j)} \sum_{k\in\mathcal{N}_2}\xi_{kj}\mathbf{u}_{kj}\mathbf{u}_{kj}^{\mathrm{T}}$
  - Power shift $\widetilde{\mathbf{x}} = \mathbf{x} + \mathbf{x}_0$

EFIM

$$\mathbf{J}_{\mathrm{p}}(\mathbf{x}) = \mathbf{J}_0 + \sum_{j\in\mathcal{N}_1}\sum_{k\in\mathcal{N}_2}\xi_{kj}x_j\cdot\mathbf{u}_{kj}\mathbf{u}_{kj}^{\mathrm{T}} = \mathbf{J}_{\mathrm{e}}(\widetilde{\mathbf{x}}) = \sum_{j\in\mathcal{N}_1}\sum_{k\in\mathcal{N}_2}\xi_{kj}\widetilde{x}_j\cdot\mathbf{u}_{kj}\mathbf{u}_{kj}^{\mathrm{T}}$$

↓

SPEB

$$\mathcal{P}_{\mathrm{p}}(\mathbf{x}) = \mathrm{tr}\{\mathbf{J}_{\mathrm{p}}^{-1}(\mathbf{x})\} = \mathrm{tr}\{\mathbf{J}_{\mathrm{e}}^{-1}(\widetilde{\mathbf{x}})\} = \mathcal{P}(\widetilde{\mathbf{x}}) = \frac{4\cdot\mathbf{1}^{\mathrm{T}}\mathbf{R}\,\widetilde{\mathbf{x}}}{\widetilde{\mathbf{x}}^{\mathrm{T}}\mathbf{R}^{\mathrm{T}}\mathbf{\Lambda}\mathbf{R}\,\widetilde{\mathbf{x}}}$$

↓

Same Structure as the objective of $\mathscr{P}$

Problem

$$\mathscr{P}_{\mathrm{p}}: \quad \min_{\{\mathbf{x}\}} \ \mathrm{tr}\{\mathbf{J}_{\mathrm{p}}^{-1}(\mathbf{x})\} \quad \text{s.t.} \ \mathbf{1}^{\mathrm{T}}\cdot\mathbf{x}\le 1, \ \mathbf{x}\succeq\mathbf{0}$$

$$\Rightarrow \quad \widetilde{\mathscr{P}}_{\mathrm{p}}: \quad \min_{\{\widetilde{\mathbf{x}}\}} \ \boxed{\mathrm{tr}\{\mathbf{J}_{\mathrm{e}}^{-1}(\widetilde{\mathbf{x}})\}} \quad \text{s.t.} \ \mathbf{1}^{\mathrm{T}}\cdot\widetilde{\mathbf{x}}\le 1+\mathbf{1}^{\mathrm{T}}\cdot\mathbf{x}_0, \ \widetilde{\mathbf{x}}\succeq\mathbf{x}_0$$

Power Allocation Strategy: General Networks

- Consider a network with m transmitting nodes: we have $\binom{m}{3}$ combinations to select three out of m transmitting nodes.
- For each simple network, we evaluate the SPEB according to our strategy and choose the best one

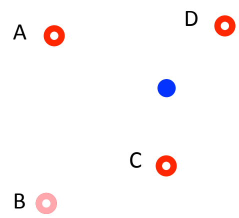

Combination	SPEB(m^2)
A, B and C	2.1
A, B and D	2.8
A, C and D	1.2
B, C and D	2.8

- The total computational complexity grows as $O(m^3)$
- Impact of sparsity: $O(m^{\mathbf{3}})$
  Compare to the worst-case complexity $O(2^m)$ [Godrich et al., 2011]

Outline

- Background
- Problem Formulation
- Sparsity of Optimal Power Allocation Vector
- Optimal Power Allocation Strategies
- **Numerical Results**
- Conclusion

Numerical Results

- Illustration
  - Anchors are deployed on vertices of an equilateral triangle
  - The optimal strategy employs anchors
    - B and C if the agent is in region I
    - A and B if the agent is in region II
    - A and C if the agent is in region III
    - A, B, and C if the agent is in region IV

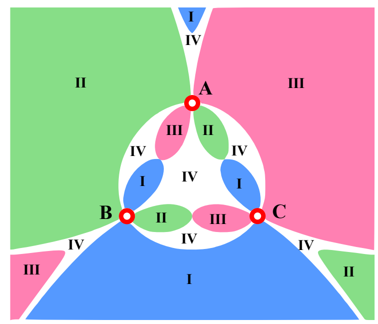

- Remarks
  - Region IV is relatively small, i.e., in most cases only two anchors need to be activated for the optimal localization accuracy
  - The optimal strategy employs two active anchors for agents in "far field" regions
  - In practice, two anchor case may use vicinity knowledge to resolve ambiguity

Wireless Network Localization

- Strategies: uniform allocation strategy π_{U} , near-optimal strategy π_2 (use only two anchors), optimal strategy π^*
- SPEB decreases with the number of anchors

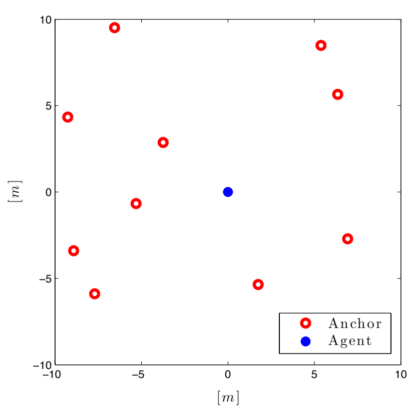

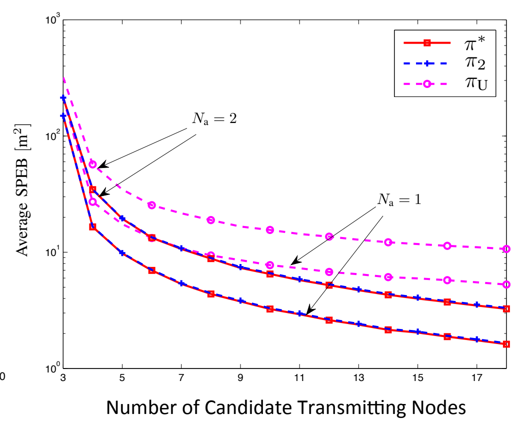

Radar Network Localization

- Target position is (0, 0) and transmitting antennas and receiving antennas uniform in [-10,10] by [-10,10] region
- Comparison between the optimal strategy $\pi^*$and uniform strategy π_{U} (power equally allocated to each transmitting node)

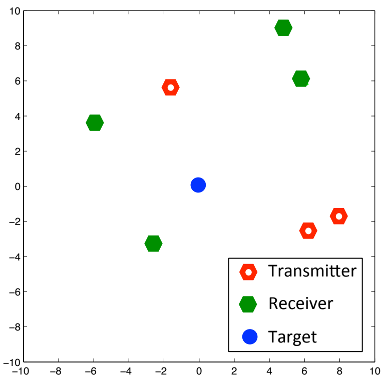

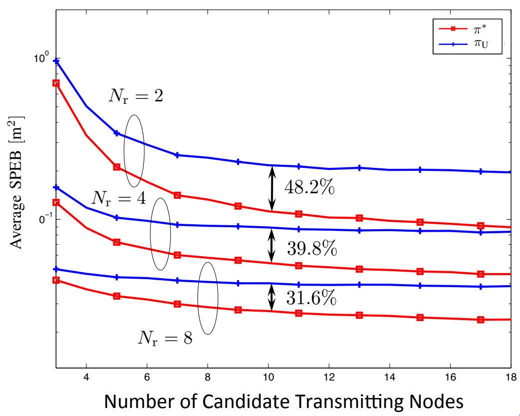

Outline

- Background
- Problem Formulation
- Sparsity of Optimal Power Allocation Vector
- Optimal Power Allocation Strategies
- Numerical Results
- Conclusion

Conclusion

- Developed an analytical framework for network localization which unifies WNL and RNL
- Determined the sparsity property of network localization, i.e., in a d -dimensional network, at most $\binom{d+1}{2}$ transmitting nodes need to be activated to achieve the optimal localization accuracy
- Proposed optimal power allocation strategies
  - for simple networks with three transmitting nodes, we provided the closed-form expression for the optimal strategy
  - for general networks with m transmitting nodes, we provided the power allocation strategy with computation complexity $\mathcal{O}(m^3)$
- Demonstrated that
  - The optimal strategy employs two active anchors for agents in "far field" regions
  - The optimal strategy outperforms the uniform power allocation strategy significantly
  - The SPEB decreases with the number of candidate transmitting nodes

References

- W. Dai, Y. Shen, and M. Z. Win, "Resource allocation for network localization: A computational geometry framework," *IEEE Trans. Inf. Theory*, 2016, to appear.
- M. Z. Win, A. Conti, S. Mazuelas, Y. Shen, W. M. Gifford, D. Dardari, and M. Chiani, "Network localization and navigation via cooperation," *IEEE Commun. Mag.,* vol. 49, no. 5, pp. 56–62, May 2011.
- W. Dai, Y. Shen, and M. Z. Win, ''Sparsity-inspired power allocation for network localization,'' in *Proc. IEEE Int. Conf. on Commun.,* Budapest, Hungary, May 2013, pp. 1-6.
- W. W.-L. Li, Y. Shen, Y. J. Zhang, and M. Z. Win, "Robust power allocation for energy-efficient location-aware networks," *IEEE/ACM Trans. Netw.*, vol. 21, no. 6, pp. 1918-1930, Dec. 2013.
- Y. Shen, W. Dai, and M. Z. Win, ''Power optimization for network localization,'' *IEEE/ACM Trans. Netw.*, vol. 22, no. 4, pp. , Aug. 2014.
- W. Dai, Y. Shen and M. Z. Win, "On the minimum number of active anchors for optimal localization," in *Proc. IEEE Global Telecomm. Conf.,* Anaheim, CA, Dec. 2012, pp. 1–6.
- Y. Shen and M. Z. Win, "Energy efficient location-aware networks," in *Proc. IEEE Int. Conf. on Commun.,* Beijing, China, May 2008, pp. 2995–3001.

Ranging

Cooperative Localization

Diversity Navigation

NETWORK EXPERIMENTATIONS

Characterization of Cooperative Systems

- It requires experiments specifically designed for cooperative algorithms and their comparisons under the same setting

- In the context of cooperative location-aware wireless networks, two different kinds of measurements are necessary:

  - *ranging measurements*: required as inputs for range-based localization algorithms;

  - *waveforms measurements*: required to estimate TOA and detect the state of the channel, such as non-line-of-sight (NLOS) condition.

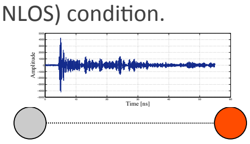

A. Conti et al., "Network experimentation for cooperative localization," IEEE J. Sel. Areas Commun., Feb. 2012

Network Experimentation

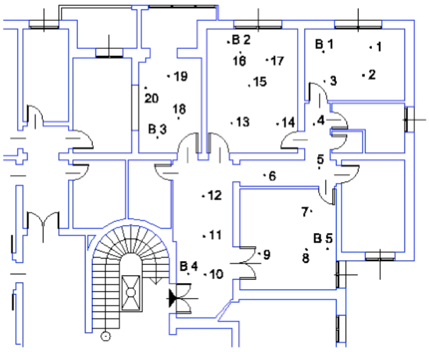

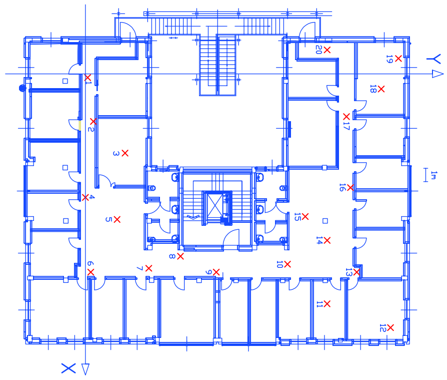

ID	x, y, z [cm]	ID	x, y, z [cm]
B1	1841.7, 2090.0, 88.5	8	1768.0, 1219.4, 76.0
B2	1423.6, 2130.2, 88.5	9	1562.2, 1204.2, 76.0
B3	1111.4, 1711.9, 82.8	10	1321.1, 1109.3, 76.0
B4	1246.9, 1112.1, 82.8	11	1315.7, 1278.2, 76.0
B5	1860.2, 1223.0, 88.7	12	1312.6, 1451.1, 76.0
1	2050.9, 2108.3, 76.0	13	1438.8, 1772.8, 76.0
2	2019.2, 1985.3, 76.0	14	1641.3, 1773.3, 76.0
3	1848.4, 1958.5, 76.0	15	1541.7, 1940.9, 76.0
4	1800.7, 1770.1, 76.0	16	1473.7, 2085.1, 76.0
5	1823.1, 1576.3, 76.0	17	1593.9, 2054.1, 76.0
6	1583.9, 1541.5, 76.0	18	1203.5, 1793.5, 76.0
7	1788.4, 1385.8, 76.0	19	1160.1, 1981.4, 76.0
		20	1060.1, 1929.4, 76.0

ID	x, y, z [cm]	ID	x, y, z [cm]
1	28.0, 16.9, 113.0	11	1740.3, 1831.1, 113.0
2	360.2, 60.4, 113.0	12	1920.6, 2311.3, 113.0
3	599.9, 300.2, 113.0	13	1500.4, 2055.5, 113.0
4	934.9, 0, 113.0	14	1260.3, 1831.4, 113.0
5	1102.0, 240.1, 113.0	15	1080.0, 1665.4, 113.0
6	1500.4, 40.5, 113.0	16	861.0, 2008.2, 113.0
7	1471.5, 480.0, 113.0	17	323.8, 1978.0, 113.0
8	1380.3, 720.1, 113.0	18	114.4, 2241.2, 113.0
9	1500.0, 991.2, 113.0	19	-116.1, 2371.8, 113.0
10	1440.3, 1531.2, 113.0	20	-181.2, 1831.3, 113.0

Case Study

The methodology is general and valid for others kinds of indoor/outdoor environments

The equipment consisted of a pair of UWB devices operating 3.2–7.4 GHz (radios provide samples of received signals and TOA-based range measurements, estimating the TOA based on the first path using a thresholding technique)

1500 measurements per pair of nodes

Ranging error and model

Measurements to characterize the positive bias in ranging errors due to NLOS conditions and ranging errors in LOS conditions

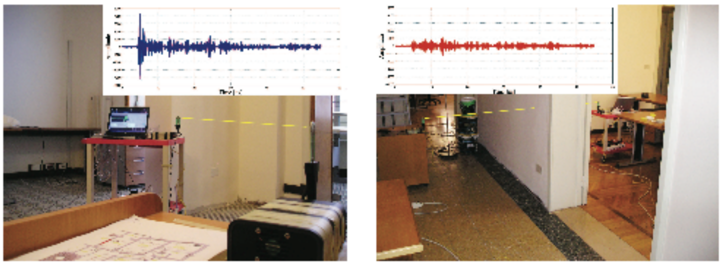

(a) Ranging and waveform measurement between a pair of nodes.   (b) Measurement of direct path (DP) excess delay.

Measurements for LOS and NLOS

range

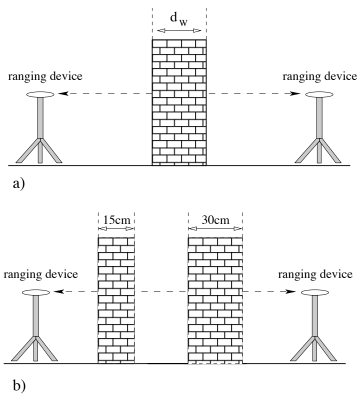

1500 measurements for each condition to characterize the positive bias in ranging errors due to NLOS and in LOS conditions

TABLE 1: Mean and standard deviation of ranging error for different wall thicknesses.

Layout, d_W [cm]	Mean [cm]	std dev [cm]
1 wall, 15.5	16.4	3.7
1 wall, 30	29.5	3.2
2 walls, 15.5 + 30	45.2	3

✓ the bias appears to increase linearly with the thickness of the wall

✓ low std indicates that the estimation error is dominated by the effects of excess delay rather than multipath or distance-dependent noise.

Measurements results

To derive a simple statistical model for ranging error, we categorized measurements in environment A for different LOS or NLOS conditions (# of walls)

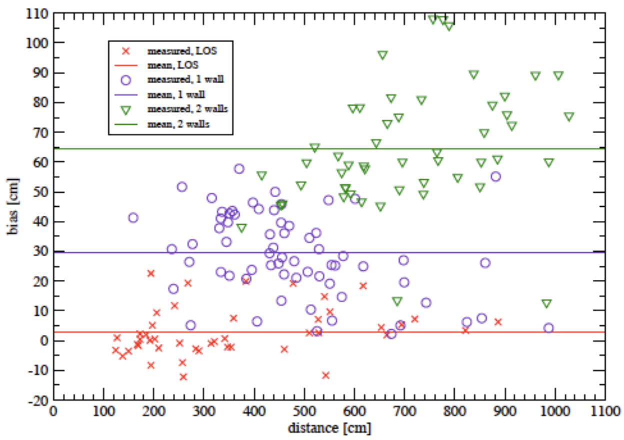

Choice of features for NLOS detection

• Features are extracted from the received waveform v(t) observed within the interval T under a particular channel condition.

• Temporal dispersion (RMS delay spread) (*higher for NLOS*)

$$\tau_{\mathrm{rms}} = \left[\frac{\int_T (t-\tau_{\mathrm{m}})^2 \, |v(t)|^2 \, dt}{\int_T |v(t)|^2 \, dt}\right]^{1/2}$$

mean excess delay

$$\tau_{\mathrm{m}} = \frac{\int_T t \, |v(t)|^2 \, dt}{\int_T |v(t)|^2 \, dt}$$

For N=1 is like comparison with a proper threshold

$$\text{Decide}: \begin{cases} \text{LOS} & \text{if } \tau_{\mathrm{rms}} < \lambda_\tau \\ \text{NLOS} & \text{if } \tau_{\mathrm{rms}} > \lambda_\tau \end{cases}$$

• Kurtosis $\mathcal{K} = \frac{1}{\sigma_{|v|}^4 T} \int_T (|v(t)| - \mu_{|v|})^4 \, dt$

(*higher for LOS*)

For N=1 is like comparison with a proper threshold

$$\text{Decide}: \begin{cases} \text{NLOS} & \text{if } \mathcal{K} < \lambda_{\mathcal{K}} \\ \text{LOS} & \text{if } \mathcal{K} > \lambda_{\mathcal{K}} \end{cases}$$

Set-up for localization testing (no coop)

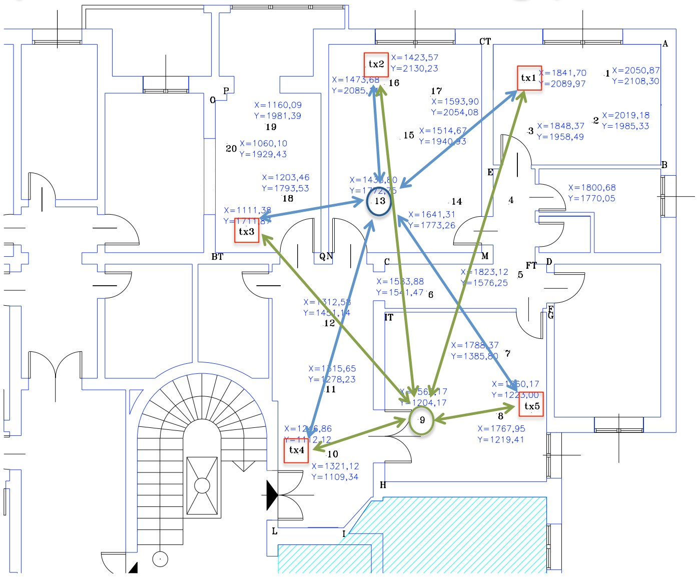

Set-up for localization testing (coop)

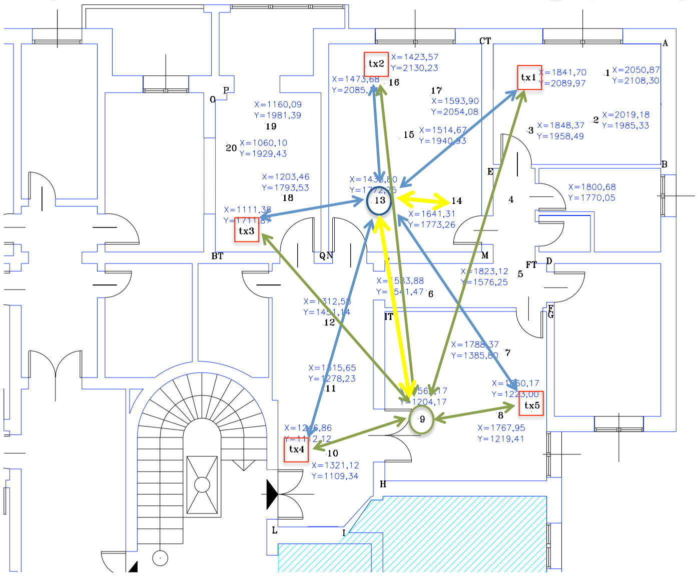

Experimental results

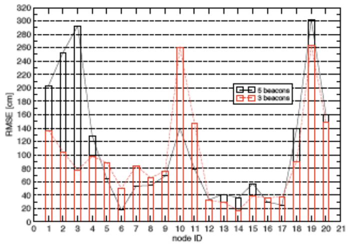

Fig. 5. RMSE as a function of target position in the absence of priori information. $N = 3$ (tx1,tx3,tx5) and $N = 5$ beacons are considered.

- Ranging Robustness
- Environment Knowledge
- Nodes Cooperation
- Cooperation Criterion
- Algorithm

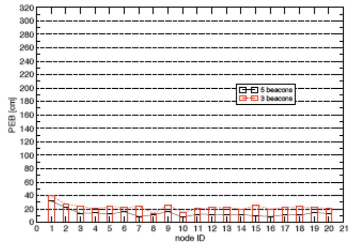

Fig. 8. PEB as a function of target position with 3 and 5 beacons.

Experimental results: LS

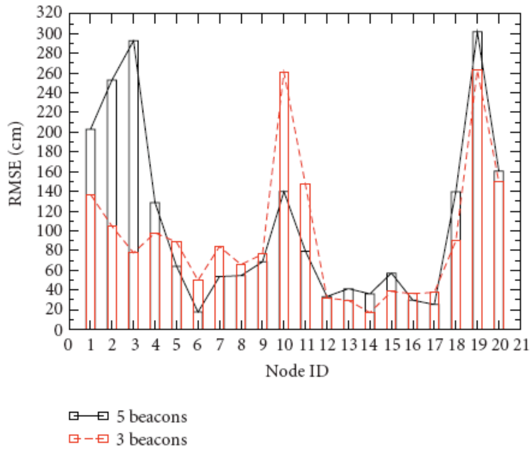

FIGURE 5: RMSE as a function of target position in the absence of priori information. $N = 3$ (tx1,tx3,tx5) and $N = 5$ beacons are considered.

Experimental results: LS

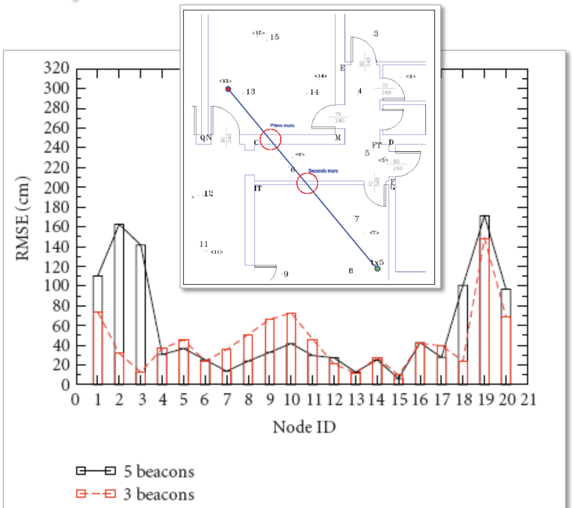

FIGURE 6: RMSE as a function of target position in the presence of priori information (two-step algorithm). $N = 3$ (tx1,tx3,tx5) and $N = 5$.

Experimental results: coop. LS

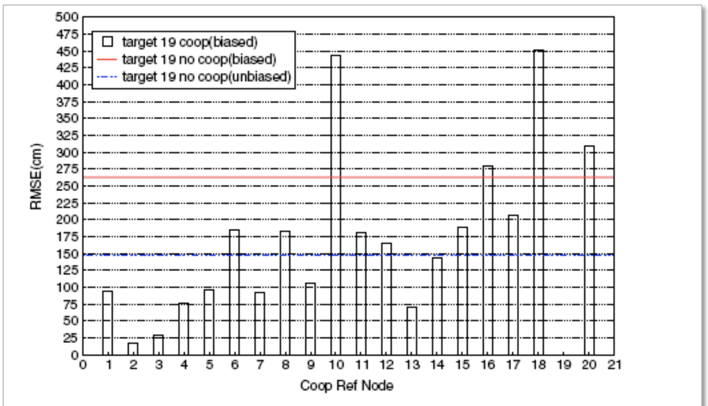

Fig. 5. RMSE for the target 1 located in position 19, when it cooperates with target 2 (cooperative reference node) in varying positions reported in abscissa.

Experimental results: ML

xmin := 1030
xmax := 2200
ymin := 920
ymax := 2190

Dx := 100.
Dy := 100.

Values in cm.

beaconprof := {1,1,1,1,1}
delbias := 0
measiniz := 200
numrealz := 10

ID=01, RMSE=	48.12
ID=02, RMSE=	104.25
ID=03, RMSE=	165.23
ID=04, RMSE=	79.32
ID=05, RMSE=	57.22
ID=06, RMSE=	28.79
ID=07, RMSE=	92.98
ID=08, RMSE=	50.86
ID=09, RMSE=	38.54
ID=10, RMSE=	56.91
ID=11, RMSE=	36.59
ID=12, RMSE=	52.86
ID=13, RMSE=	41.29
ID=14, RMSE=	38.83
ID=15, RMSE=	68.18
ID=16, RMSE=	16.41
ID=17, RMSE=	21.13
ID=18, RMSE=	125.68
ID=19, RMSE=	119.44
ID=20, RMSE=	45.19

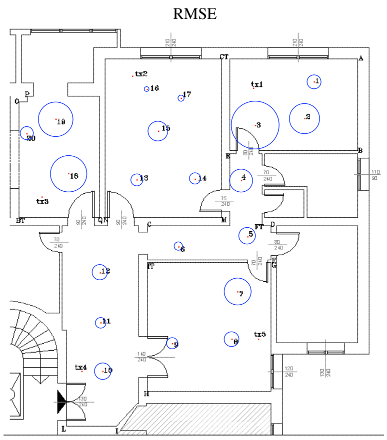

Experimental results: ML

xmin = 1030
xmax = 2200
ymin = 920
ymax = 2190

Dx = 25.
Dy = 25.

Values in cm.

beaconprof := {1,1,1,1,1}
delbias := 0
measiniz := 200
numrealz := 10

ID=01, RMSE=	82.83
ID=02, RMSE=	131.38
ID=03, RMSE=	136.61
ID=04, RMSE=	92.66
ID=05, RMSE=	48.18
ID=06, RMSE=	18.68
ID=07, RMSE=	40.61
ID=08, RMSE=	44.33
ID=09, RMSE=	71.87
ID=10, RMSE=	59.22
ID=11, RMSE=	45.77
ID=12, RMSE=	27.40
ID=13, RMSE=	10.43
ID=14, RMSE=	43.11
ID=15, RMSE=	29.30
ID=16, RMSE=	23.20
ID=17, RMSE=	28.45
ID=18, RMSE=	87.092
ID=19, RMSE=	105.76
ID=20, RMSE=	33.13

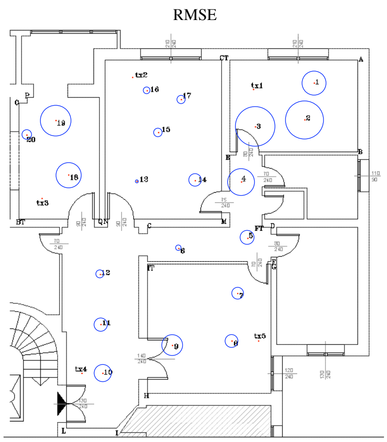

Experimental results: ML (bias removed)

xmin = 1030
xmax = 2200
ymin = 920
ymax = 2190

Dx = 100.
Dy = 100.

Values in cm.

beaconprof := {1,1,1,1,1}
delbias := 1
measiniz := 200
numrealz := 10

ID=01, RMSE=	145.70
ID=02, RMSE=	110.56
ID=03, RMSE=	66.63
ID=04, RMSE=	20.68
ID=05, RMSE=	93.00
ID=06, RMSE=	28.79
ID=07, RMSE=	41.08
ID=08, RMSE=	52.01
ID=09, RMSE=	68.20
ID=10, RMSE=	73.28
ID=11, RMSE=	64.87
ID=12, RMSE=	79.24
ID=13, RMSE=	41.29
ID=14, RMSE=	38.83
ID=15, RMSE=	72.42
ID=16, RMSE=	16.41
ID=17, RMSE=	85.22
ID=18, RMSE=	80.08
ID=19, RMSE=	22.94
ID=20, RMSE=	62.67

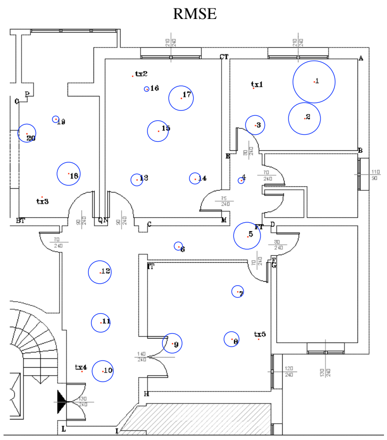

Experimental results: Hierarchical ML

xmin = 1030
xmax = 2200
ymin = 920
ymax = 2190

Dx = 200.
Dy = 200.

Values in cm.

η := 2
Nger := 4

beaconprof := {1,1,1,1,1}
delbias := 0
measiniz := 200
numrealz := 10

ID=01, RMSE=	272.62
ID=02, RMSE=	184.41
ID=03, RMSE=	26.64
ID=04, RMSE=	56.20
ID=05, RMSE=	47.85
ID=06, RMSE=	141.66
ID=07, RMSE=	75.97
ID=08, RMSE=	152.61
ID=09, RMSE=	139.49
ID=10, RMSE=	193.53
ID=11, RMSE=	163.06
ID=12, RMSE=	135.06
ID=13, RMSE=	200.38
ID=14, RMSE=	40.77
ID=15, RMSE=	99.53
ID=16, RMSE=	155.79
ID=17, RMSE=	194.17
ID=18, RMSE=	172.14
ID=19, RMSE=	127.35
ID=20, RMSE=	17.87

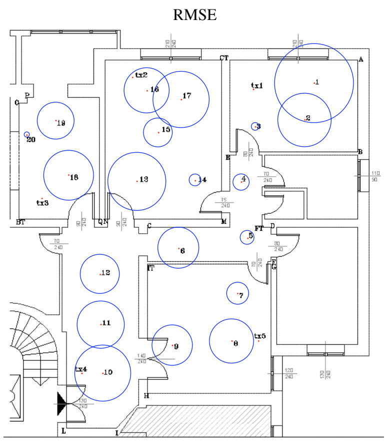

Experimental results: SPAWN coop

COOPERATIVE SPAWN LOCALIZATION RMSE $e(\mathbf{p})$ [CM] FOR EACH NODE POSITION (ID) WITH $N_B = 3$ IN VARIOUS SITUATIONS (A)-(G).

ID	(A)	(B)	(C)	(D)	(E)	(F)	(G)
1	65.5	48.3	65.5	48.3	48.2	48.5	14.5
2	111.5	21.2	111.5	21.2	21.1	21.2	9.0
3	83.0	38.3	83.0	38.3	38.3	38.3	30.7
4	111.8	66.4	111.8	66.4	66.4	66.4	25.7
5	100.8	41.2	100.8	41.2	41.3	40.9	46.8
6	39.5	18.9	39.5	18.9	18.9	-	55.8
7	90.8	61.9	90.8	61.9	61.9	61.9	33.8
8	-	-	99.1	38.8	38.9	39.0	16.1
9	58.2	67.4	58.2	67.4	67.4	67.4	18.7
10	31.1	34.9	31.1	34.9	34.9	34.9	25.4
11	46.1	47.0	46.1	47.0	47.0	47.0	19.2
12	16.1	39.8	16.1	39.8	39.8	39.8	12.2
13	62.0	44.8	62.0	44.8	44.9	45.0	33.9
14	48.9	39.3	48.9	39.3	39.3	39.3	23.9
15	77.0	26.5	77.0	26.5	-	-	29.6
16	47.8	48.7	47.8	48.7	48.7	48.7	31.5
17	56.7	46.5	56.7	47.5	46.5	46.5	20.6
18	59.3	46.6	59.3	46.6	46.6	46.6	43.9
19	98.3	62.0	-	-	62.0	62.0	45.4
20	59.2	36.6	59.2	36.6	36.6	36.6	12.7

(A) coop. with agent 8, no ranging refinement
(B) coop. with agent 8, ranging refinement (WED)
(C) coop. with agent 19, no ranging refinement
(D) coop. with agent 19, ranging refinement (WED)
(E) coop. with agent 15, ranging refinement (WED)
(F) coop. with agents 6 and 15, ranging refinement (WED)
(G) coop. with all agents in 5m, ranging refinement (statistical)

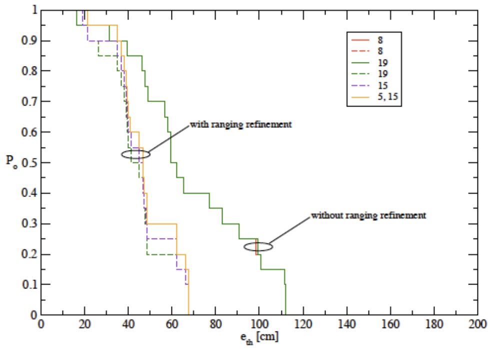

Fig. 5. LEO versus e_{th} [cm] for cooperative SPAWN with $N_b = 3$ with (continuos) and without (dashed) ranging refinement. Various combinations of cooperative agents are considered: 8 (red), 19 (green), 15 (orange), 5 and 15 (magenta).

Some lessons learned

- A priori information on the environment improves the position estimate
- Cooperation helps but only if it is carefully exploited
- Localization techniques to be used are related to the environment

Tracking experimentation

- Network navigation
- Measurements with UWB and Zigbee radios
- Data fusion
- Mobility models



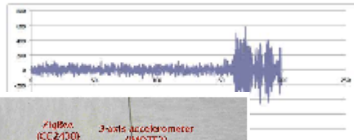
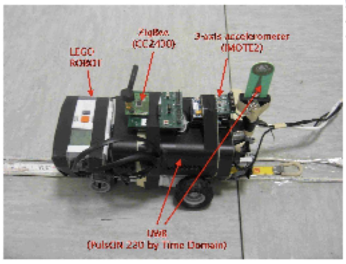

A. Conti et al., "Experimental Characterization of Diversity Navigation," IEEE Systems Journal., Mar. 2014

UWB and ZigBee nodes deployment

UWB anchor nodes

Ranging based on TOA estimation

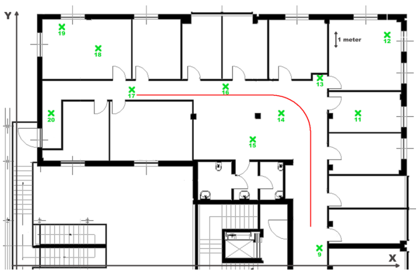

ZigBee anchor nodes

Ranging based on RSSI measurements

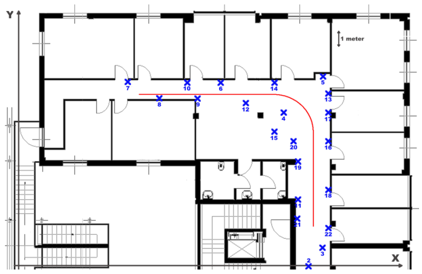

In addition: inertial measurements and data fusion

Estimated trajectory

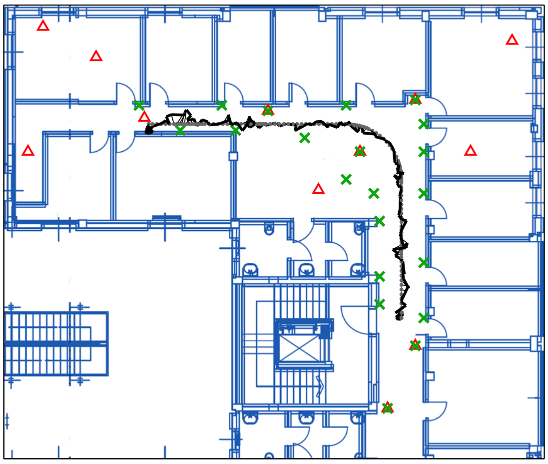

Fig. 12. Real (gray) and estimated (black) trajectory of the robot for the diversity navigation system. UWB (triangles) and ZigBee (crosses) anchors are indicated.

UWB navigation performance

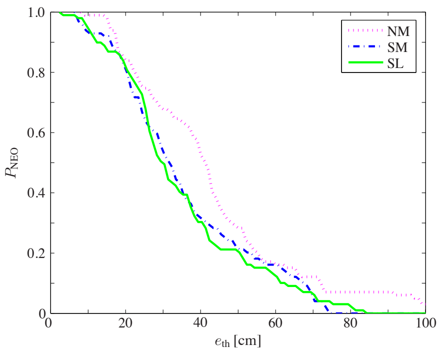

Fig. 7. NEO for the UWB system; constant speed scenario; three mobility models: NM, SM, and SL with optimum window size.

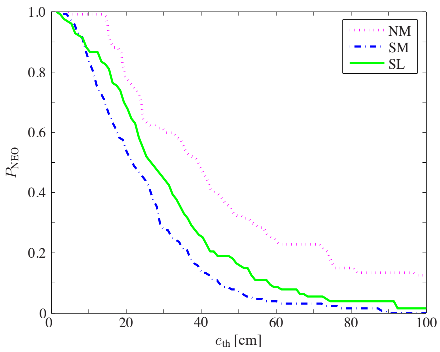

Fig. 8. NEO for the UWB system; variable speed scenario; three mobility models: NM, SM, and SL with optimum window size.

UWB, Zigbee, & data fusion

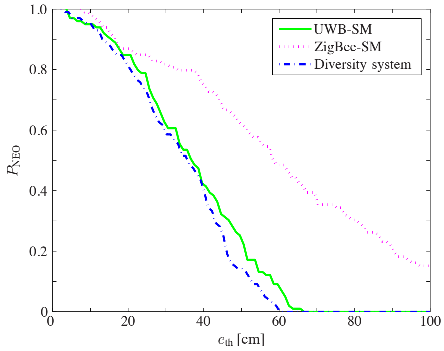

Fig. 9. NEO for UWB, ZigBee, and diversity system; constant speed scenario is considered.

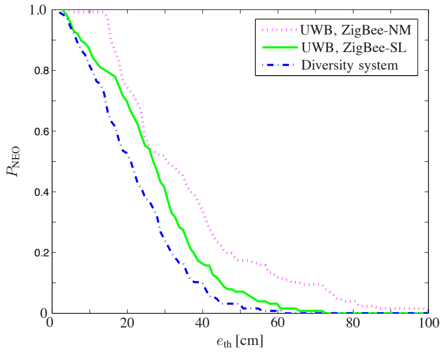

Fig. 11. NEO for UWB and ZigBee technologies with models NM, SL, and SM in variable speed scenario. Optimum window size is considered for SL.

SENSOR RADAR NETWORKS

Passive localization

- Ranging based on backscattered signals
- Sensor radar networks (network of monostatic or bistatic radars)

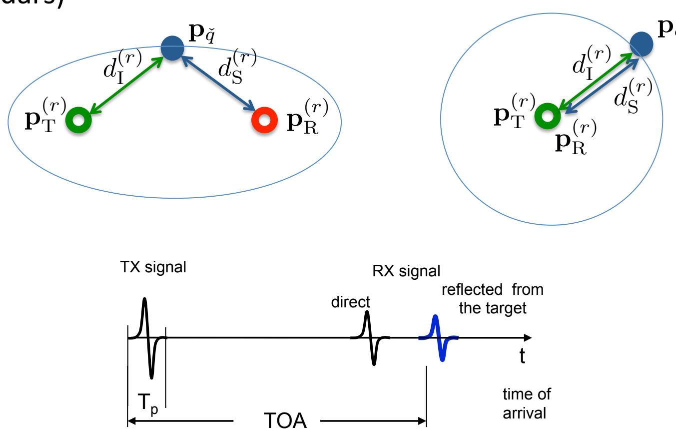

Bistatic radar coverage limits

- To detect the target the echo must be resolvable with respect to the direct pulse, i.e., the two pulses are separated by at least a delay γ (minimum resolvable delay)

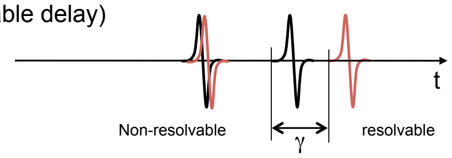

There is a ***minimum ellipse*** where a target inside
is invisible to the bistatic pair.

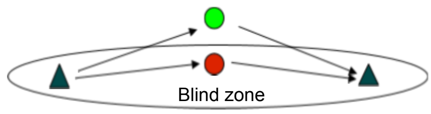

$$D_{\min} = \sqrt{(Rx_{\mathrm{x}} - Tx_{\mathrm{x}})^2 + (Rx_{\mathrm{y}} - Tx_{\mathrm{y}})^2} + \gamma c\,.$$

$$\sqrt{(x_{\mathrm{T}} - Tx_{\mathrm{x}})^2 + (y_{\mathrm{T}} - Tx_{\mathrm{y}})^2} + \sqrt{(x_{\mathrm{T}} - Rx_{\mathrm{x}})^2 + (y_{\mathrm{T}} - Rx_{\mathrm{y}})^2} - D_{\min}$$

<0 Undetectable
>0 Detectable

Bistatic radar coverage limits

- Received power from the target

$$P_{\mathrm{r}} = \int_{f_{\mathrm{L}}}^{f_{\mathrm{U}}} \frac{S_{\mathrm{t}}(f) G_{\mathrm{t}}(f) G_{\mathrm{r}}(f) \sigma}{(l_1 l_2)^{\beta} (4\pi)^3} \left(\frac{c}{f}\right)^2 df$$

IEEE 802.15.4a RCS

Equi-power positions are the locus of points whose ***product*** of the distances from the TX node and the RX node $l_1\, l_2$ is constant (e.g., Cassini oval in free-space β=2)

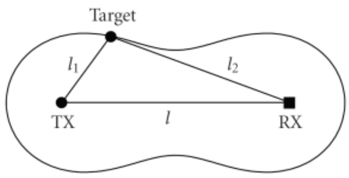

- Receiver sensitivity requirement:

$$P_{\mathrm{r}} \geq P_{\mathrm{rth}} \Rightarrow l_1 l_2 \leq (l_1 l_2)_{\mathrm{th}}$$

$$(l_1 l_2)_{\mathrm{th}} \triangleq \left[\int_{f_{\mathrm{L}}}^{f_{\mathrm{U}}} \frac{S_{\mathrm{t}}(f) G_{\mathrm{t}}(f) G_{\mathrm{r}}(f) \sigma}{P_{\mathrm{rth}} (4\pi)^3} \left(\frac{c}{f}\right)^2 df \right]^{1/\beta}$$

There is a ***maximum oval*** where a target outside
is invisible to the bistatic pair due to receiver sensitivity.

UWB sensor radar networks

- Network of monostatic or bistatic sensor radars

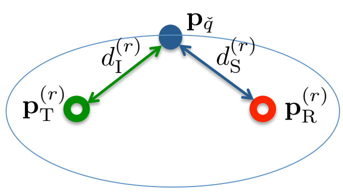

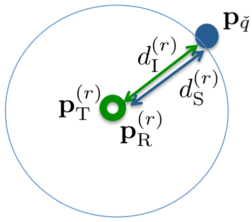

Obstructed line of sight conditions (OLOS)

$$\varepsilon_i(\mathbf{p}) \sim \mathcal{N}(\mu_i(\mathbf{p}), \sigma_i^2(\mathbf{p}))$$

$$\mu_i(\mathbf{p}) \simeq \Delta/c$$

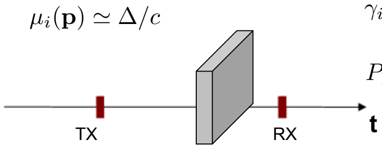

$$\gamma_i(\mathbf{p}) = \frac{P_{\mathrm{R},i}(\mathbf{p})}{\mathsf{PRF} N_0}$$

$$P_{\mathrm{R},i}(\mathbf{p}) = \int_{f_{\mathrm{L}}}^{f_{\mathrm{U}}} \frac{T_i(f)\eta_i(f,\boldsymbol{\Theta}_{\mathrm{i}})^2 \Sigma(f)}{(4\pi)^3 L_i(f,\mathbf{p}) \left(\frac{f_0 d_0}{c}\right)^2 \ell_i^{2\beta}(\mathbf{p}) \left(\frac{f}{f_0}\right)^{2\kappa+2}}$$

$$L_i(f,\mathbf{p}) = \sum_{w=1}^{W_i(\mathbf{p})} 2\, n_{w,i}(\mathbf{p}) X_w(f)$$

Ranging and tracking

- Energy detection based TOA estimation
- Tracking via particle filtering
- Mobility models

$$p(\mathbf{x}_{k,i}|\mathbf{x}_{k-1,i}) = \frac{1}{\sqrt{2\pi}\sigma_{\mathrm{m,k}}} e^{\frac{||\mathbf{x}_{k,i}-\boldsymbol{\mu}_{k,i}||^2}{2\sigma_{\mathrm{m,k}}^2}} \qquad \text{Gaussian model}$$

  - Speed known direction unknown

$$\boldsymbol{\mu}_{k,i} = \mathbf{x}_{k-1,i} + \mathbf{v}_i\, \Delta_T \qquad (\theta_i \sim \mathcal{U}[-\pi,\pi])$$

$$\sigma_{\mathrm{m,k}} = \frac{v\, \Delta_T}{\sqrt{2}\,\mathrm{erfc}^{-1}(1-q)} \qquad (\mathbb{P}\left\{|\mathbf{x}_{k,i} - \boldsymbol{\mu}_{k,i}| \leq v\, \Delta_T\right\} = q)$$

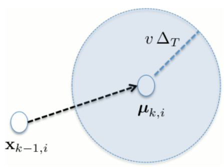

  - Speed direction learning

$$\boldsymbol{\mu}_{k,i} = \mathbf{x}_{k-1,i} + \mathbf{v}_{k-1}\, \Delta_T \qquad \mathbf{v}_{k-1} = \frac{1}{N_v\, \Delta_T} \sum_{m=1}^{N_v} (\mathbf{x}_{k-m} - \mathbf{x}_{k-m-1})$$

$$\sigma_{\mathrm{m},k} = \frac{|\mathbf{v}_{k-1}|\, \Delta_T}{\sqrt{2}\,\mathrm{erfc}^{-1}(1-q)}$$

Case study on sensor radars

Monostatic WSR

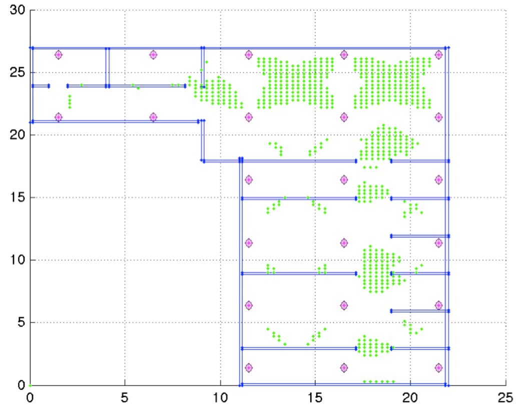

$$S_t(f) = -42\text{dBm/MHz}$$

European lower band $f_L = 3.1\text{GHz}$

$$f_U = 4.8\text{GHz}$$

$$\beta = 2$$

$$P_{rth} = -95\,\text{dBm}$$

$$T_{int} = 4\text{ns}$$

$$T_g = 120\text{ns}$$

$$A = -7.39$$

$$B = -0.0875$$

$$\xi_{dB}^{(L)} = 0.8\text{dB}$$

$$\xi_{dB}^{(H)} = 17\text{dB}$$

$$\Delta_{SNR} = -5, 0, 5, 10\text{dB}$$

Numerical sesults

SKDU

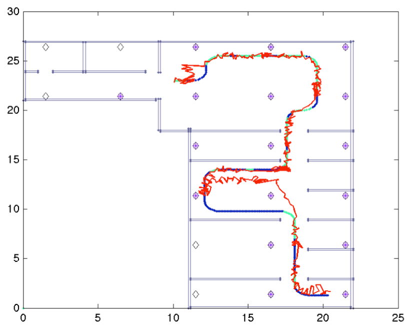

$e_{RMS} = 1.2\text{m}$

SDL

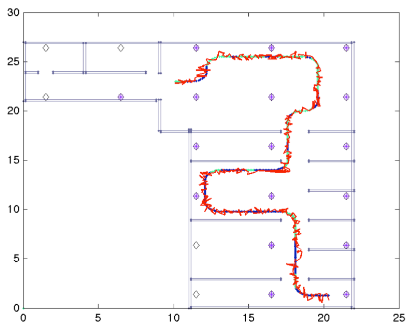

$e_{RMS} = 0.35\text{m}$

S. Bartoletti et al., "Sensor Radar Networks for Indoor Tracking," IEEE Wireless Commun. Letters, Feb. 2014

Numerical results

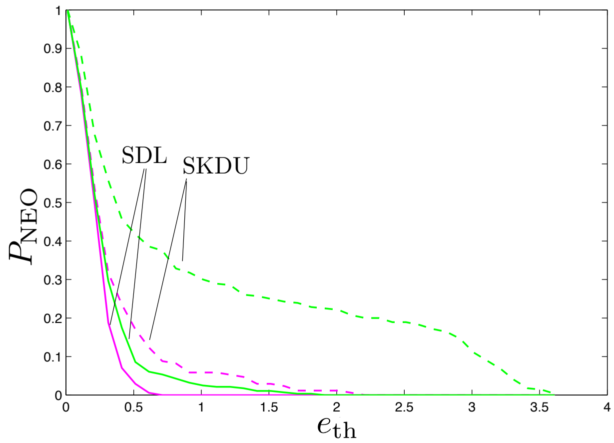

		SKDU	SDL	
$P_{\mathrm{NEO}} < 0.2$		$e_{\mathrm{th}} = 0.5\mathrm{m}$	$e_{\mathrm{th}} = 0.3\mathrm{m}$	LOS
		$e_{\mathrm{th}} = 2.7\mathrm{m}$	$e_{\mathrm{th}} = 0.4\mathrm{m}$	OLOS

SEMIPASSIVE TAGS

From RFID to RADIAL

- Radio-frequency identification (RFID) of objects in real-time enables new important applications (e.g., logistic, automotive, surveillance, and automation)
- Such applications require also high-accuracy localization/tracking capability even in harsh propagation environments

radio **d**etection, **i**dentification, **a**nd **l**ocalization

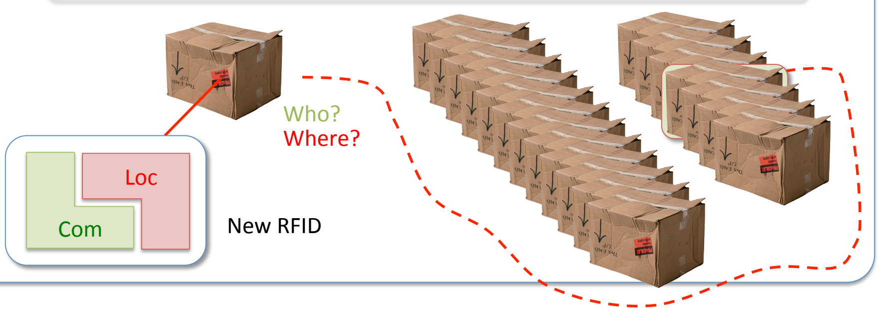

Backscattering modulation

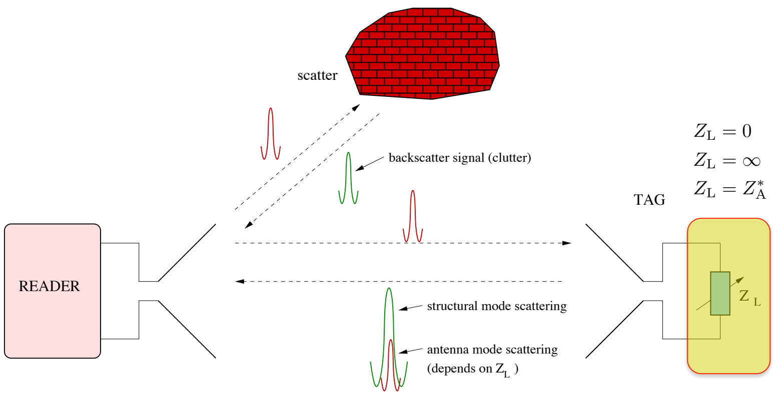

- The backscattering modulation is obtained by changing the tag's antenna load according to the information to be transmitted, e.g. identifier (+ payload).

Antenna backscattering

- It is essential to model antenna backscattering characteristics
- Structural mode
  - Reflection of e.m. waves depending on antenna's shape and material, independently of the load
- Antenna mode
  - Reflection of e.m. waves depending on the load → data can be sent back to the reader through variations of Z_L, without requiring a dedicated power source

Order of Arrival Estim. via UHF-UWB RFID

- Conveyor belt
- Reader network
- Monitored area
- Objects with multiple tags

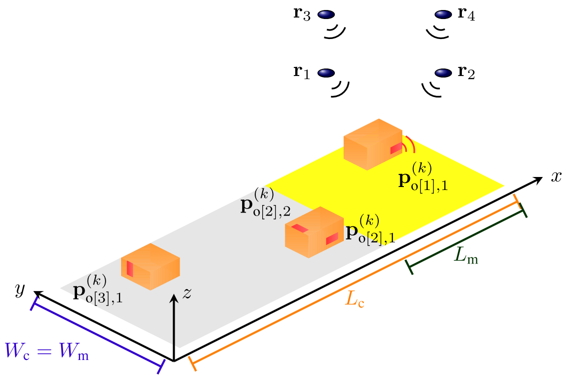

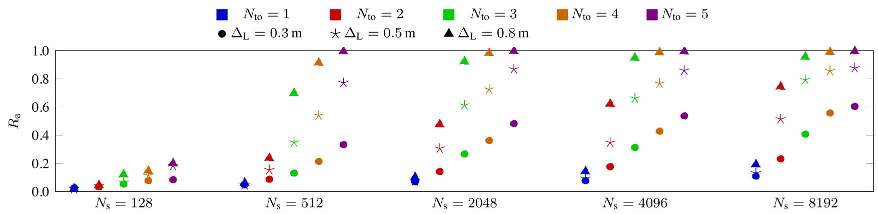

Relaying

- Poor coverage calls for higher transmitted power or/and relaying, especially in the presence of obstacles

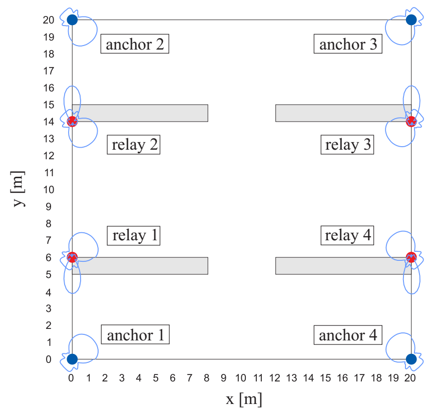

N. Decarli et al., "Non-Regenerative Relaying for Network Localization," IEEE Trans. on Wireless Commun., Jan. 2014

Relaying

- Poor coverage calls for higher transmitted power or/and relaying, especially in the presence of obstacles

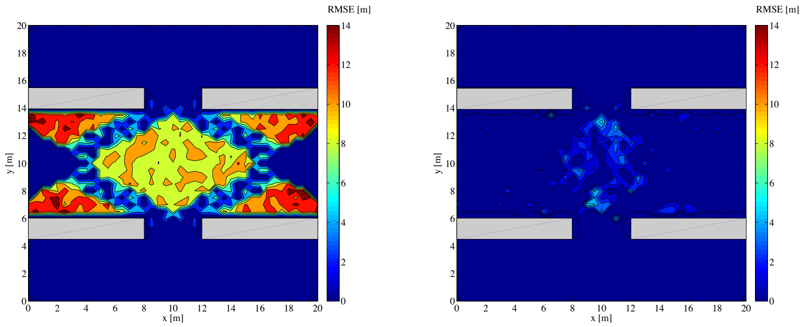

(a) Without relays (b) JF relays

Figure 5.7: RMSE contour map in the 2D environment.

Green tags

- Next frontier is to design a green tag (>80% of the tag on organic materials)

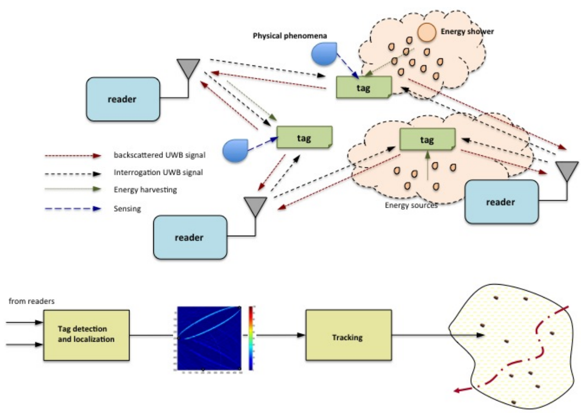

Green tags

- Substrate integrated wave technology
- Energy harvesting

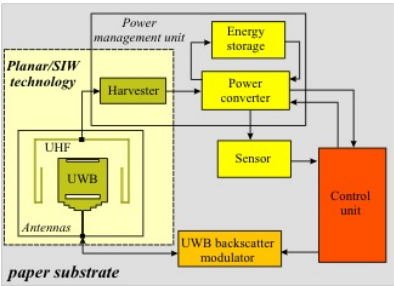

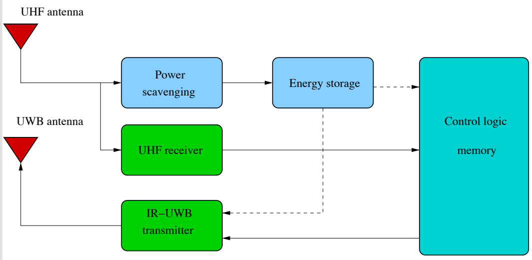

Location-Aware Networks = Team Effort

http://wgroup.lids.mit.edu/publication.html

- W. Dai, Y. Shen, and M. Z. Win, "Resource allocation for network localization: A computational geometry framework," *IEEE Trans. Inf. Theory*, 2016, to appear.
- J. Chen, W. Dai, Y. Shen, V. K.N. Lau, and M. Z. Win, "Power management for cooperative localization: A game theoretical approach," *IEEE Trans. Signal Process.*, 2016, to appear.
- T. Zhang, A. Molisch, Y. Shen, Q. Zhang, Ha. Feng, and M. Z. Win, "Optimal joint power and bandwidth allo- cation in cooperative wireless localization networks," *IEEE Trans. Wireless Commun.*, 2016, to appear.
- J. Prieto, S. Mazuelas, and M. Z. Win, "Context-aided inertial navigation via belief condensation," *IEEE Trans. Signal Process.*, vol. 64, no. 12, pp. 3250–3261, Jun. 2016.
- K. Witrisal, P. Meissner, E. Leitinger, Y. Shen, C. Gustafson, F. Tufvesson, K. Haneda, D. Dardari, A. F. Molisch, A. Conti, and M. Z. Win, "High-accuracy localization for assisted living," *IEEE Signal Process. Mag.*, vol. 33, no. 2, pp. 59–70, Mar. 2016.
- Y. Han, Y. Shen, X. Zhang, M. Z. Win, and H. Meng, "Performance limits and geometric properties of array localization," *IEEE Trans. Inf. Theory*, vol. 62, no. 2, pp. 1054–1075, Feb. 2016.
- T. V. Nguyen, Y. Jeong, H. Shin, and M. Z. Win, "Least-square cooperative localization," *IEEE Trans. Veh. Technol.*, vol. 64, no. 4, pp. 1318–1330, Apr. 2015.

Location-Aware Networks = Team Effort

http://wgroup.lids.mit.edu/publication.html

- S. Bartoletti, A. Giorgetti, M. Z. Win, and A. Conti, "Blind selection of representative observations for sensor radar networks," *IEEE Trans. Veh. Technol.*, vol. 64, no. 4, pp. 1388–1400, Apr. 2015.
- S. Bartoletti, W. Dai, A. Conti, and M. Z. Win, "A mathematical model for wideband ranging," *IEEE J. Sel. Topics Signal Process.*, vol. 9, no. 2, pp. 216–228, Mar. 2015.
- W. Dai, Y. Shen, and M. Z. Win, "Distributed power allocation for cooperative wireless network localization," *IEEE J. Sel. Areas Commun.*, vol. 33, no. 1, pp. 28–40, Jan. 2015.
- Y. Shen, W. Dai, and M. Z. Win, "Power optimization for network localization," *IEEE/ACM Trans. Netw.*, vol. 22, no. 4, pp. 1337–1350, Aug. 2014.
- M. Leng, W. P. Tay, C. M. S. See, S. G. Razul, and M. Z. Win, "Modified CRLB for cooperative geolocation of two devices using signals of opportunity," *IEEE Trans. Wireless Commun.*, vol. 13, no. 7, pp. 3636–3649, Jul. 2014.
- S. Bartoletti, A. Conti, A. Giorgetti, and M. Z. Win, "Sensor radar networks for indoor tracking," *IEEE Wireless Commun. Lett.*, vol. 3, no. 2, pp. 157–160, Apr. 2014.
- T. Wang, Y. Shen, S. Mazuelas, H. Shin, and M. Z. Win, "On OFDM ranging accuracy in multipath channels," *IEEE Syst. J.*, vol. 8, no. 1, pp. 104–114, Mar. 2014.
- A. Conti, D. Dardari, M. Guerra, L. Mucchi, and M. Z. Win, "Experimental characterization of diversity navigation," *IEEE Syst. J.*, vol. 8, no. 1, pp. 115–124, Mar. 2014.

Location-Aware Networks = Team Effort

http://wgroup.lids.mit.edu/publication.html

- N. Decarli, A. Guerra, A. Conti, R. D'Errico, A. Sibille, and D. Dardari, "Non-regenerative relaying for network localization," *IEEE Trans. Wireless Commun.*, vol. 13, no. 1, pp. 174–185, Jan. 2014.
- W. W.-L. Li, Y. Shen, Y. J. Zhang, and M. Z. Win, "Robust power allocation for energy-efficient location-aware networks," *IEEE/ACM Trans. Netw.*, vol. 21, no. 6, pp. 1918–1930, Dec. 2013.
- Y. Shen and M. Z. Win, "Intrinsic information of wideband channels," *IEEE J. Sel. Areas Commun.*, vol. 31, no. 9, pp. 1875–1888, Sep. 2013.
- S. Mazuelas, Y. Shen, and M. Z. Win, "Belief condensation filtering," *IEEE Trans. Signal Process.*, vol. 61, no. 18, pp. 4403–4415, Sep. 2013.
- F. Montorsi, S. Mazuelas, G. M. Vitetta, and M. Z. Win, "On the performance limits of map-aware localization," *IEEE Trans. Inf. Theory*, vol. 59, no. 8, pp. 5023–5038, Aug. 2013.
- J. Lien, U. J. Ferner, W. Srichavengsup, H. Wymeersch, and M. Z. Win, "A comparison of parametric and sample- based message representation in cooperative localization," Interna- tional Journal of Navigation and Observation, vol. 2012, pp. Article ID 281 592, 1–10, 2012.
- Y. Shen, S. Mazuelas, and M. Z. Win, "Network navigation: Theory and interpretation," *IEEE J. Sel. Areas Commun.*, vol. 30, no. 9, pp. 1823–1834, Oct. 2012.
- H. Wymeersch, S. Maranò, W. M. Gifford, and M. Z. Win, "A machine learning approach to ranging error mitigation for UWB localization," *IEEE Trans. Commun.*, vol. 60, no. 6, pp. 1719–1728, Jun. 2012.

Location-Aware Networks = Team Effort

http://wgroup.lids.mit.edu/publication.html

- A. Conti, M. Guerra, D. Dardari, N. Decarli, and M. Z. Win, "Network experimentation for cooperative localization," *IEEE J. Sel. Areas Commun.*, vol. 30, no. 2, pp. 467–475, Feb. 2012.
- S. Mazuelas, Y. Shen, and M. Z. Win, "Information coupling in cooperative localization," *IEEE Commun. Lett.,* vol. 15, no. 7, pp. 737–739, Jul. 2011.
- M. Z. Win, A. Conti, S. Mazuelas, Y. Shen, W. M. Gifford, D. Dardari, and M. Chiani, "Network localization and navigation via cooperation," *IEEE Commun. Mag.*, vol. 49, no. 5, pp. 56–62, May 2011, **IEEE Communications Society Fred W. Ellersick Prize.**
- Y. Shen and M. Z. Win, "Fundamental limits of wideband localization – Part I: A general framework," *IEEE Trans. Inf. Theory*, vol. 56, no. 10, pp. 4956–4980, Oct. 2010.
- Y. Shen, H. Wymeersch, and M. Z. Win, "Fundamental limits of wideband localization – Part II: Cooperative networks," *IEEE Trans. Inf. Theory*, vol. 56, no. 10, pp. 4981–5000, Oct. 2010.
- S. Maranò, W. M. Gifford, H. Wymeersch, and M. Z. Win, "NLOS identification and mitigation for localization based on UWB experimental data," *IEEE J. Sel. Areas Commun.*, vol. 28, no. 7, pp. 1026–1035, Sep. 2010.
- D. Dardari, R. D'Errico, C. Roblin, A. Sibille, and M. Z. Win, "Ultrawide bandwidth RFID: The next generation?" *Proc. IEEE*, vol. 99, no. 7, pp. 1570–1582, Jul. 2010.

Location-Aware Networks = Team Effort

http://wgroup.lids.mit.edu/publication.html

- Y. Shen and M. Z. Win, "On the accuracy of localization systems using wideband antenna arrays," *IEEE Trans. Commun.*, vol. 58, no. 1, pp. 270–280, Jan. 2010.
- D. Dardari, A. Conti, U. J. Ferner, A. Giorgetti, and M. Z. Win, "Ranging with ultrawide bandwidth signals in multipath environments," *Proc. IEEE*, vol. 97, no. 2, pp. 404–426, Feb. 2009.
- H. Wymeersch, J. Lien, and M. Z. Win, "Cooperative localization in wireless networks," *Proc. IEEE*, vol. 97, no. 2, pp. 427–450, Feb. 2009.
- D. Dardari, A. Conti, J. Lien, and M. Z. Win, "The effect of cooperation on localization systems using UWB experimental data," *EURASIP J. Appl. Signal Process.*, vol. 2008, pp. 1–11, Article ID 513 873, 2008.
- D. Dardari, C.-C. Chong, and M. Z. Win, "Threshold- based time-of-arrival estimators in UWB dense multipath channels," *IEEE Trans. Commun.*, vol. 56, no. 8, pp. 1366–1378, Aug. 2008.
- D. B. Jourdan, D. Dardari, and M. Z. Win, "Position error bound for UWB localization in dense cluttered environments," *IEEE Trans. Aerosp. Electron. Syst.*, vol. 44, no. 2, pp. 613–628, Apr. 2008, **IEEE Aerospace and Electronic Systems Society M. Barry Carlton Award.**
- C. Falsi, D. Dardari, L. Mucchi, and M. Z. Win, "Time of arrival estimation for UWB localizers in realistic environ- ments," *EURASIP J. Appl. Signal Process.*, vol. 2006, pp. 1–13, Article ID 32 082, 2006.